SERUM, URINE, AND KIDNEY MICRORNA AND GENE EXPRESSION CHARACTERIZATION IN DOGS WITH CHRONIC KIDNEY DISEASES

A Dissertation

by

PEI-HUA CHU

Submitted to the Office of Graduate and Professional Studies of
Texas A&M University
in partial fulfillment of the requirements for the degree of

DOCTOR OF PHILOSOPHY

Chair of Committee,	Mary B. Nabity
Committee Members,	Jan S. Suchodolski
	Ivan Ivanov
	Alan R. Dabney
Head of Department,	Ramesh Vemulapalli

August 2018

Major Subject: Veterinary Pathobiology

Copyright 2018 Pei-Hua Chu

ABSTRACT

Chronic kidney disease (CKD) is a significant cause of death in dogs. However, the gene and microRNA (miRNA) expression profile that affects progression in CKD has only been partially characterized. Dogs with X-linked hereditary nephropathy (XLHN) have a glomerular basement membrane defect that leads to progressive juvenile-onset renal failure, and their disease is analogous to Alport syndrome in humans. Therefore, dogs with XLHN not only serve as a good model of canine CKD but also an animal model for Alport syndrome in humans. In the report, kidney tissue mRNA and small RNA sequencing were used to aid in the characterization of CKD progression in colony dogs with XLHN. Further, biofluid miRNA expression in serum and urine was characterized to serve as potential biomarkers in canine patients with natural-occurring glomerular diseases.

Differentially expressed genes (DEGs) and differentially expressed miRNAs (DE miRs) were identified via mRNA and small RNA sequencing in serial kidney biopsies obtained from dogs with XLHN. The DEGs and the top-ranked miRNA target genes derived from DE miRs were used to identify enriched biological processes, over-represented pathways, and upstream regulators that contribute to kidney disease progression. Differentially expressed genes and DE miRs identified over 3 clinical time points revealed upregulation of inflammatory pathways, and TGF-β1 was identified as the primary upstream regulator. These results provide new insights into the underlying

molecular mechanisms of disease progression in XLHN, and the identified DEGs and DE miRs can be potential biomarkers and therapeutic targets translatable to all CKDs.

Biofluid miRNA detection was performed in carrier female dogs with XLHN. This preliminary study helped optimize RNA isolation and library preparation methods for canine serum and urine. A biofluid miRNA biomarker study was then performed in dogs with 3 types of glomerular diseases diagnosed histopathologically: focal segmental glomerulosclerosis, immune complex glomerulonephritis, and amyloidosis. Compared with healthy control dogs, DE miRs were identified in the serum and urine from dogs with mild or advanced tubulointerstitial fibrosis in all 3 diseases. Several miRs showed promise in their ability to distinguish among these 3 glomerular diseases. These results will provide non-invasive options for diagnosing canine glomerular diseases.

To my husband,

Bill,

for loving me as who I am

To the amazing animals I have met,

Aggie, Mimi, Little White, Little Honey,

and the Sundance cats,

for inspiring me to become a better veterinarian

ACKNOWLEDGEMENTS

As a veterinarian who grew up in Hsinchu City, Taiwan, College Station, Texas is considered my second home. Five years ago, Dr. George Lees kindly forwarded my position-seeking email to Dr. Mary Nabity. Words can't express my appreciation to Dr. Nabity, who spotted my potential and accepted me as her first Taiwanese student. In the past four years, there has never been a moment that I am not grateful for having a mentor as patient, understanding, and knowledgeable as her who guides me through the PhD study. Dr. Nabity inspired me to step on the path of becoming a veterinary clinical pathologist. She will continue to be the role model of my career path.

I would also like to thank the members of my committee: Dr. Jan Suchodolski, who always provided constructive suggestions to my study and generously shared the resources of the GI Laboratory with me; Dr. Ivan Ivanov, for providing me valuable teaching opportunities in his graduate-level course, Analysis of Genomic Signals, to enrich my teaching experience; Dr. Alan Dabney, for offering his statistical expertise and encouragement throughout my PhD study.

Several other mentors that I encountered also encouraged me to pursue my dream of becoming a veterinary clinical pathologist. My labmates, Dr. Jessica Hokamp, taught me how a person could work hard while preserving a sense of humor, and Dr. Sabrina Clark showed me how to stay positive during the dark moments. I thank Dr. Mark Johnson who always has high expectations in me and witnesses how much I have grown during

these years. The people that I met at Purdue University during my summer externship are also my strong supporters. I enjoyed the friendly learning environment built by Dr. John Christian, Dr. Joanne Messick, Dr. Craig Thompson, Dr. Andrea Santos. Dr. Ashley Leisering, and Dr. Mara Varvil. Particularly, I appreciate having the opportunity to be Dr. Rose Raskin's Chinese interpreter and local guide during her visit to Taiwan. Her energy, curiosity, and humbleness constantly remind me of whom I want to be as a "grown-up."

All of my projects couldn't be carried out without the technical assistance provided by our veterinary technician, Mary Sanders. Her special care and dedication toward our dog colony and the International Veterinary Renal Pathology Service (IVRPS) is the pivotal part of our research. I would also like to thank So Young Park, the Diagnostic Laboratory Supervisor of the GI Laboratory, for her endless support in helping me set up experimental protocols. I appreciate the encouragement from Dr. Michael Criscitiello since I joined A&M, and the help from several departmental staff: Betty Suehs and Jeanine Malazzo, our previous HR, a.k.a. my "American Mama," for the warm care they had given to me; Katie Cosby, Kathie Smith, Dee Cooper, and Katharina Ojala, the past and current graduate program coordinators I have interacted with, for their efficient assistance.

Thanks also to my Taiwanese fellows for having each other in our memories of studying abroad: Yu-Heng, who always made hilarious yet insightful comments; Heng-Heng, Ah-Hung, and Stephen, with whom we shared a road trip to Colorado and Oklahoma; Amy, Carol, and Meow-Meow, my dear neighbor and girlfriends, for joy we have of being together; Ya-An, my bestie at the College of Veterinary Medicine, for supporting each other during the past 3 years.

Most importantly, I thank my husband, Bill, for his respect, love, and affection since the age of 16. We are blessed to share almost half of our lives together and to witness the growth of each other in the past 11 years. I am grateful to have his company during my overseas PhD study. He believes in me, provides me with never-ending supports, and awakens my inner strength to overcome obstacles. He is no doubt my driving force in the way of pursuing an academic career.

CONTRIBUTORS AND FUNDING SOURCES

This work was supervised by a dissertation committee consisting of Professor Mary B. Nabity of the Department of Veterinary Pathobiology, Professor Jan S. Suchodolski of the Department of Small Animal Clinical Sciences, Professor Ivan Ivanov of the Department of Veterinary Integrative Biosciences, and Professor Alan R. Dabney of the Department of Statistics.

The RNA samples analyzed for Chapter II were isolated by Dr. Jessica Hokamp of the Department of Veterinary Pathobiology and Mia Aguilar of the Doctor of Veterinary Medicine program, the histopathology results were evaluated by Dr. Rachel E. Cianciolo of the Department of Veterinary Biosciences at The Ohio State University, the statistical analyses were conducted in part by Dr. Alan R. Dabney of the Department of Statistics, the project was co-designed by Dr. Candice Brinkmeyer-Langford of the Department of Veterinary Integrative Biosciences, the samples analyzed were collected by Dr. George E. Lees and Dr. Mary B. Nabity of the Department of Veterinary Pathobiology. The results were published in 2017.

The RNA samples analyzed for Chapter III were isolated by Dr. Wenping Song at Sanofi, and the data analyses were provided, in part, by Dr. Ethan Xu at Sanofi. Part of the RNA samples used for Chapter III were isolated by Dr. Jessica Hokamp of the Department of Veterinary Pathobiology and Mia Aguilar of the Doctor of Veterinary Medicine program. The project was co-designed by Dr. Shiguang Liu at Sanofi. Professor

Mary B. Nabity of the Department of Veterinary Pathobiology supervised the whole project.

The histopathology results for Chapter V were evaluated by Dr. Rachel E. Cianciolo of the Department of Veterinary Biosciences at The Ohio State University. Dr. Mary B. Nabity of the Department of Veterinary Pathobiology supervised the whole project.

All other work conducted for the dissertation was completed by the student independently.

My graduate study was supported by the Government Scholarship to Study Abroad from the Ministry of Education in Taiwan. This work was made possible in part by the National Institutes of Health under Grant Number DK57676 and DK64273, the American Kennel Club Canine Health Foundation Grant No. 02066 and 02152, the Texas A&M Genomics Seed Grant Program, the CVM Graduate Student Core Facility Experiential Learning Program at Texas A&M University, and the Callie Cook Endowment for Kidney Disease Research.

NOMENCLATURE

A385	Absorbance at 385 nm
A414	Absorbance at 414 nm
AKI	Acute kidney injury
ALT	Alanine aminotransferase
AMYL	Amyloidosis
AS	Alport syndrome
BGN	Biglycan
BUN	Blood urea nitrogen
CD248/ TEM1	Endosialin or tumor endothelial marker 1
CKD	Chronic kidney disease
COL4A5	Type IV collagen alpha 5
Cq	Quantification cycles
ddPCR	Droplet digital polymerase chain reaction
DE miR	Differentially expressed microRNA
DEG	Differentially expressed gene
DN	Diabetic nephropathy
ECFC	Endothelial colony-forming cells
eGFR	Estimated glomerular filtration rate
ENCODE	ENCyclopedia of DNA Elements

ERCC	Extracellular RNA communication consortium
FN1	Fibronectin-1
FSGS	Focal segmental glomerulosclerosis
GBM	Glomerular basement membrane
GEO	Gene expression omnibus
GFR	Glomerular filtration rate
GN	Glomerulonephritis
GO	Gene ontology
GS	Glomerulosclerosis
HDL	High-density lipoproteins
HGB	Hemoglobin
HS	Hemolysis score
ICGN	Immune complex-mediated glomerulonephritis
IgAN	IgA nephropathy
IHC	Immunohistochemistry
IPA	Ingenuity pathway analysis
ISEV	International society for extracellular vesicles
ITGA2	Integrin subunit α 2
IVRPS	International veterinary renal pathology service
KCP	Kielin/chordin-like protein
LN	Lupus nephritis
LOX	Lysyl oxidase

LOXL2	Lysyl oxidase homologue 2
MIQE	Minimum information for publication of quantitative real-time PCR experiments
MiR	MicroRNA
MiRNA	MicroRNA
MMP	Matrix metalloproteinase
MT1-MMP	Membrane type 1- matrix metalloproteinase
NCBI	National center for biotechnology information
NF	Normalization factor
NPM1	Nucleophosmin 1
NRQ	Normalized relative quantities
NRT	No reverse transcriptase
NTC	No template controls
OAT3/ SLC22A8	Organic anion transporter 3
PC1	Principal components 1
PC2	Principal components 2
PCA	Principal component analysis
Pre-miRNA	Precursor miRNA
Pri-miRNA	Primary miRNA
PRLR	Prolactin receptor
qRT-PCR	Quantitative reverse transcription polymerase chain reaction
RBC	Red blood cell

RDML	Real-time polymerase chain reaction data markup language
RIN	RNA integrity number
RISC	RNA-induced silencing complex
RNA-seq	RNA sequencing
ROS	Reactive oxygen species
RQ	Relative quantities
RQN	RNA quality number
RT	Reverse transcription
SCD5	Stearoyl-CoA desaturase 5
sCr	Serum creatinine
SDMA	Symmetric dimethylarginine
SI	Sucrase-isomaltase
SOD2	Superoxide dismutase 2
SRA	Sequence read archive
TCF7L2	Transcription factor 7-like-2
TGF-β1	Transforming growth factor beta 1
TI	Tubulointerstitial
TK1	Thymidine kinase 1
UPC	Urine protein to urine creatinine ratio
WBC	White blood cell
XLAS	X-linked Alport syndrome
XLHN	X-linked hereditary nephropathy

TABLE OF CONTENTS

LIST OF FIGURES

LIST OF TABLES

CHAPTER I

INTRODUCTION

Canine chronic kidney disease

Chronic kidney disease (CKD) is defined as the presence of structural or functional abnormalities of one or both kidneys that have been present for an extended period, usually 3 months or longer.[1] CKD is a significant cause of morbidity and mortality in dogs, as the median survival time from diagnosis in dogs is less than one year.[2] While early treatment of CKD has been shown to slow disease progression[3-6], early stage CKD has no obvious clinical signs and many non-invasive diagnostic tests are poorly sensitive and not specific to the etiology, causing CKD to remain unrecognized until late in the disease process in many patients.

The gold standard method for assessing kidney function is the estimated glomerular filtration rate [7] using clearance techniques.[7,8] However, due the high technical demand and expense of these clearance techniques, serum creatinine (sCr) concentration is most often used as an estimate of glomerular filtration rate [7] for the diagnosis of CKD. Creatinine is thought to increase only after the loss of approximately 75% of the functional nephron mass[9], and it is affected by other non-renal factors such as muscle mass, body weight, age, and breed[10], often resulting in failure of early diagnosis. Recently, symmetric dimethylarginine (SDMA) has received growing attention as it is can detect CKD earlier than creatinine in dogs and cats.[11,12] While SDMA is not affected by lean body mass in

dogs[13], its concentration is significantly influenced by time on food[13] and breed.[14] Proteinuria can allow for early detection of CKD in dogs with glomerular diseases and is, in fact, often the first abnormal finding in such patients. However, none of the above diagnostic methods is specific for the etiology of CKD.

The majority (>80%) of proteinuric dogs with CKD have glomerular diseases such as immune-complex glomerulonephritis, glomerulosclerosis, or amyloidosis.[15] Renal biopsy is necessary to identify specific causes. Knowing the cause of the glomerular disease is important as it can affect treatment strategy. For example, evidence of an active immune-mediated pathogenesis would benefit from immunosuppressive therapy; however, such therapy could contribute to more rapid progression for dogs with amyloidosis.[16,17] Therefore, the development of a highly sensitive, non-invasive, and etiology-specific biomarker would be beneficial for dogs with CKD that have contradictions for renal biopsy.

Canine X-linked hereditary nephropathy

To characterize gene and microRNA expression in dogs with CKD, colony dogs with X-linked hereditary nephropathy (XLHN) housed at Texas A&M University[18] were used as a canine model for CKD in this report. Canine XLHN is caused by a naturally-occurring, 10-base deletion in the gene located on the X chromosome encoding the type IV collagen α5 chain (*COL4A5*).[19] The inability to synthesize complete α5 chains impedes the formation of the α3.α4.α5 heterotrimer of type IV collagen in the glomerular basement membrane, leading to juvenile-onset CKD that progresses to end-stage renal disease in affected males (hemizygous), and the development of proteinuria in carrier female dogs

(heterozygous).[18,20] These dogs serve as a suitable large animal model for X-linked Alport Syndrome (XLAS) in human patients because they both exhibit similar clinical manifestations[21] and shared the mutation of the same X-linked *COL4A5* gene in 80% of XLAS cases.[22]

Studies done in dogs with XLHN have characterized the protein and gene expression during CKD progression to some extent. Early studies of protein expression in end-stage dogs with XLHN mainly focused on matrix metalloproteinases (MMPs): MMP-2, MMP-3, MMP-7, MMP-9, and membrane type 1-MMP (MT1-MMP or MMP-14).[23,24] Elevated expression of MMP-2, MMP-9, and MT1-MMP was found in the fibrotic renal cortex of affected dogs[23], likely activated by MMP-3 and MMP-7 as indicated by their increased protein and mRNA expression in kidney tissue.[24] To expand the scope of gene characterization, microarray was used to characterize more genes in the end-stage kidney tissue of the affected dogs.[21] Overall, 133 genes showed significant changes in affected dogs compared to age-match littermates, including upregulated genes (*WFDC2*, *CLU*, *SPP-1*, *COL1A1*, and *TIMP-1*) and downregulated genes (*EGF* and *APOA2*).[21] These findings have contributed to the understanding of the pathogenesis of CKD[25-27] and could contribute to the development of a therapeutic for XLAS in humans.[28]

While these studies on gene expression at end-stage disease have enhanced our understanding of CKD, changes in gene expression before extensive kidney damage would provide even more insight into CKD progression. A recent study in dogs with XLHN examined the morphological changes as well as selective gene expression in kidney tissues of affected dogs at 4, 6, and 9 months of age.[29] Overall upregulation of

CDH2 (or *NCAD*), *CLU*, *TGFB1*, *CTGF*, *PDGFD*, *MMP-2*, *MMP-9*, *TIMP-1* and downregulation of EGFR was seen, including genes upregulated as early as 4 months of age (*TGFB1* and *CTGF*) and at later timepoints (*CLU*, *TIMP-1*).[29] This age-based staging approach provided novel findings as compared to previous studies that solely focused on dogs with end-stage CKD.[21,23,24] In this report, we compared the gene expression in dogs with XLHN at different clinical stages of CKD, hoping to mitigate the difference seen in progression rate of affected dogs in the traditional age-based approach.[29] Also, we expanded the scope of the study by incorporating next-generation sequencing. RNA sequencing[30] is a non-species-dependent, high-throughput method that has high flexibility in the identification of gene expression.[31] In theory, every gene present in a sample has the potential to be identified through RNA sequencing.[30] Results of RNA-seq have been shown to be accurate and strongly correlate with the gold-standard method of PCR[32-36], even at the fold change level.[37] Using RNA-seq, we aimed to fully characterize the gene expression in dogs with XLHN and gain new insights into the disease progression of CKD.

MicroRNA

MicroRNAs (miRNAs or miRs) are short non-coding RNAs (21–25 nucleotides long) that bind to the 3' untranslated region[38] of messenger RNA to post-transcriptionally regulate gene expression.[39-41] The biogenesis of mammalian miRNAs starts from several kilobase-long primary miRNAs (pri-miRNAs) that are transcribed either from independent transcription units or from a part of the intron (or exon) in genes.[42,43] Pri-miRNAs are further cleaved by microprocessors (Drosha and DGCR8)[44] into approximately 70 nucleotide-long stem-loop precursor miRNAs (pre-miRNA) in the

nucleus. Pre-miRNAs are then exported to the cytoplasm by the nuclear Exportin-5 protein.[45] In the cytoplasm, the endonuclease Dicer cleaves out the stem-loop structure, leaving an approximately 22 nucleotide-long double-stranded miRNA duplex.[46] One strand is loaded onto the Argonaute proteins, forming the RNA-induced silencing complex (RISC). This strand is referred as the mature miRNA (the "guide" strand). The other, often degraded strand is called the "passenger" strand.[47] A single mature miRNA can bind to multiple mRNAs, and one mRNA can be regulated by multiple miRNAs. Such an extremely complex miRNA-mRNA interaction influences a wide range of physiological changes and pathological processes.[40]

To date, 48,885 mature miRNA sequences have been identified in 271 species (miRbase v22 released on March 12, 2018). Information about these miRNAs is stored in a miRNA repository database, miRBase (www.mirbase.org/).[48] In humans, 2693 mature miRNA sequences have been identified[48], representing approximately 1% of the human gene repertoire. However, these miRNAs are estimated to regulate more than 60% of all protein-coding genes.[49] With the maturation of next generation sequencing technologies, researchers are now interested in comprehensive miRNA profiling and novel miRNA discovery in other species. Thus far, 1045 mature miRNAs have been documented in the cattle genome. Of these 19.8% have sequences identical to those of human miRNAs. Respective numbers in other species are horse (720; 36.4%), dog (504; 36.7%), goat (436; 34.2%), pig (461; 36.5%), and sheep (153; 28.1%). Interestingly, feline miRNAs have not yet been described in the miRBase.[48] Since miRNAs are highly conserved across

species[50,51], miRNA profiling in a less characterized species is made possible by using references in other species.[52]

miRNAs are present in cells and in cell-free biological fluids (biofluids), such as cerebrospinal fluid, vitreous humor, saliva, serum, plasma, urine, and semen.[53] Binding to Argonaute proteins provides protection against endogenous RNase degradation.[54] High-density lipoproteins (HDL)[55] and nucleophosmin 1 (NPM1)[56] have also been observed to bind to miRNAs. However, HDL binds to only a small proportion of circulating miRNAs[57], and binding of miRNA with NPM1 has not been identified *in vivo*.[58]

miRNA can also be enclosed in extracellular vesicles[59-61] called exosomes.[62] Exosomes are 40-100 nm structures that originate from multivesicular bodies. They have received considerable attention because they are more consistent in size than other vesicles. Furthermore, exosomes contain a significant proportion of small RNAs (20-200 nt) and small amounts of proteins, mRNAs, and ribosomal RNA.[61,63-65] Even though all body fluids contain miRNAs, the proportion present in exosomes varies.[66,67] This review will focus on circulating total RNA and urinary exosomal RNA for 2 reasons. First, although some contradictory evidence has been proposed[68], most circulating miRNAs are thought to be associated with proteins rather than exosomes.[54,56,58,69,70] Second, urinary miRNAs are enriched and more stable in urine-derived exosomes than in cell-free urine.[63,71]

MicroRNA as biomarkers

In biofluids, miRNAs are association with proteins and exosomes.[72] Intriguingly, miRNA content in biofluids was found to be distinct from the miRNA content in cells

from which the miRNA originated, supporting that miRNAs might be selectively secreted into biofluids.[61,73-75] Alternatively, this distinct miRNA content might be a result of sequence-dependent decay, isolation bias, and the affinity of miRNA to the outer-layer of multivesicular vesicles.[58,76-79] The exact mechanism for selection of miRNAs for exportation and the regulation of the sorting and exportation remain elusive.[80] As of now, 3 routes have been proposed in the literature: cell lysis and apoptosis (non-selective), exosome secretion (random selection or selective protein sorting), and cellular export of protein-binding RNAs.[54-58,63]

Studies of tissue miRNA during development[81,82] and in diseases[83,84] are well-documented. In these cases, miRNAs from tissue samples might serve as early biomarkers for various diseases before histopathologic changes occur.[85] However, tissue collection might not be possible for certain organs or in every patient. Thus, tissue-based miRNA evaluation is not a practical option for routine diagnosis and monitoring of diseases. To overcome this challenge, there has been a shift toward "liquid biopsy," a minimally invasive technique that obtains cells or nucleic acids from biofluids. Therefore, investigations into obtaining biofluid miRNAs and linking pathological changes with levels of miRNA expression are increasing in popularity. For example, liver necrosis was found to result in miR-122 and miR-192 release into the bloodstream. When both miRNAs were used to monitor acetaminophen toxicity in a mouse model, miR-122 and miR-192 were more sensitive than alanine aminotransferase (ALT) for detecting hepatocellular necrosis.[86] Similarly, urine exosomal miRNAs have diagnostic potential for urinary-system diseases, including kidney diseases[87-90] and urological tumors.[91-94] Some evidence

exists that miRNAs can be transferred from cell to cell via exosomes in a paracrine or autocrine fashion[58,61,95,96] and that exosomal miRNAs serve as functional components in cell-to-cell communication, cell growth promotion, and cancer cell invasion.[92,97-99] A list of miRNAs with identified origin and recipient cells that utilize exosomal transportation can be found in another review.[72]

In domestic animals, many studies have shown the correlation between differentially expressed circulating and urinary exosomal miRNAs with diabetes mellitus[52], kidney function and histopathological changes[100], hepatocellular injury and hepatobiliary diseases[101,102], cardiovascular diseases[103-105], infectious diseases[106-111], lymphoma[112], neuromuscular diseases[113-115], estrous cycle and pregnancy[116-119], and toxin exposure[120,121] (Table 1). The following sections will discuss preanalytical considerations and isolation methods that were addressed in these studies.

Table 1. Summary of circulating and urinary miRNA studies in domestic animals (2011-present).

Topic (sample size)	Sample type	Sample vol.	Isolation method(s)	RNA quantity and measurement method	Profiling method(s)	Library prep.	Seq. platform	Seq. results	qRT-PCR internal control or normalization	Ref.
Bovine										
Foot-and-mouth disease virus infection (n=2)	Serum	N/A	QIAamp Circulating Nucleic Acid Kit (Qiagen)	N/A	PCR array, qRT-PCR	N/A	N/A	N/A	bat-miR-127	[122]
Bovine viral diarrhea virus infection (n=9)	Serum	N/A	miRNeasy serum/plasma kit (Qiagen)	N/A	Small RNA-seq	NEBNext Multiplex Small RNA Library Prep Set for Illumina	Illumina HiSeq 2500	Total reads: 197M Mapped reads: 0.9M	N/A	[123]
Pregnancy (n=15)	Serum	500 μL	Plasma/Serum Circulating and Exosomal RNA Purification Mini Kit (Norgen)	N/A	qRT-PCR	N/A	N/A	N/A	miR-25- 3p	[124]
Foot-and-mouth disease virus infection (n=12)	Serum	200 μL	miRNeasy serum/plasma kit (Qiagen)	N/A	PCR array, qRT-PCR	N/A	N/A	N/A	Cel-miR-39 (Spike-in), snoRNA, and snRNA	[107]
Early pregnancy (n=22)	Plasma	700 μL	TRIzol LS (ThermoFisher Scientific)+glycogen	N/A	Small RNA-seq, qRT-PCR	TruSeq Small RNA Preparation Kit	Illumina HiSeq 2000 system (36SE)	Total reads: 16.1M/sample Mapped reads: 8.0M MiRNA reads: 5M	Cel-miR-39 (Spike-in), miR-128	[125]
Metritis (n=8)	Serum	150 μL	miRNeasy serum/plasma kit (Qiagen)	N/A	qPCR array	N/A	N/A	N/A	Cel-miR-39 (Spike-in), SNORD42B, SNORD69, SNORD61, SNORD68, SNORD96A, RNU6-2, miRTC, and PPC	[126]

Table 1. Continued.

Topic (sample size)	Sample type	Sample vol.	Isolation method(s)	RNA quantity and measurement method	Profiling method(s)	Library prep.	Seq. platform	Seq. results	qRT-PCR internal control or normalization	Ref.
Estrous Cycle variation (n=8)	Plasma	1.05 mL	TRIzol LS(ThermoFisher Scientific)+glycogen	N/A	Small RNA-seq, qPCR array, qRT-PCR	TruSeq Small RNA Preparation Kit	Illumina HiSeq 2000 system (36SE)	Total reads: 9.1M/sample Mapped reads: 4.3M miRNA% out of mapped reads: 70% no. of miRNA: 313	Cel-miR-39 (Spike-in)	[116]
Early pregnancy (n=24)	Plasma	1.05 mL	TRIzol LS(ThermoFisher Scientific)+glycogen	N/A	Small RNA-seq, qPCR array, qRT-PCR	TruSeq Small RNA Preparation Kit	Illumina HiSeq 2000 system (36SE)	Total reads: 9.2M/sample Mapped reads: 4.0M MiRNA reads: 2.8M	Cel-miR-39 (Spike-in)	[117]
Healthy (n=4)	Serum	200 μL	Total RNA Purification Kit (Norgen)	9.25ng (QB mIRNA)	Small RNA-seq, qRT-PCR	TruSeq Small RNA Preparation Kit (input: 5 μL of total RNA)	Illumina HiSeq 2000 system (50SE)	Total reads: 29,692,695 MiRNA% out of mapped reads: 6.9% miRNA	U6, miR-127, miR-744, miR-93	[127]
M. bovis infection (n=16)	Serum	200 μL	miRNeasy serum/plasma kit (Qiagen)		Small RNA-seq	NEBNext Multiplex Small RNA Library Prep Set for Illumina	Illumina Hi-Seq	miRNA reads: 1.3M	N/A	[108]
M. paratuberculosis infection (n=20)	Serum	1 mL	miRNeasy Mini Kit (Qiagen)	708-2640 pg/μL (BA small RNA)	Small RNA-seq	TruSeq Small RNA Preparation Kit	Illumina HiSeq 2500 Rapid (50SE)	Total reads: 311,475,358 MiRNA% out of mapped reads: 2.7%	N/A	[109]

Table 1. Continued.

Topic (sample size)	Sample type	Sample vol.	Isolation method(s)	RNA quantity and measurement method	Profiling method(s)	Library prep.	Seq. platform	Seq. results	qRT-PCR internal control or normalization	Ref.
M. paratuberculosis infection (n=12)	Serum	1 mL	miRNeasy Mini Kit (Qiagen)	N/A	Small RNA-seq	TruSeq Small RNA Preparation Kit	Illumina HiSeq 2500 Rapid (50SE)	Total reads: 325,249,513 miRNA% out of total reads: 4.3%	N/A	[110]
Reference gene study (n=49)	Serum	Unknown	miRNA purification kit (Genolution)	N/A	qRT-PCR (input: 100ng of RNA)	N/A	N/A	N/A	geNorm, NormFinder, and BestKeeper	[128]
Controlled ovarian hyperstimulation (n=10)	Plasma	200μL	miRNeasy kit (Qiagen)	N/A	E panel	N/A	N/A	N/A	global normalization method	[129]
Healthy (n=9)	Plasma	9 mL	miRNeasy Serum/Plasma Kit (Qiagen)	36.3-210.4 ng (QB total RNA)	Small RNA-seq	NEBNext Multiplex Small RNA Library Prep Set	Illumina HiSeq 2000	Total reads: 10,465,348 miRNA% out of total reads: 5%	N/A	[118]
Canine										
Kidney disease carrier (pooled sample from n=7)	Serum	2 mL	Modified Direct-zol RNA MiniPrep (Zymo Research)	0.918 ng/μL (Fragment analyzer)	Small RNA-seq	NEXTflex Small RNA Library Prep Kit	Illumina HiSeq 2500R to obtain at least 10 million 50bp single end reads per sample	Total reads: 9,700,565 Mapped%: 95.65% miRNA% out of mapped reads: 11.47% miRNA reads: 1,344,094	N/A	Chu, unpublished data
Transitional cell carcinoma (n=70)	Whole blood and urine cell pellets	2.5 mL and 5 mL	PAXgene blood miRNA kit (PreAnalytiX) and miRNeasy (Qiagen)	N/A	qRT-PCR	N/A	N/A	N/A	Cel-miR-39 (Spike-in) and RNU6	[130]

Table 1. Continued.

Topic (sample size)	Sample type	Sample vol.	Isolation method(s)	RNA quantity and measurement method	Profiling method(s)	Library prep.	Seq. platform	Seq. results	qRT-PCR internal control or normalization	Ref.
Myxomatous mitral valve disease (n=27)	Plasma	400 μL	TRIzol LS(ThermoFisher Scientific) and miRNeasy (Qiagen)	N/A	qRT-PCR	N/A	N/A	N/A	Geometric mean	[131]
Pancreatic injury (n=4)	Serum	50 μL	TaqMan miRNA ABC purification kit – human panel A	N/A	Digital droplet PCR (ddPCR)				Ath-miR-159a (Spike-in)	[132]
Kidney diseases (n=84)	Urine (exosome)	1 mL or 5 mL	Urine Exosome RNA Isolation Kit (Norgen)	N/A	Small RNA-seq, qRT-PCR	TruSeq Small RNA Preparation Kit	Illumina HiSeq2000	miRNA out of mapped reads: 0.12-0.42%	N/A	[100]
Hepatic biliary diseases (n=57)	Serum	100 μL	miRNeasy serum/plasma kit (Qiagen)	N/A	qRT-PCR	N/A	N/A	N/A	Cel-miR-39 (Spike-in)	[101]
Hepatocellular injury (n=66)	Serum	100 μL	miRNeasy serum/plasma kit (Qiagen)	N/A	qRT-PCR	N/A	N/A	N/A	Cel-miR-39 (Spike-in)	[102]
Meningoencephalomyelitis of unknown origin(n=13)	Serum	200 μL	miRNeasy Micro kit (Qiagen)	N/A	qRT-PCR	N/A	N/A	N/A	Cel-miR-39 (Spike-in) and mean expression value	[133]
Pancreatic toxicity (n=6)	Serum	100 μL	miRNeasy (Qiagen)	N/A	qRT-PCR	N/A	N/A	N/A	Synthetic miR-55-3p (Spike-in)	[134]
Myxomatous mitral valve disease (n=18)	Serum	200 μL	miRNeasy serum/plasma kit (Qiagen)	N/A	qRT-PCR	N/A	N/A	N/A	Mean expression value	[103]

Table 1. Continued.

Topic (sample size)	Sample type	Sample vol.	Isolation method(s)	RNA quantity and measurement method	Profiling method(s)	Library prep.	Seq. platform	Seq. results	qRT-PCR internal control or normalization	Ref.
Lymphoma (n=6)	Serum	200 μL	miRNeasy Mini kit (Qiagen)	N/A	qRT-PCR	N/A	N/A	N/A	MiR-26b, RNU6-2, SNORD61-1, miR-16-2, SNORD95-1, SNORD96A-1	[112]
Muscular dystrophy (n=5)	Serum	300 μL	miRNeasy (Qiagen)	N/A	Small RNA-seq, qRT-PCR	See original paper	Illumina HiSeq 36b	MiRNA reads: 0.8-1.2M	MiR-16	[114]
Chronic degenerative valvular disease (n=24)	Plasma	N/A	MiRCURY RNA isolation kit – biofluids (Qiagen)	N/A	qRT-PCR	N/A	N/A	N/A	miR-16-5p	[135]
D. immitis infection (n=4)	Plasma	7.5-10 mL	Plasma/Serum Circulating RNA Purification Maxi Kit (Norgen)	112-554ng (ND total RNA)	Small RNA-seq, qRT-PCR	TruSeq Small RNA Preparation Kit	Illumina GAIIx	Total reads: 15,378,851	miR-223	[106]
Dilated cardiomyopathy (n=8)	Serum	400 μL	miRNeasy Mini kit (Qiagen)	158-262ng (ND total RNA)	Microarray (customized miRNA array based on dog and mouse miRNA)	N/A	N/A	N/A	RNUA1_1, RNU6B_2	[105]
Muscular dystrophy (n=10)	Serum	50 μL	mirVana (Ambion)	N/A	qRT-PCR	N/A	N/A	N/A	Cel-miR-39 (Spike-in), miR-16	[113]
Equine										
Endurance exercise (n=4)	Plasma	500 μL	MiRUCY RNA isolation kit – biofluids (Exiqon)	N/1	Small RNA-seq	NEBNext Multiplex Small RNA Library Prep Set for Illu-mina	Small RNA-seq, qRT-PCR	MiRNA reads: 1-15M	N/A	[136]

Table 1. Continued.

Topic (sample size)	Sample type	Sample vol.	Isolation method(s)	RNA quantity and measurement method	Profiling method(s)	Library prep.	Seq. platform	Seq. results	qRT-PCR internal control or normalization	Ref.
Insulin resistance (n=6)	Serum	N/A	TRIzol BD (Molecular Research Center)	N/A	qRT-PCR	N/A	N/A	N/A	Geometric mean	[137]
Hendra virus infection (n=6)	Whole blood	N/A	miRNeasy Mini Kit (Qiagen)	N/A	Small RNA-seq, qRT-PCR	TruSeq Small RNA Preparation Kit	Illumina HiSeq 2000	MiRNA reads: 6-10M	miR-103	[138]
Endurance exercise (n=14)	Whole blood	N/A	PAXgene Blood RNA kit (Qiagen)	N/A (ND and BA total RNA)	Microarray (custom Equine miRNA array), qRT-PCR	N/A	N/A	N/A	hsa-miR-191	[139]
Healthy (n=141)	Plasma and Serum	2 mL	miRNeasy Serum/Plasma Kit (Qiagen)	40-8760pg/µL (BA small RNA)	Small RNA-seq	unknown	Illumina HiSeq	Total reads: 7.1-16.5M	N/A	[140]
Healthy (n=35)	Serum	2 mL	Modified miRNeasy serum/plasma kit	2-428 ng/µl, (QB total RNA) 69-89% miRNA (BA small RNA)	Small RNA-seq	NEBNext Multiplex Small RNA Library Prep Set	Illumina HiSeq 2500 with 50 sequencing cycles. total of 12 M reads on average	miRNA% out of total reads: 2.3 to 62.9% (18.8% on average)	N/A	[141]
Reference gene study (n=3)	Plasma	unknown	TRIzol (ThermoFisher Scientific)	N/A	Small RNA-seq	TruSeq Small RNA Preparation Kit	Illumina HiSeq2000	Total reads: 21.8-25.6M Total processed reads: 21.7-25.4 MiRNA reads and % out of processed reads: 10.3-15.8M, 45.3-72.7%	N/A	[142]

Table 1. Continued.

Topic (sample size)	Sample type	Sample vol.	Isolation method(s)	RNA quantity and measurement method	Profiling method(s)	Library prep.	Seq. platform	Seq. results	qRT-PCR internal control or normalization	Ref.
Feline										
Diabetes mellitus (n=18)	Serum	400 μL	miRNeasy Mini kit (Qiagen)	138-432ng (ND total RNA)	Microarray (custom miRNA array based on mouse miRNA), qRT-PCR	N/A	N/A	N/A	RNUA1_1, RNU6B_2	[52]
Ovine										
Prion disease (n=21)	Plasma	200 μL	Norgen Total RNA Purification kit (Norgen Biotek)	N/A	qRT-PCR	N/A	N/A	N/A	Cel-miR-39 (Spike-in)	[119]
Fetal Alcohol Exposure (n=10)	Plasma	unknown	MagMAX Viral RNA Isolation kit (Ambion)	N/A	E panel	N/A	N/A	N/A	Mean expression value	[120]
Seasonal variation (n=5)	Urine (cell-free total RNA)	500 μL	mirVana kit (Invitrogen)	N/A	Small RNA-seq	SOLiDTM Total RNA-Seq Kit	SOLIDTM sequencer (Applied Biosystems, CA)	miRNA reads: 4,926 per sample	N/A	[143]
Porcine										
Thoracic Spinal Cord Injury (n=16)	Serum	1 mL	modified mirVana PARIS kit (ThermoFisher)	N/A	Small RNA-seq	TruSeq Small RNA Preparation Kit	Illumina MiSeq or HiSeq 2500	no. of miRNA detected: 314	N/A	[115]
Trichuris suis Infection (n=12)	Serum	unknown	miRNeasy serum/plasma kit (Qiagen)	N/A	qRT-PCR	N/A	N/A	N/A	miR-423-5p, miR-19b, let-7c, miR-21, let-7a, miR-23a	[111]
Acetaminophen-Induced Acute Liver Failure (n=9)	Plasma	unknown	miRNeasy Mini kit (Qiagen)	N/A	qRT-PCR	N/A	N/A	N/A	miR-26a	[121]

Table 1. Continued.

Topic (sample size)	Sample type	Sample vol.	Isolation method(s)	RNA quantity and measurement method	Profiling method(s)	Library prep.	Seq. platform	Seq. results	qRT-PCR internal control or normalization	Ref.
Cardiogenic shock (n=12)	Plasma	unknown	TRIzol LS(ThermoFisher Scientific)+miRNeasy mini kit (Qiagen)	N/A	qRT-PCR	N/A	N/A	N/A	miR-16	[144]
ST elevation myocardial infraction model (n=6)	Serum	unknown	TRIzol LS (ThermoFisher Scientific)+miRNeasy mini kit (Qiagen)	N/A	qRT-PCR	N/A	N/A	N/A	Normalized against baseline values and the maximum value in each pig	[104]

Abbreviations: A, Affymetrix Microarray; BA small RNA: Bioanalyzer Small RNA kit(Agilent); E, miRCURY LNA Universal RT microRNA PCR (Qiagen); EP, miRCURY microRNA QC PCR Panel (Qiagen); N/A, not mentioned in the paper; ND, NanoDrop (Thermo Fisher Scientific); Q, miScript miRNA Assays (Qiagen); QB miRNA, Qubit microRNA assay kit (Thermo Fisher Scientific); QB total RNA, Qubit RNA/RNA High Sensitivity assay kit (Thermo Fisher Scientific);T, TaqMan miRNA Assays (Life Technologies); TLDA, TaqMan low-density arrays; U, unspecified qRT-PCR.

Preanalytical considerations

The study of extracellular miRNAs faces many challenges well before RNA isolation. Common preanalytical factors that might introduce variability in conventional veterinary clinical pathology testing should be considered for miRNA studies as well.[145] Whenever possible, researchers should use consistent sample types, collection tubes, collection methods, animal conditions (diurnal duration, nutritional status, fasting or non-fasting, hydration status, stress, exercise etc.), sample processing, and storage to minimize preanalytical variability.

Serum versus plasma

Serum and plasma are common sources of circulating miRNAs. The biggest difference between serum and plasma is the presence of coagulation proteins, particularly fibrinogen, in plasma. In some studies, the miRNA expression in serum and plasma was highly correlated[146,147] while in other studies, differences were observed.[59,70,148,149] In one of the studies demonstrating high correlation based on sequencing results, differences can be seen depending on the RNA isolation method used.[147] The comparison of 2 qRT-PCR platforms also revealed high correlations between serum and plasma.[148] However, one study found a higher overall miRNA concentration in serum than plasma and speculated it was caused by miRNAs released from WBCs, RBCs, or platelets during coagulation.[59] In another study comparing paired heparinase-treated heparin plasma and serum concluded that no significant correlation was found in miRNA expression levels of serum and plasma.[150] Possible explanations other than heparinase digestion include degradation

of serum components because of the delay in time for clot formation[145], or trapping of exosomes in the clot.[150] Taken together, these studies support that various factors might explain differences in miRNA profiling between serum and plasma. Beyond consistency within a particular study, there is currently no preference for using one over the other.[149]

EDTA, heparin, and citrate plasma

In veterinary medicine, sodium or potassium-EDTA plasma is commonly used in hematology, heparin plasma is commonly used in biochemistry[145], and citrated plasma is used for coagulation testing. In RNA studies, heparin and citrated plasma are not recommended for follow-up analysis because both anticoagulants interfere with PCR[151-153] and consequently, hamper nearly all profiling methods, including qRT-PCR, microarray, and small RNA-seq. For example, one study using qRT-PCR reported overall lower concentrations of miRNA for samples collected in citrate tubes than in serum.[154] Although corrective methods using heparinase and lithium chloride have been proposed to reduce the heparin concentration in heparinized plasma, administration of heparin in patients (*in vivo*) and addition of heparin to EDTA-plasma (*in vitro*) will selectively change the expression spectrum of endogenous miRNAs as well as exogenous miRNAs that were introduced during isolation.[155] As this procedure induces variation and increases expense, EDTA-plasma is preferred over heparinized plasma.[72,156]

Biological variation

Various biological factors affect hematology and biochemistry results in veterinary clinical pathology, such as species, breed, sex, nutritional status and diet, stress,

medications, biological rhythms, exercise, and environmental conditions.[145] Several of these preanalytical factors also affect miRNA expression.[124,129,141,143] This is not surprising given the ubiquity of miRNAs in biofluids and their broad regulation. For example, Pacholewska et al[141] described 50 differentially expressed serum miRNAs (7.05- to 6.4-fold) between ponies and Warmblood horses. Seasonal variations led to a dramatic (up to 27-fold) change in expression levels of 40 urinary miRNAs in goats.[143] Hormonal changes also caused a slight increase (up to 2.2-fold) in 4 miRNAs in cattle.[116] In early pregnancy, cattle showed 1.7- to 3.1-fold upregulation of miR-26a.[117,125] In humans, women in the third trimester of pregnancy showed a more than 600-fold increase in expression levels of miR-526a and miR-527.[157] Nutritional status and dietary factors might change the level of carrier proteins and lipid components and indirectly affect the species and proportions of miRNAs or miRNome in blood and urine.[55] Alternatively, increased lipid content in biofluids (ie, lipemia) could introduce variation in miRNA isolation.[158] Several studies have shown dietary factors to impact circulating miRNAs.[159-161] Stress, exercise, and hydration status might also affect miRNA expression in an exercise- and miRNA-specific manner, with some miRs increasing or decreasing nearly 20-fold after exercise in human subjects.[149,162-165] In horses, one study showed endurance exercise minimally (1.25- to 2-fold) changed whole blood miRNA expression[139] while another study showed up to a 7-fold increase in certain plasma miRNAs.[136] Recently, studies have investigated the interplay between miRNAs and circadian rhythms.[166-169] However, one study comparing paired plasma from human subjects in the morning and afternoon did not identify differentially expressed miRNAs (DE miRs).[170] For consistency, in human medicine,

morning urine samples are commonly used for investigation of urinary exosomes.[71,88,171,172]

Overall, biological variation may influence the expression of miRNAs, but effects appear to be minimal except during vigorous exercise and reproductive changes (for example, pregnancy and estrus). Ideally, sample selection and collection time should be as consistent as possible.[173] However, a more stringent cutoff value in differential expression (at least 2-fold or 3-fold change) could serve as an alternative method to facilitate biomarker discovery in diverse populations.

Biofluid sample collection and processing

In veterinary medicine, common methods for collecting urine include cystocentesis, catheterization, and voided/free catch. Cystocentesis is the preferred method to reduce the prokaryotic transcriptome from contaminating bacteria.[171] A full urinalysis (physical appearance, chemical analysis, and sediment evaluation) should be performed at the time of urine collection to exclude urine samples with active urine sediments. This is because exosomes might be released from RBCs and WBCs and adversely affect the interpretation of results.

There is no consensus for standard processing of urine before long-term storage. In studies that involved isolation of urinary exosomes, the majority of them processed the urine first using ultracentrifugation to obtain exosome pellets before storage at -80°C.[88-90,174-177] The remaining studies left urine unprocessed[178,179], or performed minimal centrifugation at 1000-2000 *g* for 1-10 minutes to remove cellular debris.[92,180,181] In rare situations, urine was mixed with guanidinium thiocyanate[182] or filtered through a 0.8 μm

filter[183] for long-term storage. To our knowledge, there have been no comprehensive studies comparing different urine collection and processing methods for exosomal miRNA investigation. Since the time-consuming nature of ultracentrifugation impedes its application in the clinical setting (see "Evaluation of miRNA isolation method" section), we recommend an initial minimal centrifugation to remove cellular debris followed by long-term storage at -80°C. Readers are referred to other resources for general guidelines regarding urine sample collection.[184,185]

Currently there appear to be no published studies evaluating the effects of variables such as needle gauge, free flow, syringe size, and vacuum tube on circulating miRNA profiling for blood collection. Therefore, guidelines for minimizing preanalytical factors should be adopted when designing miRNA profiling studies.[145] Recommendations include using a large enough needle to minimize hemolysis, applying minimal negative pressure while withdrawing blood, and discarding the first few milliliters of blood to avoid tissue and cell contamination from the vascular puncture site.[145,173] For multiple vacuum tubes, a specific collecting order is recommended in human medicine to minimize possible carryover of additives to other tubes.[186] After centrifugation, one should carefully aspirate only the supernatant and avoid any disturbance of the buffy coat or fibrin to minimize contamination from cellular miRNAs. This can be accomplished by aspirating the top three-fourths of the supernatant or leaving at least 5 mm of residual volume above the buffy coat or fibrin layer.[187] Processing time should also be minimized (ie, separating serum or plasma within 2-4 hours of collection).[158,188] This recommendation is based on a study in which significant changes in expression levels of miRNAs was observed

depending on whether the time between blood collection and centrifugation was 2 or 6 hours.[189] For serum-derived miRNA, no study appears to have investigated the difference between tubes (plain versus gel separator) or the effect of the time allowed for coagulation. However, consistency within a given study is recommended to reduce confounding factors. For instance, a standard temperature and time (eg, clot at 25°C for 30 mins) should be used.[158,187] Readers are referred to other resources for general guidelines regarding processing of serum and EDTA plasma samples.[184,185]

Cellular contamination in serum and plasma

In evaluating cell-free circulating miRNAs, it is crucial to minimize cellular miRNA contamination from white blood cells (WBCs), platelets, and red blood cells (RBCs) that might affect the miRNA concentration or expression profile. Hunter et al[59] demonstrated different overall miRNA expressions across human plasma microvesicles, WBCs, and platelets; however, there was an extensive overlap among the top 10 highly expressed miRNAs. Additional studies found substantial overlap between miRNAs from human plasma and those from blood cells, supporting the hypothesis that blood cells are the major contributors to circulating miRNAs.[85,190] This finding also indicates the potential for misleading results if cellular components are not completely removed prior to miRNA isolation. WBC contamination is less worrisome since WBC-free biofluid is achievable by standard centrifugation. However, contamination with platelets and lysed RBCs is of greater concern. Merkerova et al[191] profiled 13 miRNAs in human hematopoietic cells and found miR-223 to be highly expressed in platelets. Another study showed that miR-223, miR-142-3p, and let-7a were more highly expressed in human platelet concentrate than in

plasma.[187] Also, higher expression of miR-15b, miR-16, and miR-24 (up to a difference of 5 quantification cycles (Cq)) have been associated with platelet contamination in human plasma.[70] Additional processing, such as centrifugation at 1940 *g* or 15,000 *g* and filtering through a 0.22 μm filter, decreased the expression level of these miRNAs in human plasma significantly but only minimally influenced the expression in serum (which is naturally platelet-poor).[70,187]

Kirschner et al[192] and MacLellan et al[159] showed an increased overall miRNA expression and number of detectable miRNAs in hemolyzed human plasma or serum. In human RBCs, miR-16 and miR-451 are highly expressed.[191] Therefore, Kirschner et al[192] assessed if these miRs could be candidate reference miRNAs for hemolysis. They found that the expression levels of miR-16 and miR-451 were stable in grossly non-hemolyzed human plasma. In another study, serum miR-15 and miR-16 were substantially increased when hemolysate was added to mimic hemolysis.[70] Other miRNAs that appear to be affected by hemolysis include miR-17, miR-21, miR-92a, miR-106a, miR-210, and miR-486.[193,194] Given the influence of RBC miRNAs released upon hemolysis, it is important to exclude hemolyzed samples before miRNA analysis. Visual hemolysis assessment lacks sensitivity and is subject to interpretation.[195] However, hemoglobin (HGB) concentration can be easily assessed by inspecting the absorbance at 414, and, to a lesser extent, 541 and 576 nm, using spectrophotometry.[196] A prominent peak at 414 nm using spectrophotometry provides objective measurements and correlates with visual assessment of hemolysis as well as the expression of miRNAs that might be altered due to hemolysis.[149] A strong linear correlation has been observed between the absorbance at

414 nm (A414) and the concentration of lysed RBCs. However, A414 is also influenced by the presence of lipemia.[197] Therefore, Appierto et al[197] proposed incorporating the absorbance at 385 nm (A385) to generate a lipemia-independent hemolysis score using the following equation:

Hemolysis score (HS) = A414 - A385 + lipemia correlation factor x A385.[197]

Researchers are then encouraged to use the mean (HS) + 3 x SD (HS) obtained from many non-hemolyzed samples as a cutoff value for sample exclusion.[197] In some cases, only purified RNA may be accessible without corresponding information regarding hemolysis. In these samples, quantification of RBC-enriched miRNAs (eg, miR-16 and miR-451, both of which demonstrated up to an 8-fold increase in samples containing free HGB[192]) has been proposed as an alternative method to determine the degree of hemolysis.[198]

Storage and stability

Blood and urine have high RNase activity; therefore, the stability of miRNA in these fluids relies on miRNA binding with proteins and lipids and enclosure within exosomes.[59-61,199] Veterinary research often relies heavily on archived samples, making the stability of miRNA in long-term storage, short-term storage, and freeze-thaw cycles an important consideration.

For urine, Zhou et al[172] demonstrated that exosomes remained intact in human urine stored for up to 7 months at -80 °C, but a significant loss in exosomes was observed in urine stored at -20 °C. Similarly, another study found that the storage of human urine for 24 hours at -20 °C led to a 40% loss of RNA yield (measured by RiboGreen); the percentage of miRNA was, however, not affected.[200] In another study, up to a 58% and

65% decrease in specific miRNAs (miR-16 and miR-21) was observed in human urine based on qRT-PCR after 5 days of storage at 4°C or room temperature, respectively.[201] In addition to storage temperature and time, vigorous vortexing of human urine after thawing can substantially increase exosome recovery from urine samples as determined by expression of exosome-associated proteins.[172] However, no separation of cells was performed before the procedure, and the perceived increased in exosome recovery may have been due to cell rupture.

For circulating miRNAs, long-term stability at -80°C was demonstrated by the recovery of 177 miRNAs in human plasma stored at -80°C for more than 12 years. The Cq values obtained were not significantly higher than those obtained from freshly frozen plasma from different patients.[189] Over 400 miRNAs can still be detected via qRT-PCR in human serum that has been through long-term storage (40 years) at -25 °C, although library preparation for sequencing failed in certain samples.[202] Short-term storage at higher temperatures was examined by incubating serum and plasma samples at room temperature or 4 °C. In one study, Cq values for miR-122 and miR-145 increased after incubation of serum at 4 °C for up to 24 hours.[203] Another study evaluated the expression of 4 miRNAs (miR-16, miR-24, miR-181a, and miR-451) isolated from human plasma that had been incubated at 4 °C for 2 weeks. The Cq values of all but miR-16 increased.[204] Further, other studies done at room temperature have demonstrated that the expression of 20 miRNAs in human serum[157] and 3 miRNAs (miR-15b, miR-16, and miR-24) in human plasma[146] remain stable after incubating the serum and plasma for up to 4 hours and (up to) 24 hours, respectively. The ability to still detect miRNAs after incubation of serum at room

temperature for 10 days demonstrates marked stability of circulating miRNAs.[205] For freeze-thaw cycles, the expression levels of miR-15b, miR-16, and miR-24 in human plasma remain stable after 8 freeze-thaw cycles.[146] In human serum, let-7a, miR-16, miR-103, and miR-210 remained stable after 10 freeze-thaw cycles[85] whereas the Cq values for miR-24, miR-93, miR-223, and miR-451 were slightly increased (approximately by 2 Cq).[205]

Stability of miRNAs could also be influenced by species differences. Currently, only a few studies have evaluated miRNA stability in domestic animals. Archived equine EDTA blood that was stored at -80 °C for 5 to 11 years did not show significant changes in RNA yield as compared to short-term stored samples from different horses. Some archived samples produced over 7 million reads, but sequencing results were not disclosed.[140] For bovine serum stored at -20 °C for over 10 years, the miRNA fractions did not show significant differences compared to those from different samples stored at -80 °C for less than 1 year, and the identified miRNAs were largely identical.[109] Only 4 miRNAs (let-7a, miR-16, miR-23a, and miR-26a) in canine serum and plasma have been evaluated after short-term storage of the sample at room temperature.[206] In contrast to a previous human study[146], the miRNA expression was stable for 1 hour but not for 24 hours at room temperature.[206]

Overall, miRNAs appear to be relatively stable in urine, serum, and plasma despite prolonged storage, even in suboptimal temperatures and after repeated freeze-thaw cycles. Nevertheless, the inconsistency between studies in determining the expression of specific miRNAs could be related to the stability of the miRNA in question. To prevent drawing

conclusions on a limited number of miRNAs, global profiling using small RNA-seq is beneficial.[109] Furthermore, to minimize the interference of preanalytical factors, readers are advised to use samples that are less than one year old and stored at -80 °C for miRNA studies.

Standardized reporting of preanalytical factors

Because of the impact that preanalytical factors can have on analytical results, researchers should strive for standardization of these factors to facilitate comparison of miRNA profiling results across laboratories.[207] Below is a summary of these various factors:

1. Animal conditions: breed, sex, age, neuter status, and fasting/non-fasting.
2. Sample collection: sample type, collection site, collection time, needle gauge, and collection method (free flow, syringe, butterfly needle, or vacuum tube with specific collection order), blood collection tube type (ie, separator gel or not), tube size, and brand (name of manufacturer).
3. Sample processing: total processing time from collection to storage, time and temperature during clotting (for serum), centrifuge temperature, time, and speed.
4. Sample storage: temperature and container.
5. Quality control: methods for excluding hemolyzed samples (ie, visual assessment, spectrophotometry, measuring RBC-derived miRNAs).

Overview of small RNA-seq workflow

As mentioned previously, global profiling is ideal to obtain a comprehensive assessment of the miRNA composition in a particular sample. For this, small RNA-seq provides the most comprehensive approach currently available. A typical small RNA-seq experiment starts with RNA isolation, followed by library preparation, sequencing, and data analysis (Figure 1). Researchers should tailor each step to optimize cost. The choice of optimal RNA isolation method is based on sample type, volume, ability to modify the protocol, RNA yield, and performance based on profiling results available in the literature. Next, library preparation kit, sample pooling, the effective size of biological replicates to reach ideal statistical power, sequencing platform, and sequencing depth also need to be considered. For data analysis, different platforms are available for all skill levels in computational biology. Before staring RNA isolation, one also needs to consider if qRT-PCR verification is needed since synthetic miRNA might need to be spiked-in during RNA isolation for qRT-PCR normalization. These topics will be discussed in detail in the following sections.

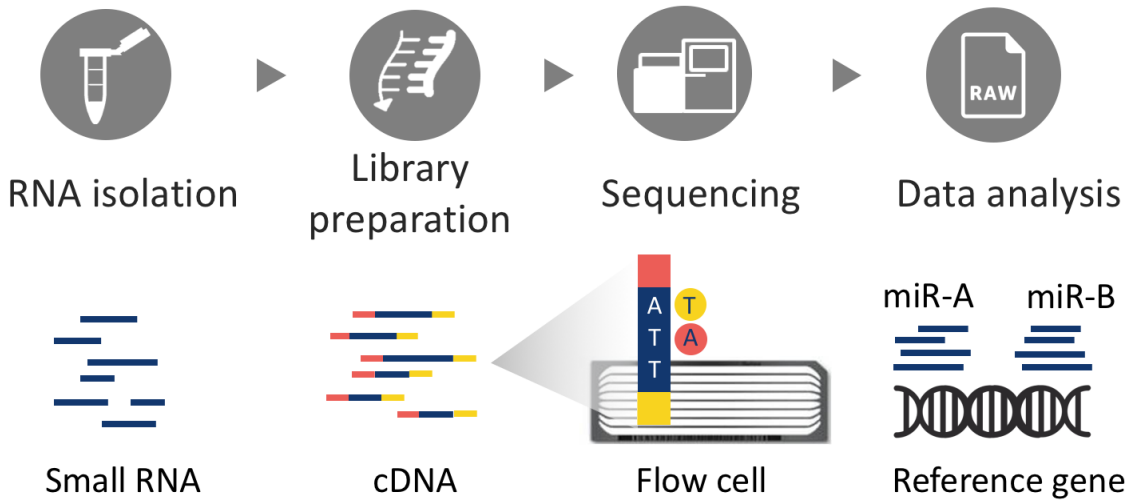

Figure 1. Small RNA-seq workflow. The upper circles represent each step in small RNA-seq and the lower diagrams illustrate the content of each step. For library preparation, RNA is reverse-transcribed into cDNA and is bound to adaptors. One or multiple libraries can be multiplexed and sequenced in one or more lanes on the flow cell (the sequencing surface). The sequencing machine sequences a complete flow cell at a time. In the data analysis, raw reads generated by the machine are aligned to miRNAs present in a reference database. Differential analysis is performed to identify differentially expressed miRs.

Evaluation of miRNA isolation method

Currently, there is no gold standard for biofluid miRNA isolation.[208] For urine samples, the traditional approach is to use ultracentrifugation (100,000-167,000 *g*) to pellet the exosomes.[209] In a 2016 survey by the International Society for Extracellular Vesicles, ultracentrifugation (including differential centrifugation) was reported to be the most commonly used method for isolating extracellular vesicles (reported by 81% of investigators who were polled) for various downstream applications.[210] However, ultracentrifugation is time-consuming[154], requires a large input volume, and co-precipitates macromolecules.[209] These limitations have hampered the application of

ultracentrifugation in the clinical setting. The same survey also revealed that only 64% of investigators would use ultracentrifugation if less than 1 mL of starting material was available.[210] Alternatively, investigation of an expedited isolation process involving precipitation, membrane filtration, gel filtration, and affinity purification has been performed.[63,211,212] However, co-precipitation of proteins and other microvesicles was found to be a limitation of these commercial precipitation-based methods.[213] For explanations of exosome isolation principles, readers are referred to other recent reviews.[154,214,215]

Five studies from 2012 to 2016 compared urinary exosome isolation methods with qRT-PCR and sequencing. In total, 8 methods were used to isolate urinary exosomes from 5-19 mL of urine.[71,87,178,200,216] Ultracentrifugation was the most frequently compared method, followed by the Urine Exosome RNA Isolation Kit (Norgen Biotek), which was identified as the best exosome isolation method in 3 of the studies.[71,178,216] Depending on the method used, the resulting total RNA concentration ranged widely, from 0.4 to 30 ng per mL of urine (Table 2).[87,200,217]

Table 2. Urinary exosome isolation method comparison based on qRT-PCR or sequencing.

Ref.	[217]	[178]	[71]	[200]	[87]
Sample vol. (mL)	10	5	5-19 See below	10-25 See below	10-15 See below
RNA isolation input (μL)	70	Unknown	Unknown	unknown	unknown
Elution vol. (μL)	35	Unknown	100	30	unknown
Verification	T	T	N/A	T	T
Number of miRNA/RNAs examined	8 RNAs	7 RNAs +1 miRNA	Sequencing	2 miRNAs	2 miRNAs
Ultracentrifugation	●	●	● 19 mL	● 25 mL	◎ 15 mL
Ultracentrifugation + 30% sucrose cushion					◎ 15 mL
Ultracentrifugation + 0.22μm filtration					◎ 15 mL
Nanomembrane ultrafiltration concentrator (Vivaspin 20, Sartorious)				★ 25 mL (RB total RNA: 4.69 ng/mL of urine)	◎ 15 mL
ExoQuick-TC Exosome Precipitation Solution (System Biosciences)	●			● 10 mL	● 15 mL
Total Exosome Isolation Reagent (Invitrogen, Life Technology)	●				● 15 mL ☆ 10 mL (lower Cq)
Urine Exosome RNA Isolation Kit (Norgen Biotek)	☆ (BA total RNA[a]: 2.7ng/mL of urine) (most transcripts detected)	★ (BA total RNA[a]: 15-346 ng/μL)	☆ 5 mL (BA miRNA: 30 ng/mL of urine) (most miRNA detected)		
Biotinylated *Solanum tuberosum* lectin (Vector Laboratories)	◎				

Denotations: ●, Unmodified (follow manufacturer's protocol); ◎/☆, modified (refer to the ref for modification); ★/☆, Best method according to paper, could be the one that produces the highest total RNA or small RNA yield, the lowest Cq values, or the one that identifies the most miRNAs (read descriptions inside the parenthesis for details); [a]RNA 6000 Pico kit; [b]Small RNA kit (6-40 nt); [c]Small RNA kit (14-29 nt).

Abbreviations: A, Affymetrix Microarray; BA: Bioanalyzer (Agilent); E, miRCURY LNA Universal RT microRNA PCR (Qiagen); EP, miRCURY microRNA QC PCR Panel (Qiagen); ND, NanoDrop (Thermo Fisher Scientific); Q, miScript miRNA Assays (Qiagen); RG, RiboGreen RNA quantification kit; T, TaqMan PCR/TaqMan miRNA Assays (Life Technologies); TLDA, TaqMan low-density arrays; U, unspecified qRT-PCR.

For circulating RNA isolation, TRIzol-based and silica-based methods are commonly used. TRIzol-based extraction is the traditional method in which serum or plasma is first homogenized with guanidinium thiocyanate solution (ie, TRIzol, QIAzol, or other comparable products). This is followed by phase separation using chloroform and RNA precipitation with isopropanol. Increasingly, commercial kits have been employing silica-based columns to absorb RNA. After initial homogenization and phase separation (as described above), the mixture of isopropanol (or ethanol) and RNA-containing solution is transferred to the column. After several washing steps, the absorbed RNA is eluted with RNase-free water. Table 3 compares studies that evaluated the performance of different commercial kits for isolating circulating miRNAs based on either qRT-PCR or microarray.[207,218-227] For several of these studies, an inconsistent starting volume (of plasma or serum) and different input volume of miRNA (for qRT-CPR or microarray) were used for comparing different isolation methods within the study.[218,221,222,224] Since the low concentration of miRNA in biofluids impedes accurate quantification, a fixed starting volume of biofluid for miRNA isolation and a fixed input for qRT-PCR are necessary for comparing isolation methods. The starting volume of plasma and serum needed for performing qRT-PCR ranges from 50-500 μL, and, depending on the kit, the recommended elution volume ranges from 14 to 100 μL. Among all 15 commercial kits tested, miRNeasy Serum/Plasma kit (Qiagen), miRCURY RNA Isolation Kit-biofluids (Qiagen), NucleoSpin miRNA Plasma kit (Macherey-Nagel), and mirVana PARIS kit (Ambion) were the most frequently tested. These are all column-based methods, and each was determined as the best method in approximately half of the trials (Table 3).

Table 3. Circulating RNA isolation method comparison based on qRT-PCR and microarray.

Ref.	[218]	[219]	[220]	[228]	[221]	[222]	[223]	[224]	[225]	[226]	[207]	[227]
Sample type	Serum	Plasma and Serum	Plasma	Plasma	Plasma	Plasma	Plasma	Serum	Plasma	Plasma	Plasma	Serum
Sample vol. (μL)	400	200	200	200	200-400 See below	200-300 See below	50	200-300 See below	100	400	500	200
Elution vol. (μL)	unknown	50	50	See below	See below	See below	50	See below	See below	See below	unknown	50
Spike-in	No	No	Yes	Yes	Yes	Yes	Yes	No	Yes	No	No	Yes
Verification	T	Q and T	TLDA	Q	Q and T	EP	E	TLDA	T	A	U	T
Number of miRNAs examined	6	90	756	5	2	9	10	380	6	1733	4	2
Direct-zol RNA MiniPrep Kit (Zymo Research)				● 14 μL		● 200->50 μL	●					
exoRNeasy Serum/Plasma Kit (Qiagen)				● 14μL								
mirVana (Ambion)							◎		● 100 μL			
mirVana PARIS (Ambion)					★ 400->100 μL (lower Cq)					● 100 μL (ND total RNA: 0.54ug)	★ (lower Cq)	● (BA small RNA[c]: 29.3pg/μL)
MiRCURY Cell&Plant (Qiagen)									● 50 μL			
MiRCURY RNA Isolation Kit –biofluids (Qiagen)		● (BA total RNA[a]: 147.2pg/μL)	◎ (no. of miR: 111)		★ 200->50 μL (lower Cq)	★ 200->50 μL (lower Cq)	◎		★ 50 μL (lower Cq)			

Table 3. Continued.

Ref.	218	219	220	228	221	222	223	224	225	226	207	227
NucleoSpin miRNAs Plasma kit (Macherey-Nagel)				★ 30 µL (lower Cq)	★ 400->50 µL (lower Cq)	● 300->30 µL		★ 300->30 µL (ND total RNA: 0.273ng; BA small RNA[b]: 80pg/µL, no. of miR: 84)				
Plasma/Serum Circulating RNA purification kit (Norgen)				★ 30 µL (lower Cq)	● 400->50 µL	● 250->100 µL		● 200->50 µL (ND total RNA: 0.267ng; BA small RNA[b]: 11pg/µL; no. of miR: 41)				
RNAzol-RT (Sigma-Aldrich)	★ (ND total RNA yield: 378.8±28.45ng/µL)											
RNeasy Mini kit (Qiagen)							☆ (lower Cq)					
miRNeasy Mini kit (Qiagen)			☆ (no. of miR: 313)	● 30 µL			☆ (lower Cq)	● 300->30 µL (ND total RNA: 0.198ng; BA small RNA[b]: 22pg/µL				

Table 3. Continued.

Ref.	218	219	220	228	221	222	223	224	225	226	207	227
miRNeasy Serum/Plasma kit (Qiagen)		◎ (BA total RNA[a]: 184pg/μL)		★ 14 μL (lower Cq)	● 200->25 μL	● 200->14 μL			● 14 μL	★ 28 μL (ND total RNA: 42ug)		★ (BA small RNA[c]: 48.8pg/μL, lower Cq)
TaqMan miRNA ABC Purification kit (ThermoFisher Scientific)		◎ (BA total RNA[a]:14pg/μL)										
Total RNA Purification Kit (Norgen)												● (BA small RNA[c]: 11.7pg/μL)
TRIzol LS (ThermoFisher Scientific)									◎ 100 μL	● 100 μL (ND total RNA: 6.01ug)	●	
In-house method	● (ND total RNA yield: 226.5±13.34ng/μL)	☆ (BA total RNA[a]: 1.06±0.44 ng, lower Cq)										

Denotations: ●, Unmodified (follow manufacturer's protocol); ◎/☆, modified (refer to the ref for modification); ★/☆, Best method according to paper, could be the one that produces the highest total RNA or small RNA yield, the lowest Cq values, or the one that identifies the most miRNAs (read descriptions inside the parenthesis for details); [a]RNA 6000 Pico kit; [b]Small RNA kit (6-40 nt); [c]Small RNA kit (14-29 nt).
Abbreviations: A, Affymetrix Microarray; BA: Bioanalyzer (Agilent); E, miRCURY LNA Universal RT microRNA PCR (Qiagen); EP, miRCURY microRNA QC PCR Panel (Qiagen); ND, NanoDrop (Thermo Fisher Scientific); Q, miScript miRNA Assays (Qiagen); T, TaqMan miRNA Assays (Life Technologies); TLDA, TaqMan low-density arrays; U, unspecified qRT-PCR.

miRNA quantification

For miRNA profiling, both RNA quantity and quality typically predict success. It is therefore helpful to accurately quantify the miRNA present in a sample. The most common tool used to measure RNA quantity is the spectrophotometric-based analysis, such as the NanoDrop (Thermo Fisher Scientific). For cell- and tissue-derived total RNA, the concentration is typically high enough to be accurately quantified by this method. In addition, potential protein and phenol contamination can be determined.[158,229,230] However, the concentration of total RNA derived from biofluids often falls below the detection limit of spectrophotometry (4-10 ng/μL).[207] In this case, the total RNA concentration measured by this method is unreliable.[171] Furthermore, the proportion of miRNA cannot be discerned.[231] Therefore, the NanoDrop is not recommended for quantifying extracellular RNA, and care should be taken when reviewing RNA yield, as it may not correlate with the concentration measured using more specific quantification methods.[218,224]

Alternatively, fluorometric methods, such as the Qubit (Thermo Fisher Scientific) and Quant-iT RiboGreen (Thermo Fisher Scientific) can be used for quantifying RNA. In one study, the results generated by the Qubit resembled the Bioanalyzer results (discussed below) and demonstrated less variability than those obtained using the NanoDrop.[171] The Qubit RNA High Sensitivity Assay can quantify total RNA concentrations as low as 250 pg/μL. However, for samples with low RNA concentration, a large volume of eluted RNA

(up to 20 μL) may be needed for quantification. The need for such a relatively large volume can limit the amount of RNA available for downstream applications. Use of a spike-in RNA of known quantity to decrease the volume required has been proposed to allow accurate quantification.[232]

The Agilent Bioanalyzer and Advanced Analytical Fragment Analyzer are other methods available for RNA quantification. With the Agilent RNA 6000 Pico Kit, the Bioanalyzer quantifies total RNA concentration and provides a 0-10 RNA integrity number (RIN) based on the ratio of 28S and 18S RNA to indicate RNA degradation.[233] Similarly, the RNA quality number (RQN) is generated by the Fragment Analyzer. While RINs are commonly used to determine whether the quality of RNA is high enough for downstream analysis (ie, microarray and sequencing)[234], the RIN relies on the presence of ribosomal RNA. Since RNA extracted from biofluids typically lacks ribosomal RNA, the quality of the extracted RNA cannot be determined.[70,226,227] Therefore, the Agilent Small RNA Kit is used to specifically detect the presence of small RNAs between 6 and 150 nt. It provides absolute miRNA concentration between 50 and 2000 pg/μL as well as the percentage of miRNA (miRNA/small RNA x 100).[235,236] As shown in Table 3, a comparison of 4 isolation kits showed that the NanoDrop did not distinguish performance among different kits while the Bioanalyzer results corresponded to the microarray results.[224]

qRT-PCR

The most frequently used method to determine the best RNA isolation protocols is qRT-PCR. In other words, the best isolation protocols resulted in samples for which the

spike-in miRNAs or endogenous miRNAs had the lowest Cq and standard deviation of Cq values. Most studies relied on only a few miRNAs to make this determination.[207,218,221,222,225,227,228] However, at least one RNA isolation method (the standard TRIzol protocol) has been reported to cause the loss of miRNAs with low GC content during RNA isolation from cells, particularly when cell input is low. This resulted in the retraction of one paper.[237] If miRNAs are preferentially selected during isolation, it would make qRT-PCR a questionable method for identifying the best protocol, and high-throughput analysis is required to identify whether any bias in RNA isolation methods might also apply to biofluids.[219]

Small RNA-seq

Compared with simple quantification and qRT-PCR, small RNA-seq offers a comprehensive way to compare the performance of different isolation kits based on raw reads, miRNA reads, miRNA percentage, miRNAs detected, and the miRNA distribution pattern. Gautam et al[238] examined 3 RNA isolation methods and 3 modifications with 200 μL or 350 μL of serum. While the RNA concentration was too low to be quantified by spectrophotometric measurement, successful library preparation was achieved. In the study, RNA extracted by TRIzol demonstrated the highest percent alignment to miRBase. Notably, the percentage of miRNA determined by the Bioanalyzer did not translate into the actual percentage of miRNA among processed reads in small RNA-seq. Since possible contamination of degraded mRNA might be misidentified as miRNA by the Bioanalyzer, small RNA-seq would be a better tool for comparing isolation performance. Similarly, Guo et al[239] compared 5 methods for isolating RNA from 200 μL of serum. Again, the

concentration of isolated RNA was too low for Qubit measurement, but successful Bioanalyzer measurement and library preparation were performed. Despite not having the highest concentration or the most raw reads, the TRIzol LS method was determined as the best isolation method based on the highest number of miRNA reads and miRNA percentage. These results highlight the importance of considering multiple factors when determining the best RNA isolation method.

Modification of RNA isolation protocols

Researchers commonly make in-house modifications to isolation protocols including commercially available kits in an attempt to optimize RNA isolation. Such modifications include changing starting sample volumes, increasing the proportion of TRIzol, adding carriers, manipulating the phase separation, performing 2 elutions (versus one) from the column, and altering the final elution volume. These are described in more detail below. While these modifications typically improve RNA quantity and possibly RNA quality, they complicate the systematic comparison of methods between studies. Furthermore, these modifications have most often been assessed by qRT-PCR, and their impact on sequencing results are largely unknown.

The first step in RNA isolation, protein denaturation by homogenization with TRIzol or comparable products, is considered important because the thorough mixing of the sample and denaturing solution is essential for successful phase separation. However, the volume of denaturing solution varies among kits, ranging from 2 to 5 or rarely 10 times the sample volume.[158] Li et al[227] tested different QIAzol to sample ratios in serum miRNA isolations and concluded that a 7:1 ratio produces the highest RNA quantity. However,

this result was not validated by qRT-PCR. Although increasing the denaturing solution to sample ratio might increase RNA yield, it might require the use of larger tubes (eg, 15 mL). Since larger tubes are not low nucleic acid-binding, an increase in RNA yield may not be evident as expected.

Yeast RNAs, glycogen, and linear acrylamide are carriers that have been evaluated in serum and plasma RNA isolation.[240] Carriers have been shown to increase RNA yield[226] based on lower Cq values of spike-in miRNAs during qRT-PCR evaluation.[223] However, some evidence suggests that the effect of a carrier on endogenous miRNAs is method-dependent.[225] In a small RNA-seq study, the use of an RNA carrier led to a low percentage of miRNA despite having higher processed reads compared to isolation without a carrier.[238] This indicated the presence of degraded carrier RNA, since a smearing effect was seen in the gel image of the prepared small RNA library.[238] Since carrier RNA could potentially contaminate samples, cautious use of carriers are advised.

Like protein denaturation, phase separation is a critical step in RNA isolation. In this step, the addition of chloroform followed by centrifugation separates samples into 3 layers: the upper aqueous layer containing RNA, the interface layer containing DNA, and the lower layer containing the organic phase. Duy et al[223] demonstrated that methods with a phase separation step yield a better intra-method reproducibility in spike-in miRNA expression than methods without phase separation. Another study attempted to maximize RNA recovery by introducing a second upper aqueous layer extraction, but no evidence of increased RNA recovery was seen.[140]

The last isolation step in column-based methods is elution of RNA from the column using RNase-free water. The protocols of commercially available kits are varied. For example, the recommended elution volume ranges from 14 μL to 100 μL, depending on the kit used. McAlexander et al[225] examined the influence of volume expansion using the miRNeasy Serum/Plasma kit and found that the recommended elution volume of 14 μL could recover most of the RNA compared to 50 μL or 100 μL. While it is unknown whether volume reduction in other kits can as effectively concentrate the RNA, a study has shown that the reuse of a column to do a second elution does not significantly increase the RNA yield.[140] In summary, readers should pay attention to protocol details when interpreting results for 2 main reasons. First, even a slight modification in the RNA isolation protocol could potentially cause substantial changes in results.[208] Second, most method comparison studies do not account for different elution volumes when making comparisons (Table 3).

Special considerations for RNA isolation

The challenge of biofluid miRNA research is not just limited to the low abundance of RNA, small input volume, high variation in isolation procedures, and subsequent difficulty in quantification. The potential for degradation of RNA by ubiquitous RNases is the major challenge. RNases from skin, bacteria, saliva, and dust might contaminate the work bench, glassware, plastic ware, pipettes, and pipet tips.[241] Therefore, it is important to use an RNase decontamination solution, such as RNaseZap (Invitrogen) or RNase AWAY (Invitrogen), to properly decontaminate work surfaces and pipettes. Additionally, a designated lab coat, constant changing of gloves, and avoidance of talking during RNA

extraction are all common practice. Use of RNase-free disposable plasticware is also recommended. If such plasticware is not available, baked glassware (150 °C for 4 hours) must be used, since standard autoclaving protocols cannot effectively inactivate RNases.[241]

A high variation in RNA quantity may be observed among samples, and this can be due to biological variation[227] or technical variation in column-based methods (TruSeq Small RNA Library Prep Reference Guide, Document 15004197 v02, July 2016). Therefore, if a rigid concentration is used to guide sample submission for library preparation, the isolation method should be tested on multiple samples to ensure consistency in yield.

Standardized reporting of RNA isolation

To summarize, all steps in the RNA isolation protocol should be carefully standardized within a study and clearly described in resulting manuscripts[207] to include:

1. Sample thawing condition, any additional centrifugation before isolation (centrifugation temperature, time, and speed).
2. For urine samples, details of ultracentrifugation (rotor angle, centrifugal force, and type of tubes, all of which can affect the quality of precipitated exosomes)
3. Sample starting volume for actual isolation.
4. Isolation kit (provide full name, manufacturer, and catalog number to avoid confusion).
5. Protein denaturing solution (provide full name, manufacturer, and volume used).

6. Provide the step-by-step procedure in supplementary data. Avoid using "follow manufacturer's instruction."
7. Explicitly state whether carriers and spike-in miRNAs were used or not. If used, provide the full name and concentration (manufacturer and catalog number).
8. State the elution solution and volume (column-based method) or the resuspension solution and volume (non-column-based precipitation method).
9. Quantification of RNA: provide the instrument (manufacturer), kit or assay (full name, manufacturer, and catalog number), readouts (with proper unit) provided in main text or supplementary data.

Library preparation

With the development of next generation sequencing, small RNA-seq provides unprecedented flexibility in miRNA profiling and enables discovery of novel miRNAs. However, successful extraction of RNA for qRT-PCR does not guarantee successful small RNA-seq results, as small RNA-seq requires a higher RNA concentration, and therefore a higher volume of biofluid for library preparation.[85,242] This higher volume requirement is a major limitation, particularly for retrospective studies. Table 1 includes examples where small RNA-seq was successfully performed using biofluid RNA isolated by different methods. During library preparations, RNAs were attached with 3' and 5' adapters, reverse transcribed into cDNA, amplified by PCR, and then the right size range of PCR products was selected for sequencing.

Common library preparation kits

The most commonly used library preparation kits are the TruSeq Small RNA Library Preparation Kits (Illumina) and the NEBNext Small RNA Library Prep Set for Illumina (New England BioLabs). TruSeq requires 1 μg of total RNA in 5 μL of nuclease-free water (200 ng/μL of eluent) or 10-50 ng purified small RNA in 5 μL of nuclease-free water (2-10 ng/μL of eluent). In contrast, NEBNext requires 100 ng-1 μg total RNA in 1-6 μL of nuclease-free water (17-1000 ng/μL of eluent). These total RNA concentrations are difficult to achieve from small volumes of biofluids.

Previous studies have shown that increasing the plasma input volume for RNA isolation from 5 to 50 μL[223] or from 50 to 200 μL[220,225] can increase endogenous miRNA expression in qRT-PCR. However, no comparison was conducted using larger starting volumes. Pacholewska et al[141] obtained 2-428 ng/μL total RNA (measured by the Qubit RNA HS Assay) from 2 mL of equine serum by using a column-based isolation method. Library preparation was successful using the NEBNext library preparation kit. Similarly, Shaughnessy et al[109] extracted 708-2640 pg/μL small RNA (measured by the Bioanalyzer Small RNA kit) from 1 mL bovine serum using the same isolation method, again followed by successful library preparation using the Illumina library preparation kit. In Table 3, it is evident that when the starting plasma and serum volume are lower (eg, 200 μL), the total RNA yield, as determined by the Bioanalyzer, is also substantially lower (11-147 pg/μL) than the required input for library preparation using the TruSeq library preparation kit.[219,224,227] In one study, 5 commercial kits were used to obtain 13-3674 pg/μL presumed small RNAs from 200 μL of serum. Even though only one isolation met the minimum

requirement of 2 ng/μL, the RNA samples were able to proceed with the TruSeq library preparation for the other isolations by increasing the number of PCR amplification cycles from 11 to 18.[239]

Library preparation using low input RNA

If researchers cannot increase the starting sample volume to obtain a higher RNA concentration, they may consider using the recently developed NEXTflex Small-RNA Seq Kit (Bioo Scientific). This kit requires 1 ng - 2 μg total RNA in up to 10.5 μL nuclease-free water (95 pg/μL - 190 ng/μL of eluent). Thus, the lowest feasible concentration for this kit is attainable with small biofluid volumes. The manufacturer's manual recommends altering the number of PCR cycles based on the input RNA concentration used. In our experience, we obtained approximately 0.9 ng/μL total RNA (measured by the Fragment Analyzer) from 2 mL of canine serum and successfully performed library preparation using the NEXTflex kit with 24 PCR cycles as dictated by the protocol (unpublished observations). Notably, the NEXTflex kit also detected the highest number of miRNAs in recent studies comparing the performance of different library preparation kits.[243,244]

Increasing the number of PCR amplification cycles during library preparation is a feasible method to overcome low input RNA concentration as previously mentioned.[239] For example, one study used 11 cycles for high input of starting material (1 μg) and 18 cycles for lower input (10 ng).[244] While the NEXTflex kit provides guidelines for the number of PCR cycles, Illumina does not provide such a recommendation (personal communication). Furthermore, with increasing PCR amplification cycles, the variation in both read length and GC content will result in PCR amplification bias and greater noise in

the data.[245] This bias can affect the completeness of the resulting cDNA library[246,247], and replicates can only be compared if they all have been subjected to the same number of PCR cycles.[245]

With low RNA input, researchers should be cautious about any potential bias that would not be present had a standard RNA input been used. For example, the sequencing platform and sequencing facility may not be the major contributors to variation in miRNA expression under normal circumstances.[248] However, studies done with low RNA input showed statistically significant differences in genome mapping rates between libraries that were prepared at different locations.[244] Moreover, it is worrisome that in one study, a PCA plot demonstrated a clustering of samples based on location of library preparation rather than based on the originating tissue type.[244] Although studies have shown excellent reproducibility of technical replicates for library preparation[36] regardless of library preparation kits used[249], the need for technical replicates may need to be re-evaluated for low input samples.

Sample pooling for library preparation

As described previously, sample volume is one of the limiting factors in conducting RNA-seq studies. Sample pooling before or after RNA isolation is a strategy to increase the volume of biofluid or quantity of RNA and to decrease genetic variation.[85,250-253] One study attempted to verify sample-pooling strategies for RNA-seq, but they instead compared unpooled samples with pooled technical replicates instead of pooled biological replicates.[254] We therefore re-analyzed the data to test the effect of pooling different sample combinations for library preparation in a gene-by-gene

arithmetically averaging manner to mimic sample pooling. We found that creating 4 pools from a total of 8 biological replicates (2 individuals per pool) led to more differentially expressed genes (DEGs) identified by RNA-seq, but fewer of these genes could be qRT-PCR-verified when compared to the unpooled design (4 individuals without pooling). Indeed, a similar simulation showed that genes with higher variability in expression, especially those with low expression levels, may be inappropriately recognized as differentially expressed in the pooled design.[255] Although sequencing as many biological replicates as possible is ideal, they found that sample pooling is more cost-effective for samples with large biological variation and when library preparation cost is higher than RNA isolation cost. Although sample pooling may seem to be a promising strategy, researchers need to bear in mind that sample pooling to create only one sequencing result per condition doesn't account for biological variation (see "Replicates: biological versus technical" section). Therefore, data interpretation would be challenging as a single data point would represent a combination of multiple samples.

Small RNA-seq experimental design

Replicates: biological versus technical

As in traditional experiments, replicates are included in small RNA-seq to ensure that the differential expression of miRNA between target groups represents a pathological difference. Biological replicates are biological samples obtained from different animals, whereas technical replicates represent the repeated experimental steps on the same sample for all steps of miRNA profiling. Several mRNA-seq studies examine technical replicates

at the sequencing level.[32,256] Overall, the reproducibility of technical replicates is excellent. Low count reads might show higher inconsistency between technical replicates than high count reads[33], but low count reads are typically removed before differential expression analysis.[257] Given that biological replicates introduce a much higher variation[258], technical replicates for sequencing are not necessary[32,62,259] unless the biological variation is abnormally high.[260]

More samples versus deeper sequencing

In RNA-seq, sequencing depth or coverage refers to the average number of reads that map to, or cover, the reference genomes. Since sequencing capability of each flow cell is limited, the number of samples to be sequenced is inevitably tied to the sequencing depth as a tradeoff. Under a fixed budget, the more samples to be sequenced, the less resulting sequencing depth per sample. Several studies have shown that, although increasing sequencing depth and sample size can both increase power, sample size is more potent than sequencing depth[259,261], especially when sequencing depth is ≥ 20 million reads.[262] Others also demonstrated that once a sequencing depth of 10 million reads is reached, the statistical power of increased sequencing depth deminishes.[259,263]

In general, the goal of the experiment determines the sequencing depth. An experiment aimed at novel transcript discovery would require extensive sequencing (> 30 million reads)[260], whereas, for differential analysis, a sequencing depth of 10 million reads is considered adequate.[264] On the other hand, the number of biological replicates per group depends on the inherent variation in the biological samples. Samples obtained from single-breed, same-sex animals that reside in a strictly controlled experimental environment

would have smaller inter-individual variation than samples collected from client-owned animals that are different breeds and live in various households.[264] One study proposed that 3 biological replicates in each group should be the minimal requirement for samples having the least variation (ie, inbred mice and cell lines).[255] However, in a later experiment using 42 replicates of 2 strains of *S. cerevisiae*, a subset of 3 replicates per group only identified 20-40% of DEGs compared to the full set of 42 replicates.[265] This study concluded that a minimum of 6 biological replicates per condition should be used, although 12 replicates were suggested if the goal is to identify the majority of DEGs.[265]

Multiplex and sequencing budget calculation

Multiplexing refers to the sequencing of multiple samples in a single lane of a flow cell by attaching a unique, short sequence (or barcode) to each sample library. As the data generated from each flow cell increases substantially with new developments in sequencing technology, multiplexing is becoming increasingly popular. Common library preparation kits allow users to multiplex up to 48 samples in a single lane. This approach could significantly reduce sequencing cost with the potential tradeoff of increased wait times for other lanes on the flow cell to be filled by other researchers as a flow cell can have up to 8 lanes. In calculating the sequencing budget, the number of biological replicates per condition, number of conditions, minimal sequencing depth, and sequencing cost all need to be considered. To facilitate budget calculation, we made a sequencing cost calculator that allows users to easily plug in appropriate numbers for a study to obtain an estimated cost for the desired sequencing strategy (Supplementary Table S1).

Standardized reporting of experimental design

Standardized reporting of the experimental design can help readers quickly understand the study. Recommended content should include:

1. The numbers of treatment and control groups and biological replicates per condition.
2. The library preparation kit used (full name, manufacturer, and catalog number), RNA input volume or quantity for library preparation, number of PCR cycles if different from the standard protocol, and any quality control method used.
3. The sequencing platform, multiplexing design, number of lanes of the flow cell used, anticipated amount of data generated.

Small RNA-seq data analysis

Data analysis is the most intimidating step in RNA-seq projects according to a recent poll on the RNA-Seq Blog.[30] Indeed, it is the most unfamiliar field for most veterinary researchers. The typical data analysis steps, or data analysis pipeline, include obtaining a reference gene sequence (if applicable), quality control, mapping/alignment, assigning aligned reads to genes, and differential expression (Figure 2). The ENCyclopedia of DNA Elements (ENCODE) Project Consortium[266] has proposed small RNA-seq data standards and processing pipeline[267] for data analysis. In addition, the NIH-funded Extracellular RNA Communication Consortium (ERCC)[268] also proposed a publicly available pipeline: exceRpt small RNA-seq pipeline[269] for analyzing small RNA-seq data, although only human and mouse genomes are available in this platform.

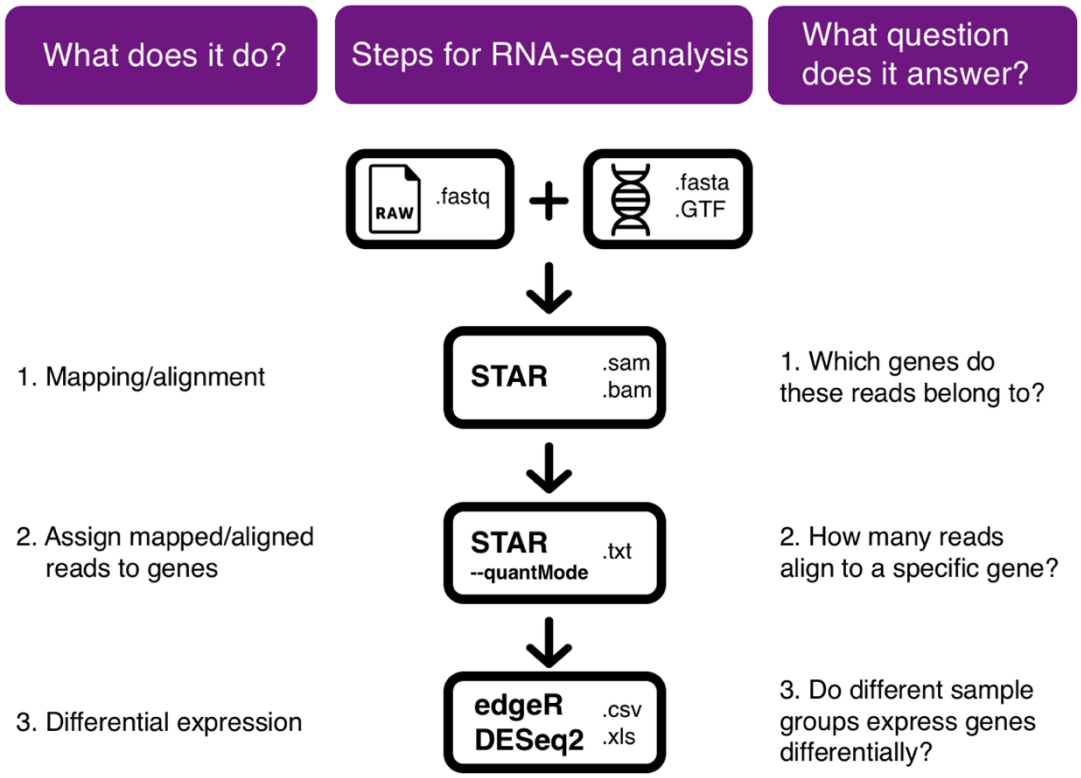

Figure 2. An example pipeline of RNA-seq data analysis up to the point of differential expression. For each box, the analysis tool is bolded, and the input file (.fastq, .fasta, and .GTF) and output file (.sam, .bam, .txt, .csv, and .xls) format are nonbolded. The alignment tool, STAR[270] and its "--quantMode" function, was selected according to the ENCODE pipeline. EdgeR[271] and DESeq2[272] are the most commonly used tools in differential analysis and thus were provided as examples.

Traditional approaches to data analysis often require the access to a high performance research computing center, command line knowledge of the Unix/Linux system, and, ideally, the R programming ability to use popular differential expression tools such as edgeR[271] and DESeq2.[272] However, as the popularity of RNA-seq grows, more and more web-based platforms that require minimal computational knowledge are available. Galaxy (http://usegalaxy.org)[273] is the most commonly used web-based platform that incorporates popular tools and a supportive forum

(https://biostar.usegalaxy.org/) to facilitate genomic research. The UEA Small RNA Workbench provides both cloud analysis and downloadable desktop software.[274,275] Also, there are many web-based pipelines for data analysis, such as CPSS 2.0[276], Oasis 2[277], and miRMaster[278] that can perform the analysis illustrated in Figure 2. An online database containing all available microRNA bioinformatic resources is available.[279] The exploration of different analysis tools is beyond the scope of this review; however, excellent review articles for RNA-seq and miRNA data analysis are available.[264,280,281] Numerous YouTube videos and online courses are also freely available for learning how to use the analysis tools. For a complete list of resources, including on-site courses, YouTube videos, tutorial websites, and online courses, readers can visit the author's post on the Biostar forum (https://www.biostars.org/p/174376/).

Standardized reporting of data analysis

Besides RNA isolation, data analysis is another major source that significantly affects reproducibility. The International Society for Extracellular Vesicles (ISEV) published a position paper that has a proposed checklist of details that should be included in publications.[62] These include:

1. Analysis platform, software/tool, and version; online tools should have their URL listed.
2. For every step of data analysis, be sure to list command line options, exclusion and inclusion criteria. For example, 'quality score of 30 was set as the cutoff value' or 'low expression genes with read count less than 5 were excluded.' If no modifications to the default settings were used, then specifying such may be all that is required.

3. Source of reference genome assemblies and release numbers.
4. Report summaries of raw data and alignment parameters (eg number of raw reads per sample, number of processed reads per sample, number of aligned reads per sample, and percentage of alignment)
5. Make customized code available to the public by posting on software development platform, such as GitHub.[282]
6. Deposit data in National Center for Biotechnology Information (NCBI) depositories such as Sequence Read Archive (SRA) and Gene Expression Omnibus (GEO).

qRT-PCR verification

Whether or not to perform qRT-PCR verification of sequencing results is still highly debated in RNA-seq. This question can be approached from 2 angles: verification in the sequenced sample groups or verification in a different cohort. For RNA-seq technology, it is questionable whether qRT-PCR validation on a few selected genes in the same sample groups that were sequencing is necessary[283], as RNA-seq may be more reliable than qRT-PCR due to its higher sensitivity and lower probe bias.[34] Also, many studies have shown extremely close correlations between qRT-PCR and RNA-seq data.[32-37] The existing evidence suggests qRT-PCR would have a higher value in validating differential expression findings in a different cohort.

Primers

To accurately detect and quantify certain mature miRNAs, the qRT-PCR primers need to be specific with minimal cross-reactivity with other non-specific targets.[284] It is

challenging to design primers for mature miRNA qRT-PCR for several reasons. First, miRNAs themselves are as long as the traditional primers for mRNAs. Second, there is no common sequence present across different miRNAs[285], and the mature miRNA sequence is also present in pri- and pre-miRNA.[286,287] Third, mature miRNA sequences are too short to be templates.[288] Two of the most popular commercial products, TaqMan miRNA Assays and miRCURY LNA miRNA PCR System, each use a different reverse transcriptase strategy to overcome this all of these challenges. TaqMan applies the stem-loop miRNA specific structure to generate cDNA, whereas miRCURY adds a poly-A tail to the 3' end of the mature miRNA sequence followed by universal poly-T primers to synthesize cDNA. The former method is highly specific, but requires more RNA and repeated RT if detection of more than one miRNA species is desired.[287] Recently, a new product, TaqMan Advanced miRNA Assays, also adapts the poly-A tailing with the ligation of adapters at the 5' end of miRNA to perform a universal RT reaction. However, the cost and reaction time using this product are much higher than the other 2 products as shown in the qRT-PCR cost calculator (Supplementary Table S2). All 3 products claim high specificity, even when differentiating sequences that differ by only 1-4 nucleotides (human miRNA let-7 family)[289-291]. Because of the challenges in creating highly specific miRNA primers, the primers are much more expensive than traditional PCR primers, and the complete sequence of each primer remains confidential. To reduce cost, researchers may use a primer design tool to develop their own miRNA primers; however, the specificity needs to be experimentally tested to minimize off-target binding.[286]

RNA input

Conventionally, RNA concentration serves as the basis for sample input for qRT-PCR; however, the use of total RNA concentration is controversial for biofluids as the total RNA content may change with the disease state.[146,292] Therefore, using a fixed volume of sample for RNA isolation and a fixed volume of resulting RNA for qRT-PCR are recommended.[146,219,227] Standardized volume of the biofluid, elution volume, and input volume for RT are applied along with normalization (discussed below) to achieve proper quantification of biofluid miRNAs. As high biological variation may be expected among samples of interest, substantial variation in RNA concentration between different samples may also be expected. Therefore, it is important to understand the necessity of normalization in addition to volume standardization when performing miRNA studies using qRT-PCR.

Internal controls and spike-ins

To identify DEGs, stably expressed housekeeping genes are used for normalization in traditional qRT-PCR experiments to facilitate comparison between samples. Similarly, several housekeeping genes in biofluids or exosomes have been proposed, demonstrating variable performance. Table 1 includes qRT-PCR internal controls and normalization methods, when available, used in circulating and urinary miRNA studies in domestic animals.

Among all housekeeping genes used as internal controls, small nuclear RNA (snRNA) U6 (snRNU6 or RNU6) and U6B (RNU6B) and miR-16 were most frequently used. Promising internal controls, such as 18S rRNA, 5S rRNA, small nucleolar RNA

(snoRNA) U43, and snRNU6 were found to be highly variable in plasma and significantly differed from blood mononuclear cells.[59] In one study, RNU6B was undetectable in cell-free plasma[192], and levels were variable in several other studies.[59,85,293-295] Another small nucleolar RNA, RNU48, was only detectable in RBC and hemolyzed plasma but not in non-hemolyzed plasma.[193] In addition to their variable detection, arguments against the use of snRNAs as internal controls are that they are not expressed at a similar level to miRNAs, and they are structurally and functionally different. Small nuclear RNAs are different than miRNAs in nucleic acid composition, in length, and in secondary structure, and their isolation and reverse transcription (RT) efficiency and stability might also be different. Additionally, snRNAU6 is exclusively located in the nucleus[296], suggesting the detection of snRNAU6 may represent cellular contamination.

Given the limitations of snRNAs as reference genes, miRNAs might serve as better internal controls as they should demonstrate a similar behavior during RNA isolation.[297] However, deciding which miRNAs to use as internal controls can be challenging. As mentioned in the section "Cellular contamination in serum and plasma," the expression of blood cell-derived miRNAs could mask the miRNAs of interest. For instance, the commonly used internal control, miR-16, was found to be inconsistent and affected by hemolysis in multiple studies.[70,85,192] Endogenous miRNA controls could also be species- and disease-specific. In one study, miRNA let-7c was identified as an internal reference for pigs infected with porcine whipworm[111] while the same miRNA was found to be expressed significantly higher in pregnant cattle versus controls.[125] While a thorough review of the literature is recommended to help identify endogenous miRNAs to use as

internal controls for a particular study, it is strongly recommended that researchers also conduct pilot qRT-PCR experiments or use small RNA-seq data to identify promising miRNAs internal controls (see below in "Normalization" section). The stability of internal controls can be discerned by the standard deviation of their Cq values among samples, the slope of the regression line when their Cq values are plotted against respective samples, and using software such as geNorm[298] (updated version incorporated in qbase+ software[299]), NormFinder[300], BestKeeper[301], and DataAssist.[302] A detailed discussion of these tools was covered by a review written by Occhipinti et al.[303]

Alternatively, exogenous synthetic miRNAs, or spike-ins, can be introduced after TRIzol homogenization as controls for qRT-PCR normalization. Among all 47 studies investigating biofluid miRNAs in domestic animals, 30 studies incorporated qRT-PCR, and almost half used cel-miR-39 as a spike-in for normalization. Despite frequent use of the spike-in for normalization using the $2^{-\Delta\Delta Cq}$ method[304] (see the following "Normalization" section), it is only suitable for assessing recovery of the RNA isolation method.[225] In other words, a spike-in can only reflect any interference after the homogenization step, and, unlike endogenous miRNAs, it does not reflect conditions regarding sample collection, processing, and storage.[222]

Normalization

The purpose of using qRT-PCR is to verify miRNAs that are differentially expressed between animals with disease and healthy controls. The goal of normalization is to minimize the technical variation within a dataset by detecting changes relevant to experimental variables. The most commonly used normalization method for qRT-PCR is

the $2^{-\Delta\Delta Cq}$ method proposed by Livak and Schmittgen.[304] Briefly, for every sample, the Cq value of the internal control is subtracted from the Cq value of target miRNA, generating the ΔCq. Next, the ΔCq of untreated samples is subtracted from the ΔCq of treated samples to obtain the ΔΔCq. Since the fluorescent signal doubles every Cq cycle, the fold change of target miRNA in treated samples versus the untreated samples can be expressed by $2^{-\Delta\Delta Cq}$.[304] However, it is often ignored that the $2^{-\Delta\Delta Cq}$ method assumes that the PCR amplification efficiencies of the target miRNA and internal controls are similar and close to 100%. This limitation inevitably narrows its application given that PCR amplification efficiency differs among target miRNAs. For the same miRNA targets, different miRNA isolation methods used may even affect the PCR amplification efficiency[305], presumptively due to co-purification of inhibitors. Therefore, Pfaffl[306] proposed an improved model that adjusts for different PCR efficiencies among the internal control and target miRNAs. The drawback of this approach is that only one internal control is allowed.

Another widely used normalization method is the mean expression value or global mean normalization.[307] The original "global mean normalization" method first set a cutoff Cq value to filter out noise signals. Then, the individual Cq values of all miRNA targets in one sample is subtracted by the arithmetic mean of all Cq values for that sample. This method calculates the difference between Cq values of specific miRNAs and the mean Cq value of all expressed miRNAs. This approach does not require identification of internal controls; however, users should be aware that this method is only valid in profiling a large number of miRNAs that do not reside in the same gene cluster. The method is based on the assumption that only a small of portion of the miRNAs is differentially expressed, with

equal numbers of up- and down-regulated miRNAs. Therefore, the presence of an outlier could potentially skew the global mean and subsequent calculations.[307,308] Alternatively, a group of internal controls that resembles the global mean expression can be used to overcome this limitation. Prior miRNome profiling data can help identify promising internal controls: First, global mean normalization is performed on the profiling data, then the standard deviations of the Cq values across all samples are calculated for each miRNA. MiRNAs with the lowest standard deviation are determined as promising internal controls. A list of 10 promising internal controls can be further analyzed by geNorm.[298] The algorithm of geNorm[298] ranks miRNAs base on their stability (M value), and the calculated normalization factor (V value), to suggest the optimal number of internal controls. Mestdagh et al.[307] concluded that both approaches for global mean normalization performed equally well. If no prior data is available for selecting promising internal controls, a set of unbiased miRNAs (more than 8) that are transcribed at different loci in a representative sample set consisting of at least 10 samples can be analyzed by geNorm[298] to consolidate a set of normalizers as described above.

The qbase+ software[299] improves upon the modified global mean normalization.[288] Briefly, after filtering out miRNAs with low expression, Cq values are converted into relative quantities (RQ). A sample specific normalization factor (NF) is then used to obtain the normalized RQ (NRQ). The software provides 2 options for the NF calculation. One is based on all expressed target miRNAs in one sample, namely the "modified global mean normalization." Alternatively, the NF can be generated using only the miRNA targets that are expressed in all samples, namely the "modified global mean normalization on common

targets." The original "global mean normalization", the "modified global mean normalization", and the "modified global mean normalization on common targets" lead to a more pronounce decrease in standard deviations for each individual miRNAs than the use of a specific internal control, and the modified approaches can further reduce the impact of missing data compared with the originally proposed calculation for "global mean normalization."[288] In qbase+ 3.1 (Biogazelle, Zwijnaarde, Belgium - www.qbaseplus.com), available normalization strategies are reference targets (as selected by geNorm[298]), modified global mean normalization, and modified global mean normalization on common targets.[288]

Standardized reporting of qRT-PCR

The Minimum Information for Publication of Quantitative Real-Time PCR Experiments (MIQE) Guideline was published in 2009[309], followed by the development of a Real-Time PCR Data Markup Language[310] to consistently report qRT-PCR data.[310] The minimum information that must be reported for a qRT-PCR experiment includes experimental design, sample type, nucleic acid extraction method, RT method, target information, oligonucleotides, protocol, validation, and data analysis. A checklist is available on the RDML website (http://www.rdml.org/MIQE_checklist.pdf) and should be submitted along with the paper. Alternatively, readers can use RDML Ninja, the reference software, or other RDML compliant third-party software to report data in the RDML file format (http://www.rdml.org/software.php).

Biofluid-derived microRNA in chronic kidney disease -- biomarker discovery

Since 2011, several studies explored the application of circulating and cell-free urinary miRNA as biomarkers in chronic kidney diseases. One of the earliest biofluid miRNA studies focused on circulating miRNA in 75 patients with CKD receiving hemodialysis.[311] The overall miRNA concentration in plasma and Cq values for individual miRNAs (miR-16, miR-21, miR155, miR-210 and miR-638) was inversely correlated with renal function as determined by eGFR (*P*-value < 0.004; correlation coefficient ranging from -0.347 to -0.723). However, the etiology of CKD was not specified, and it is unclear how the authors quantified RNA input for qRT-PCR (by volume or by quantity) and whether the Cq values were normalized or not.[311] In another study, 28 CKD patients were divided into 2 groups based on the eGFR.[179] The miRNA PCR array identified 172 upregulated and 94 downregulated circulating miRNAs isolated from plasma comparing low to high eGFR groups. However, among the top 10 DE miRs, the fold changes are relatively low (< 2-fold), and the *P*-values are of borderline statistical significance.[179] In this study, RNA input for qRT-PCR was quantified, and, RNU6B, a small nuclear RNA that is not readily expressed in serum[312-314], was used for qRT-PCR normalization.[89]

Six miRNAs (miR-29a, miR-29b, miR-29c, miR-200a, miR-200b, and miR-200c) were examined in urinary exosomes obtained from 32 patients with heterogenous glomerular diseases, including diabetic nephropathy (DN), focal segmental glomerulosclerosis, IgA nephropathy, membranous nephropathy, and mesangial proliferative glomerulonephritis.[89] Among them, miR-29c is the only miRNA identified that had a marginal significant positive correlation with eGFR (*P*-value = 0.042;

correlation coefficient = 0.365). While the quantification of RNA input for qRT-PCR was unspecified in the paper, marked differential expression (fold change: 6.59-27.24) was found between patients and controls for all miRNAs. Urinary miRNAs were also examined in the study described above.[179] Using miRNA PCR array, 248 upregulated and 136 downregulated urinary miRNAs were identified in low eGFR CKD patients compared to high eGFR CKD patients.[179] Similar to results of plasma-derived miRNAs, the low fold changes (< 2.2-fold) and borderline statistically significant *P*-values (> 0.01) were seen among the top 10 DE miRs. Also, in both studies, RNU6B was again used for qRT-PCR normalization[89,179] despite its unstable expression and questionable appearance in urine.[315]

Next-generation sequencing technology has also been used to identify differentially expressed miRNAs in humans with CKD compared to healthy subjects. A recent study sequenced urinary miRNAs from 25 samples obtained from 15 CKD patients (7 with early disease (stages I and II), and 8 with late disease (stages III and IV)) and 10 healthy controls.[316] Up to 9 upregulated miRNAs (let-7c, miR-222, miR-27a, miR-27b, miR-296, miR-31, miR-3687, miR-6769b, and miR-877) and 7 downregulated miRNAs (miR-1-2, miR-133a, miR-133b, miR-15a, miR-181a, miR-181c, and miR-34a) were identified throughout all stages of CKD patients compared to controls. Of note, the expression of miR-181a was markedly decreased (> 160-fold change) in CKD patients compared to controls. This substantial change indicates potential application of miR-181a in the diagnosis and/or pathogenesis of CKD.

Only one study has evaluated miRNAs in the urine of dogs with kidney disease. In this study, 47 dogs with elevated serum creatinine were grouped as having kidney

diseases.[100] After RNA isolation, urinary RNA samples from all 47 dogs with kidney diseases and 37 healthy controls were pooled (one pool for each group) for small RNA-seq. Due to the lack of biological replicates, no statistical analysis was performed, and candidate miRNAs and internal controls were selected based on read counts and fold change presented in the sequencing data. Urine samples obtained from dogs with kidney diseases had more reads mapped to miR-486, miR-21, miR-10a, and miR-10b than those of the control sample. However, in the following qRT-PCR verification, the differential expression of these miRs changed depending on whether miR-26a or miR-191 was used for qRT-PCR normalization.[100] In general, various preanalytical and analytical factors, such as study subjects, sample storage temperature, and experimental design, would have huge impact on data interpretation. Therefore, many studies focus on a single, biopsy-confirmed glomerular disease to optimize the specificity for biomarker discovery in CKD, as described in the following sections.

Focal segmental glomerulosclerosis

In a 2015 report analyzing 84,301 patients with end-stage renal disease attributed to glomerulonephritis (GN) from 1996 to 2011, focal segmental glomerulosclerosis (FSGS) is the most common cause (40.7%) of all GN cases, followed by lupus nephritis (LN) (19.5%) and IgA nephropathy (IgAN) (15.4%).[317] Therefore, FSGS is commonly used as a representative example of CKD due to glomerular disease[318], and there is substantial interest in identifying biofluid miRNAs as biomarkers for FSGS. In an early study, 2 miRNAs specific to mouse kidney, miR-10a and miR-30d, were investigated in the urine of FSGS patients.[319] Although it was unclear how the RNA input was quantified for qRT-

PCR, raw Cq values were normalized with spike-in synthetic plant MIR168a. Similar to the results obtained from the unilateral and bilateral renal ischemia/reperfusion mouse model performed in the same study, the urine from FSGS patients had an approximately 13- and 10-fold increase of miR-10a and miR-30d, respectively, compared to controls.[319]

Later studies implemented high-throughput microarray technology to screen for candidate miRNAs. A miRNA microarray containing 1733 mature miRNA probes has been used to discover DE miRs among patients with FSGS. Compared with sex- and age-matched controls, 39 plasma miRNAs (67% upregulated) and 135 urine miRNAs (31% upregulated) were differentially expressed. Unfortunately, the complete list of DE miRs was not provided. Among the miRNA selected for verification with qRT-PCR, urinary miR-155 was upregulated and urinary miR-1915 was down-regulated in FSGS patients. However, the qRT-PCR set up was suboptimal since a defined RNA quantity (10 ng) was used for qRT-PCR input, and RNU6B was used as an internal control.[320]

In another study focusing on FSGS patients with and without ongoing proteinuria, a microarray targeting 754 miRNAs in human plasma was carried out using snRNAU6 as internal control. They found that miR-125b, miR-186, and miR-193a-3p were upregulated in FSGS patients with active proteinuria (fold changes: 2.62-9.75). Among them, plasma miR-125b and miR-186 were differentially expressed between proteinuric patients versus patients in remission, and the expression levels of both miRNAs reduced after effective steroid treatment compared to the pre-treatment period.[321]

The same group also conducted a similar study on urinary miRNAs, identifying 27 upregulated miRNAs in FSGS patients with active proteinuria.[322] Despite using the same

internal control (snRNAU6), candidate miRNAs identified in urine (miR-196a, miR-30a-5p, and miR-490) were different from those previously described in plasma.[321] These urinary miRNAs were found upregulated among proteinuric patients versus patients in complete remission or healthy controls (fold changes: 2.81-6.74). Furthermore, decreased expression was seen after patients responded to steroid therapy, but it was not seen in the unresponsive group.[322] Next, a follow-up study focused on urinary miR-196a as the sole predictor for FSGS progression. Urinary miR-196a was differentially expressed in proteinuric FSGS patients and was associated with proteinuria, eGFR, interstitial fibrosis and tubular atrophy.[318]

A recent study used a miRNA PCR array to examine the expression of 515 miRNAs in plasma from 5 patients with FSGS compared with those from 5 healthy controls.[323] During the initial screening, 16 upregulated and 18 downregulated miRNAs were identified (P-value < 0.05, absolute fold change > 2) when cel-miR-39 was used for normalization. Among them, 4 downregulated miRNAs (miR-17, miR-451, miR-106a, and miR-19b) were subsequently selected to be candidate miRNAs. These candidate miRNAs were also downregulated with disease when tested via qRT-PCR in a larger group consist of 97 patients and 124 controls. The expression of 3 miRNAs (miR-17, miR-451, and miR-106a) was downregulated in FSGS and was found to correlate with FSGS remission. These miRNAs also appeared to be disease-specific, as their reduction was absent in patients with other kidney diseases, such as IgA nephropathy, mesangial proliferative glomerulonephritis, and membranous nephropathy. However, snRNAU6 was used as an internal control for all qRT-PCR experiments.[323]

Overall, different studies demonstrated variable results. Examining the 27 urinary DE miRs reported in a study of proteinuric FSGS patients[322], miR-30d was also differentially expressed in another FSGS study.[319] However, other DE miRs, such as miR-10a and miR-155, were not differentially expressed in other studies[319,320]. Even in the same study, miR-196a and miR-30a-5p were upregulated using qRT-PCR, but they were not significantly upregulated using microarray.[322] These discrepancies highlight the importance of standardization in all stages of a microRNA study.

Lupus nephritis

Several miRNAs (miR-141, miR-192, miR-200a, miR-200b, miR-200c, miR-205, miR-429) were examined using qRT-PCR in serum and urine of patients with lupus nephritis (LN).[324] In this study, the authors used a standard input volume of total RNA, and RNU48, a small nucleolar RNA, was used for normalization. For serum, all miRNAs except for miR-141 showed decreased expression in patients with LN while inconsistent results were seen in the urine samples. No correlation in the levels of serum and urine miRNAs was found.[324]

In a study that used microarray to examine expression of 851 miRNAs in serum, 51 miRNAs were found differentially expressed when comparing LN patients with controls.[325] Surprisingly, this study did not identify any of the DE miRs in the previous study[324] to be differentially expressed more than 2-fold.[325] Eight of the DE miRNAs were validated by qRT-PCR using cel-lin-4 as the normalizer. MiR-125a, miR-146a, and miR-155 were decreased, and miR-126, miR-16, miR-21, miR-223, and miR-451 were increased in LN patients compared to controls.[325]

In another study, expression of miR-335, miR-302d, miR-200c, miR-146a were examined in urinary exosomes obtained from patients with LN.[326] Cq values normalized by spike-in cel-miR-39 were used to compare miRNA expression between patients and controls, showing all 4 miRNAs were upregulated in LN (up to a 15-fold change in miR-146a). When focusing on patients with active LN, the fold change for all miRNAs dramatically increased, notably up to a 103-fold change in miR-146a.[326] Interestingly, the expression of urinary miR-200c was found to be increased in LN instead of decreased, as in the previous study[324], and for miR-146a, its levels were upregulated in urine versus downregulated in serum as previously reported.[325] While the discrepancy in expression of miR-200c and miR-146a could be explained by multiple factors, such as different study populations, different samples (serum, cell-free urine, and urinary exosomal pellets), and normalization methods used in qRT-PCR (RNU48, cel-lin-4, and cel-miR-39), it highlights the importance of standardization in the discovery of miRNA biomarkers.[324-326]

IgA Nephropathy

Two studies have also characterized circulating[327] and urinary[88] miRNA expression in patients with IgA Nephropathy (IgAN). In one study, the plasma miRNA signature of patients with IgAN was described based on a miRNA PCR panel to screen 20 IgAN patients and 10 healthy controls.[327] In the screening stage, 48 DE miRs were found (46 upregulated and 2 downregulated miRNAs). Later, the candidate pool of miRNAs was further downsized by performing qRT-PCR in 83 IgAN patients and 82 controls. Eventually, 4 miRNAs (miR-148a, miR-150, miR-20a, and miR-425) were identified to

be upregulated in patients with IgAN (fold change: 2.65-6.13), especially in the early stages of the disease.[327]

In the other study, RNA isolated from urine from 12 patients with IgAN and 12 healthy controls was used to perform small RNA-seq, leading to the identification of 158 urinary DE miRs.[88] Among them, 21 DE miRs with a *P*-value less than 0.01 an absolute fold change of more than 2 were identified, including 12 upregulated and 9 downregulated DE miRs. Notably, 14 out of 21 DE miRs had markedly differential expression (>400 fold change) between IgAN and controls. The results of 2 upregulated miRNAs (miR-378i and miR-215) and 2 down-regulated miRNAs (miR-135b and miR-365b) were subsequently validated by qRT-PCR in a cohort of 6 patients with IgAN and 6 controls. However, the qRT-PCR results were normalized based on RNU6B that was reported to be undetectable in human urine in another study.[315]

These studies demonstrate the potential of using biofluid-derived miRNAs in CKD to non-invasively subtype GN. The discrepancies between studies were likely from differences in multiple steps in the biomarker discovery process, including different criteria in recruiting subjects, sample processing, RNA isolation methods, and data analysis. However, the discovery of markedly DE miRs in biofluids indicates the possibility that robust biomarkers could still be detected despite the presence of substantial technical and biological variation. Large-scale studies and meta-analysis studies are needed to draw more definitive conclusions regarding miRNA biomarker discovery in biofluids.

CHAPTER II

RNA-SEQ OF SERIAL KIDNEY BIOPSIES OBTAINED DURING PROGRESSION OF CHRONIC KIDNEY DISEASE FROM DOGS WITH X-LINKED HEREDITARY NEPHROPATHY*

Introduction

XLHN in dogs leads to CKD because of a defect in type IV collagen in the glomerular basement membrane (GBM). In the XLHN dogs in this study, a naturally-occurring, 10-base-pair deletion in the *COL4A5* gene located on the X chromosome results in the inability to synthesize complete α5 chains.[19] This alteration in the type IV collagen network compromises the structure and function of the GBM in both affected (hemizygous) males and, to a lesser extent, carrier (heterozygous) female dogs.[20]

XLHN in dogs is analogous to Alport syndrome (AS) in humans, as approximately 85% of people with AS have an X-linked mutation in *COL4A5*.[328] AS is characterized by juvenile-onset CKD, ocular abnormalities, and hearing loss in affected males.[329] Thus far, only the renal abnormalities have been detected in XLHN dogs.[20] In dogs with XLHN, juvenile-onset CKD manifests as persistent proteinuria of glomerular origin as early as 3-

*Reprinted from "RNA-seq of serial kidney biopsies obtained during progression of chronic kidney disease from dogs with X-linked hereditary nephropathy" by Candice P. Chu et al., 2017, *Scientific Reports*, 7, 16776, Copyright 2017 by Candice P. Chu.

6 months of age, followed by decreasing GFR and worsening azotemia, typically leading to end-stage renal failure before 1 year of age.[18,20]

Although XLHN has been studied as an example of canine CKD caused by glomerular disease and as an animal model of human AS[20], the gene expression profile that affects progression has only been partially characterized. Furthermore, dogs with the same mutation causing XLHN display substantial variation in the rate of disease progression such that some dogs reach end-stage disease by 6 months of age and others at 12 months of age or later. Although varied times of onset and rates of progression are common among different types of mutations in people with AS[330], disease progression may also vary among members of an AS family with an identical mutation[331], as seen in dogs.[29]

While several studies have characterized gene expression in humans with CKD and in animal Alport models using microarrays[21,332] or PCR[21,23,29,333], studies that have incorporated high-throughput RNA sequencing [30] with the objective of identifying DEGs and upstream regulators are lacking. Compared with traditional approaches in gene expression analysis, RNA-seq provides unprecedented flexibility in the discovery of DEGs[31] while preserving accuracy and strong correlation with PCR[32-36], even considering fold change levels.[37]

The objective of this study was to compare the gene expression between dogs with rapid versus slow disease progression phenotypes at 3 stages of the disease. We conducted Gene Ontology (GO) and pathway analyses to characterize DEGs among sample groups at specific time points. Since all CKDs share common pathways that lead to end-stage

kidney disease[334], the results help elucidate the molecular basis of CKD progression and thus may benefit canine patients and indicate potential therapeutic targets for AS patients.

Material and methods

Animals

The dogs in this study were part of a colony with XLHN maintained at Texas A&M University.[18] XLHN is caused by a 10-base deletion in the gene encoding the α5 chain of type IV collagen. Affected males develop juvenile-onset CKD that progresses to end-stage renal disease as previously described.[18] Overall, 6 affected dogs and 2 unaffected littermates were studied. All dogs were raised according to standardized protocols, and no treatments were given to these dogs. All protocols were approved by the Texas A&M University Institutional Animal Care and Use Committee.

Clinical phenotypes

For this study, dogs were selected to represent both extremes in the speed of disease progression in this family of dogs (rapid versus slow progression). Clinical progression was determined by serial monitoring of serum and urine biomarkers of kidney disease, which allowed us to establish specific progression time points[335]: T1 (onset of proteinuria: defined as the presence of microalbuminuria for 2 consecutive weeks (E.R.D. HealthScreen Canine Urine Test Strips, Loveland, CO, USA)); T2 (onset of azotemia: serum creatinine ≥ 1.2 mg/dL); and T3 (end-stage disease: serum creatinine ≥ 5 mg/dL). Rapidly-progressing (rapid) dogs (n = 3) reached each time point at an earlier age than slowly-progressing [115] dogs (n = 3). On average, the rapid group reached T3 at 26.3 weeks

of age (range: 26-27 weeks), while the slow group reached the last clinical time point (T3) at 49 weeks of age (range: 46-52 weeks) (Supplementary Table S3).

Tissue collection

Kidney cortex was serially collected from each dog at the aforementioned 3 clinical time points (independent of age). Control dogs (n = 2) were biopsied to correspond with an affected littermate. All samples were collected by ultrasound-guided needle biopsy. This technique was appropriate for the current study as it is unlikely to induce changes that might be confused with those of CKD progression.[336] Samples for pathology evaluation and immunohistochemistry were placed in formalin and embedded in paraffin. Samples for RNA sequencing were immediately placed in RNAlater Stabilization Solution (Life Technologies, Foster City, CA, USA) and stored at -80 °C until RNA isolation.

Histopathological evaluation

Paraffin-embedded samples were processed and stained as previously described.[335] To determine the severity of interstitial fibrosis and chronic inflammation, a board-certified veterinary anatomic pathologist (REC) evaluated 5 or 20 randomly chosen 20x fields of renal cortex based on core size for each biopsy. For interstitial fibrosis, a score of 0 to 3 was assigned for each field based on the degree of tubulointerstitial architecture distortion caused by fibrosis: 0 - no fibrosis, 1 - fibrosis present but no distortion, 2 – moderate distortion, and 3 – severe distortion. For chronic inflammation, 0 – no inflammatory cells, 1 – scattered inflammatory cells, 2 – aggregates of inflammatory cells

that separate or replace tubules, and 3 – diffusely distributed inflammatory cells. Statistical analysis comparing the average scores between groups was performed using bootstrap in R (version 3.2.4) to construct simultaneous 95% confidence intervals for all 3 pairwise comparisons of mean fibrosis and chronic inflammation scores at each of the latter 2 disease stages.

RNA isolation and sequencing

The MirVana miRNA Isolation Kit (Ambion, Austin, TX, USA) was used to isolate total RNA from homogenized kidney tissue according to the manufacturer's instructions. The library preparation, sequencing, and initial quality check were performed by the Texas A&M AgriLife Genomics and Bioinformatics Service (http://www.txgen.tamu.edu/). RNA integrity was assessed by the Agilent 2100 Bioanalyzer (Agilent Technologies, Santa Clara, CA, USA). The average RIN was 3.4, and the average RNA yield was 86.2 ng/μL (Supplementary Table S3). To compensate for the low-input samples, we use the TruSeq Stranded Total RNA Library Prep Kit with Ribo-zero Gold (Illumina, San Diego, CA, USA), based on the best practice for RNA with variable qualities[337] (to remove both cytoplasmic and mitochondrial rRNA) and its compatibility with canine samples. Samples were then sequenced using the Illumina Genome Analyzer (HiSeq 2500v4 High Output). Raw sequencing data were submitted to the NCBI SRA (Accession: SRP101707; Samples: SAMN06560417, SAMN06560429-51; BioProject: PRJNA378728).

Data analysis

FastQC (version 0.11.2) was used for quality control to ensure that the quality value was above Q30. The canine (*Canis familiaris*) genome FASTA file (ftp://ftp.ensembl.org/pub/current_fasta/canis_familiaris/dna/Canis_familiaris.CanFam3.1.dna.toplevel.fa.gz) and gene annotation GTF file (CanFam 3.1 assembly; ftp://ftp.ensembl.org/pub/current_gtf/canis_familiaris/) were obtained from Ensembl. Although RNA-seq is a popular research tool, there is no gold standard for analyzing RNA-seq data. Among the available tools, we chose up-to-date open source tools for mapping, retrieving read counts, and differential analysis. We used HISAT2[338] (version 2.0.3-beta) to generate indexes and to map reads to the canine genome. For assembly, we chose SAMtools (version 1.2) and the "union" mode of HTSeq[339] (version 0.6.1), as the gene-level read counts could provide more flexibility in the differential expression analysis. Both HISAT2 and HTSeq analyses were conducted using the high performance research computing resources provided by Texas A&M University (http://hprc.tamu.edu) in the Linux operating system (version 2.6.32). Differential expression and statistical analysis were performed using DESeq2 (release 3.3) in R (version 3.2.4). DESeq2[272] was chosen as it is a popular parametric tool that provides a descriptive and continually updated user manual. DESeq2 internally corrects for library size, so it is important to provide un-normalized raw read counts as input. We used variance stabilizing transformation to account for differences in sequencing depth. *P*-values were adjusted for multiple testing using the Benjamini-Hochberg procedure.[340] A false discovery rate adjusted *P*-value (ie, q-value) < 0.05 was set for the selection of differentially expressed genes.

Gene ontology (GO), pathway, and upstream regulator analysis

GO and PANTHER pathway analyses were performed with the PANTHER Overrepresentation Test (released on July 15, 2016) in PANTHER[341] version 11.1 (http://www.pantherdb.org/, released on October 24, 2016). This program supports the canine genome. Also, Qiagen's Ingenuity Pathway Analysis (IPA, Qiagen Redwood City, www.qiagen.com/ingenuity) was used to provide overrepresented orthologous genes in human, mouse, and rat databases and to identify orthologous pathways and upstream regulators in our data. PANTHER used the binomial test and Bonferroni correction for multiple testing, while IPA used the right-tailed Fisher Exact test and displayed z-scores to indicate whether a potential regulator was activated or inhibited. We used the default settings for statistical analysis in both the PANTHER pathway and IPA. In PANTHER, only pathways and GO terms with fold enrichment > 0.2 were listed. In IPA, *P*-value < 0.05 and fold change > 2 were set as cutoff values.

Immunohistochemistry (IHC)

Three-micrometer, formalin-fixed, paraffin-embedded renal cortex sections of both affected and control dogs were stained for CD3 (n = 24) and CD20 (n = 9). After deparaffinization, the sections were placed in citrate buffer (pH 6.0) for antigen retrieval, using a pressure cooker (Decloaking Chamber, Biocare Medical). Endogenous peroxidase activity and non-specific protein binding were blocked with 3% hydrogen peroxide and Sniper protein block (Biocare Medical), respectively. After blocking, the sections were incubated with primary antibodies CD3 (1:300 dilution; Dakocytomation, Carpinteria, CA) and CD20 (1:500 dilution; Thermo Scientific, Fremont, CA) for 1 hour at room

temperature, then incubated with MACH 2 polymer for 30 minutes at room temperature. DAB (Vector Laboratories, Burlingame, CA) was used as the chromogen to demonstrate sites of antibody-antigen reaction. Mayer's hematoxylin was used for the counterstain. Photographs were obtained using a SPOT Insight 2Mp FW Color Mosaic Camera (Diagnostic Instruments, Inc., Sterling Heights, MI) and the SPOT software (version 5.2).

Results

Histopathological evaluation of kidney biopsies

Figure 3 presents representative cortical fields of the kidney biopsies and the mean interstitial fibrosis scores comparing the rapid versus slow groups. Clinical time points in affected dogs were defined as: T1 - onset of proteinuria (the earliest time point that clinical disease can be detected); T2 - onset of azotemia (sCr $\geq$ 1.2 mg/dL); and T3 - end-stage disease (sCr $\geq$ 5 mg/dL). At both T2 and T3, mean fibrosis and chronic inflammation scores were significantly higher in diseased dogs than in controls (Supplementary Table S4-S5). The degree of fibrosis in the rapid group was more severe at T2 and T3 than that in the slow group, despite the 2 groups being clinically indistinguishable; however, statistical significance between the scores was reached only at T3 (Supplementary Table S6 and Figure S1). No statistically significant difference was observed for the chronic inflammation score between the rapid and slow groups (Supplementary Table S7 and Figure S2).

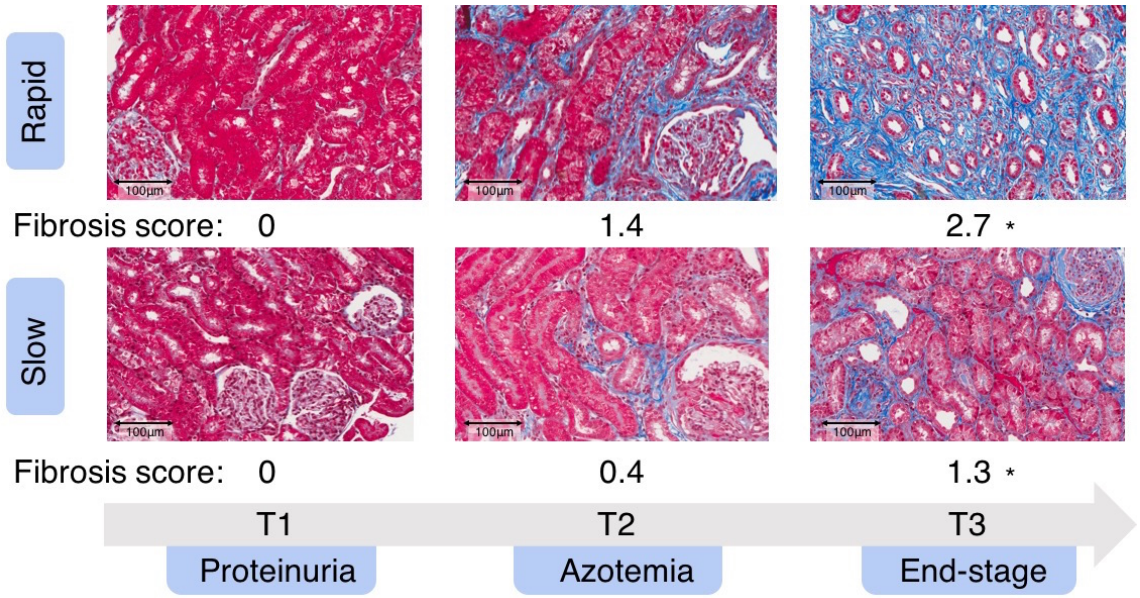

Figure 3. Kidney biopsies from representative dogs and mean interstitial fibrosis scores. Scores are ranged from 0 [normal] to 3 [severe] for each group of affected dogs at 3 time points (T1, T2, and T3). Fibrosis scores were based on evaluation of multiple 20x fields. *Statistical significant. Scale bar: 100 µm. Trichrome-stained.

RNA-sequencing of dog transcriptomes

The average RNA yield from the 24 kidney biopsies was 86.2 ng/µL, and the average RIN was 3.4 (Supplementary Table S8). Because of the variable quality of RNA, the proper library preparation kit was used to compensate for the low-input samples according to the best practice for RNA with variable qualities[337] (see "RNA isolation and sequencing" section in Methods). After performing quality control, we obtained an average of over 30 million paired-end reads from each sample (n = 24). Overall, 91-96% of reads were mapped to the canine genome (CanFam 3.1) by HISAT2.[338] Among them, 70-78% of reads were uniquely mapped (Supplementary Table S8 and Figure S3). Based

on the union setting of HTSeq[339], ambiguous reads that mapped to multiple genes were not included in our analysis.

Principal component analysis (PCA) and hierarchical clustering analysis

We performed PCA at each time point to determine whether samples in each group clustered with each other or other groups. First, we used HTSeq[339] to count reads that uniquely aligned to one gene, and these data were then imported into DESeq2[272] to generate PCA plots. At T1, the PCA results demonstrated that most samples clustered together, regardless of the grouping (Figure 4). Except for one dog, rapid and slow groups became separated from controls at T2. Although the slow group tended to be closer to the controls than the rapid group, there was no clear distinction between rapid and slow groups at T2 or T3. Furthermore, PCA scree plots confirmed that principal components 1 (PC1) and 2 (PC2) accounted for 76-90% of the total variation in gene expression at each time point (Supplementary Figure S4). To further investigate the time-dependent nature of the DEGs, we performed hierarchical clustering of the top 100 DEGs (ie, those with the smallest q-value identified in the time course analysis in DESeq2). In agreement with the PCA plots, this analysis demonstrated clustering of almost all sample groups at T1 (Figure 5A). At time points T2 and T3, the rapid and slow groups clustered together (Cluster 1 in Figure 5A) and were distinctly separated from the control group for all but one T2 sample (Cluster 2 in Figure 5A).

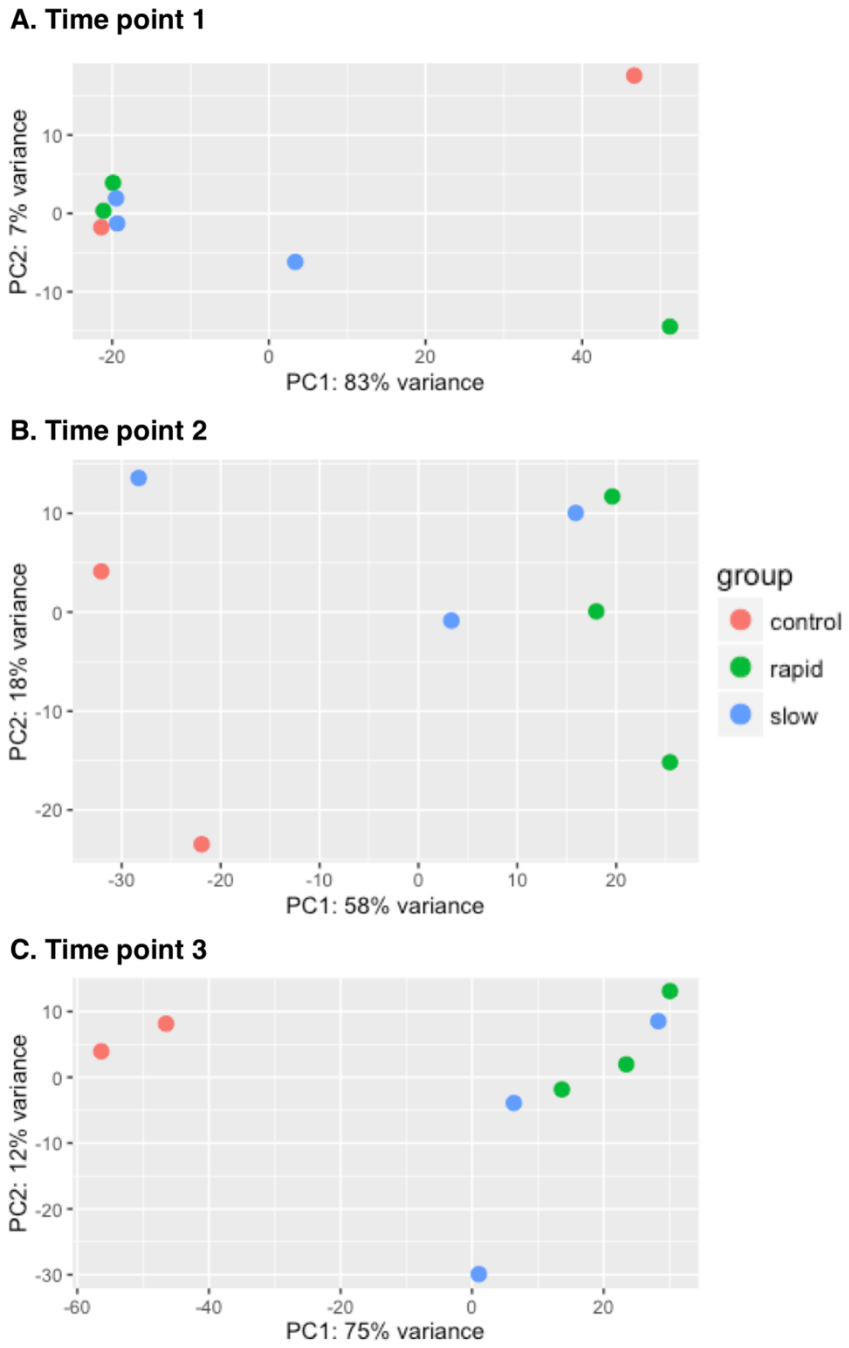

Figure 4. Principal component analysis (PCA) for all samples at 3 time points. Principal component 1 (PC1) and principal component 2 (PC2) were identified by variance stabilizing transformation in DESeq2 at the 3 time points. The percentage of variance indicates how much variance was explained by PC1 and PC2. (Red: control group; Green: rapid group; Blue: slow groups).

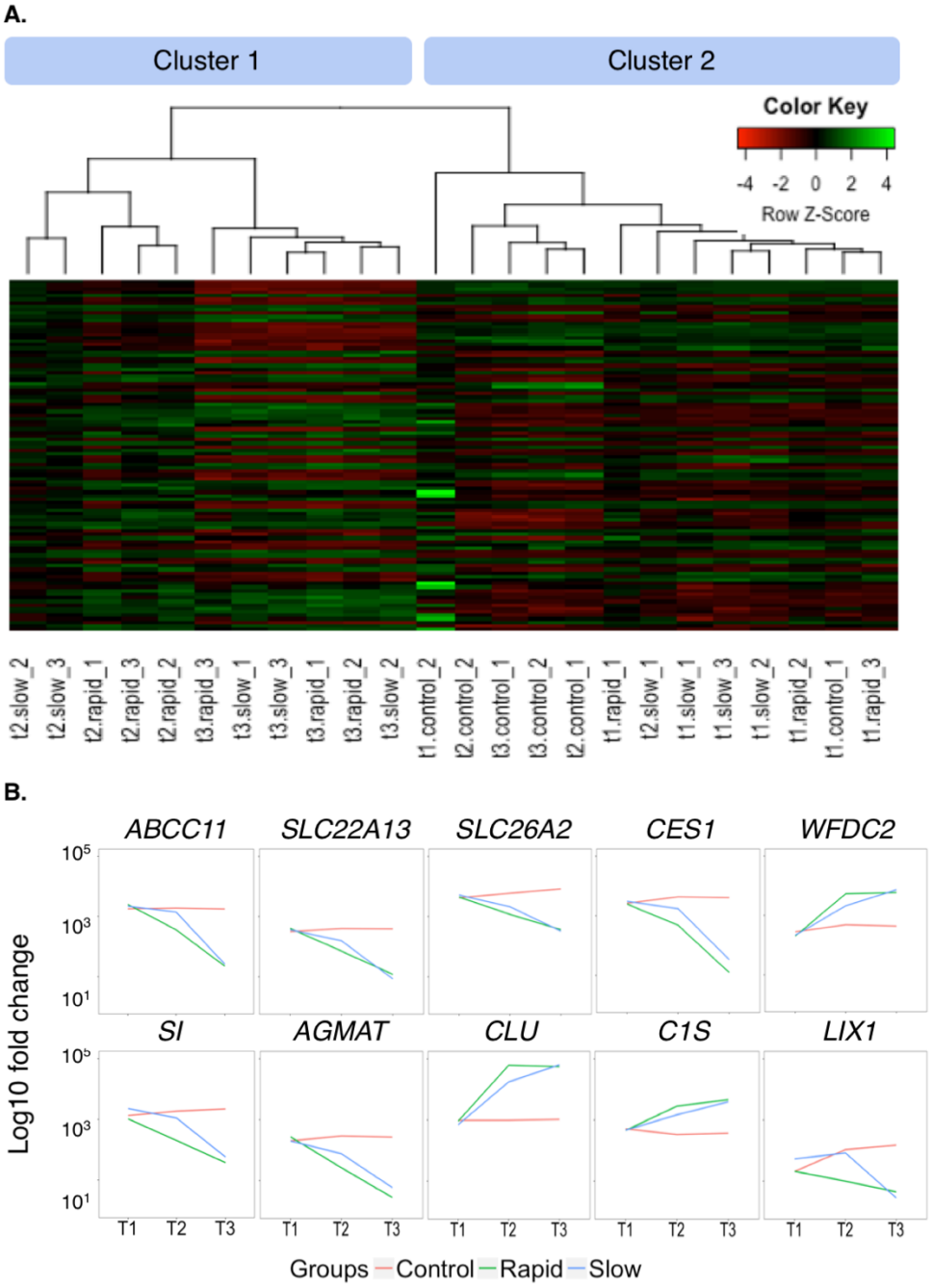

Figure 5. Hierarchical clustering analysis, heatmap, and gene expression. (A) Hierarchical clustering analysis and heatmap of the 100 genes with the smallest q-values in the time course analysis in DESeq2 (Column names: t1, t2, and t3 designate 3 clinical time points; slow, rapid and control represent grouping; _1, _2, and _3 are individual dogs in each group). (B) Trends of gene expression over time for the 10 genes with the smallest q-values (from left to right, top to bottom) (Red: control group; Green: rapid group; Blue: slow group).

Differentially expressed genes (DEGs)

In average, 20,090 genes were mapped by at least one read in each of the kidney biopsy samples (Supplementary Table S8). Overall, 1,947 DEGs with a q-value < 0.05 were detected over the 3 time points in the time course analysis of DESeq2 (Supplementary Table S9). We applied the plot counts function in DESeq2 to visualize the top 10 genes with the smallest q-values (Figure 5B). While these genes were not differentially expressed at T1, group-specific changes were observed over time, and expression in the slow group was consistently closer to that in the control group for each gene at T2 (Figure 5B).

To achieve the primary goal of this study, we identified 70 DEGs between the rapid and slow groups among all time points (q-value < 0.05) (Table 4). In this comparison, T2 demonstrated the most DEGs, with 68 of the 70 DEGs unique to T2. Two DEGs were identified at T1: stearoyl-CoA desaturase 5 (SCD5) (fold change = -3.55, q-value = 1.1×10^{-05}), which was also detected at T2, and thymidine kinase 1 (TK1) (fold change = 2.49, q-value = 0.02). At T3, no DEGs were identified when these 2 groups were compared.

Table 4. Overview of 70 significant DEGs comparing rapid and slow groups.

Up-regulated DEGs in the rapid group			
Gene Symbol	Full Name	Fold Change	q-value
COL1A1	Collagen type I alpha 1 chain	6.52	2.62E-20
COL3A1	Collagen type III alpha 1 chain	5.35	1.05E-17
COL1A2	Collagen type I alpha 2 chain	4.01	4.66E-13
COL5A1	Collagen type V alpha 1 chain	3.8	7.21E-05
COL6A3	Collagen type VI alpha 3 chain	3.27	7.08E-07
COL6A1	Collagen type VI alpha 1 chain	3.26	1.82E-05
LOX	Lysyl oxidase	3.13	1.42E-03
COL6A2	Collagen type VI alpha 2 chain	3.07	2.34E-04
PAMR1	Peptidase domain containing associated with muscle regeneration 1	2.99	5.76E-03
CDCA8	Cell division cycle associated 8	2.98	2.80E-02
COL11A1	Collagen type I alpha 1 chain	2.86	5.33E-03
COL15A1	Collagen type XI alpha 1 chain	2.82	6.24E-03
C1QTNF6	C1q and tumor necrosis factor related protein 6	2.81	4.98E-03
FNDC1	Fibronectin type III domain containing 1	2.81	3.22E-02
FN1	Fibronectin 1	2.8	4.10E-02
CCDC80	Coiled-coil domain containing 80	2.72	7.98E-04
MFSD7	Major facilitator superfamily domain containing 7	2.7	3.22E-02
FBLN1	Fibulin 1	2.69	4.10E-02
NID2	Nidogen 2	2.61	1.52E-07
COL4A2	Collagen type IV alpha 2 chain	2.6	1.42E-03
FAM69B	Family with sequence similarity 69, member B	2.6	3.42E-02
NDN	Necdin	2.59	4.39E-02
COL4A1	Collagen type I alpha 1 chain	2.59	5.76E-03
HTR7	5-hydroxytryptamine (serotonin) receptor 7, adenylate cyclase-coupled	2.58	2.60E-02
PCOLCE	Procollagen C-endopeptidase enhancer	2.58	5.83E-03
OLFML2B	Olfactomedin like 2B	2.56	6.24E-03
TK1a	Thymidine kinase 1	2.49	1.98E-02
C15orf39	Chromosome 15 open reading frame 39	2.47	2.76E-02
RCN3	Reticulocalbin 3	2.46	6.94E-04
MFAP2	Microfibrillar associated protein 2	2.45	1.42E-03
HSPG2	Perlecan	2.45	1.20E-02
PRSS35	Protease, serine 35	2.45	4.10E-02
MMP2	Matrix metallopeptidase 2	2.43	4.48E-05
FBN1	Fibrillin 1	2.37	3.57E-03
CD248	CD248 molecule	2.36	2.72E-02
FOXRED2	FAD dependent oxidoreductase domain containing 2	2.35	1.11E-02
GXYLT2	Glucoside xylosyltransferase 2	2.34	3.62E-02
FSCN1	Fascin actin-bundling protein 1	2.34	1.20E-02
ENSCAFG00000008741c	Novel gene	2.29	1.18E-02
ENSCAFG00000012963c	Novel gene	2.28	1.23E-03
BGN	Biglycan	2.19	1.85E-02

Table 4. Continued.

Up-regulated DEGs in the rapid group			
Gene Symbol	Full Name	Fold Change	q-value
FAS	Fas (TNF receptor superfamily member 6)	2.16	2.08E-02
ADAMTS2	ADAM metallopeptidase with thrombospondin type 1 motif 2	2.15	3.23E-02
PXDN	Peroxidasin	2.14	4.10E-02
SPARC	Secreted protein acidic and cysteine rich	2.13	4.48E-05
THBS1	Thrombospondin 1	2.12	1.26E-04
KCP	Kielin/chordin-like protein	2.12	4.19E-02
LRP1	LDL receptor related protein 1	2.11	7.98E-04
CERCAM	Cerebral endothelial cell adhesion molecule	2.11	4.39E-02
ITGA5	Integrin subunit alpha 5	2.07	7.03E-03
BMP1	Bone Morphogenetic Protein 1	1.88	6.74E-05
FSTL1	Follistatin Like 1	1.72	1.25E-05
PTGFRN	Prostaglandin F2 Receptor Inhibitor	1.66	2.61E-05
Down-regulated DEGs in the rapid group			
UGT1A6	UDP glucuronosyltransferase family 1 member A6	-4.77	1.23E-03
NAT8	N-acetyltransferase 8 (putative)	-4.1	1.09E-04
R3HDML	R3H domain containing like	-4.02	1.42E-03
LIX1	Limb and CNS expressed 1	-3.83	7.21E-03
PRLR	Prolactin receptor	-3.73	4.64E-04
SCD5[b]	Stearoyl-coa desaturase 5	-3.55	1.07E-05
FMO2	Flavin containing monooxygenase 2	-3.42	1.78E-02
OAT3/SLC22A8	Solute carrier family 22 member 8	-3.37	2.45E-02
SI	Sucrase-isomaltase	-3.25	1.16E-02
ENSCAFG00000003760[c]	Novel gene	-2.92	3.96E-02
SLC26A4	Solute carrier family 26 member 4	-2.79	7.14E-03
ENSCAFG00000000799[c]	Novel gene	-2.77	3.25E-02
HEPACAM2	HEPACAM family member 2	-2.66	8.81E-03
IDO2	Indoleamine 2,3-dioxygenase 2	-2.58	3.42E-02
PECR	Peroxisomal trans-2-enoyl-coa reductase	-2.57	6.24E-03
MT-ND3	Mitochondrially encoded NADH dehydrogenase 3	-2.16	3.49E-03
ABCA4	Retinal-specific ATP-binding cassette transporter	-1.91	1.08E-04

[a] DEG identified only at T1.
[b] DEG identified at both T1 and T2.
[c] Genes are displayed with ensembl IDs if gene annotations are unavailable.

We also compared the rapid and slow groups with the control group, both individually and combined as a single "affected" group (Figure 6A). In these comparisons, the number of DEGs increased with advancing disease, with the largest number of DEGs identified at T3. This phenomenon indicates that the DEGs are disease-dependent as they are more differentially expressed in the later time points (T2 and T3) than T1 (Figure 6).

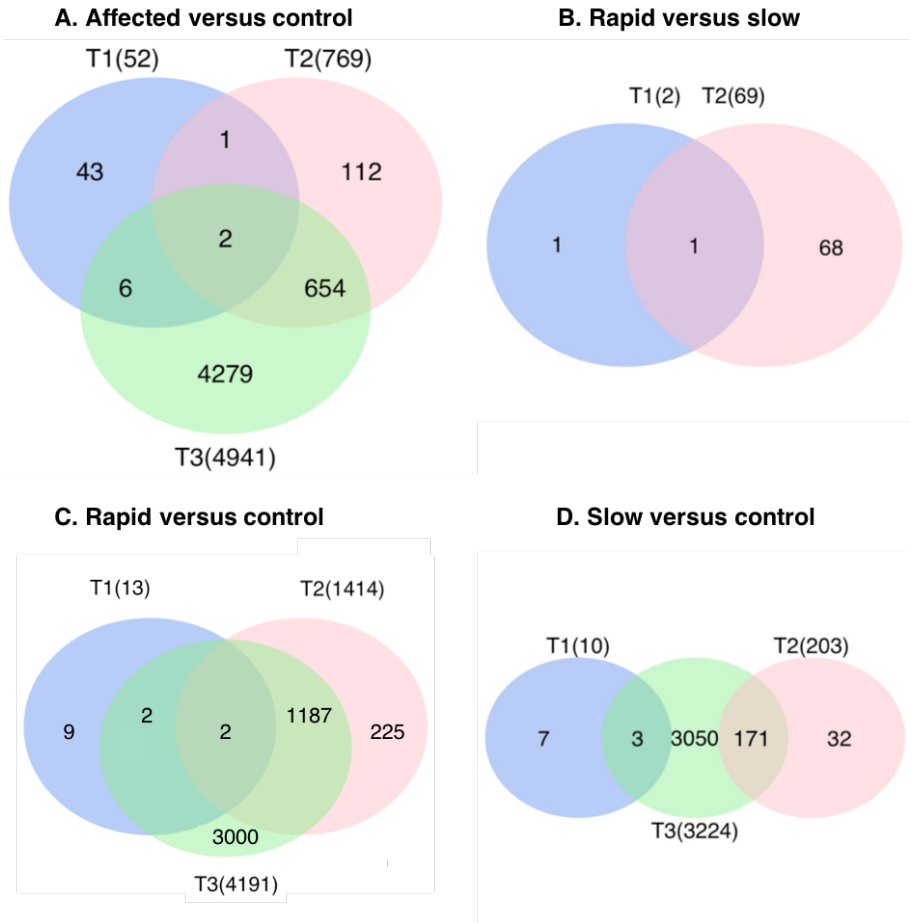

Figure 6. DEGs in different pairs of comparison at the 3 time points (T1, T2, and T3). Comparing the rapid and slow groups, 70 DEGs were found. Comparing each affected group with controls, several thousand DEGs were identified, with most of the DEGs occurring at T3. For each pair, only genes with a q-value < 0.05 were considered as DEGs. The total number of DEGs found at each time point appears in parentheses.

A substantial overlap of DEGs was present when comparing rapid and slow groups with the control group at T2 and T3 (Figure 7). The overlapping DEGs between the rapid and slow groups were more numerous at T3 (2,952 DEGs) than at T2 (190 DEGs), supporting that the 2 groups behave similarly at the end-stage disease, as expected based on Figs. 4-6. Furthermore, the number of DEGs (1,189 DEGs) identified in both T2 and T3 in the rapid group was higher than the number of DEGs (171 DEGs) identified in both T2 and T3 in the slow group. This supports the theory that rapidly-progressing dogs express end-stage DEGs at a young age. The complete lists of DEGs from the time course analysis and all pairs of comparisons appear in Supplementary Table S9.

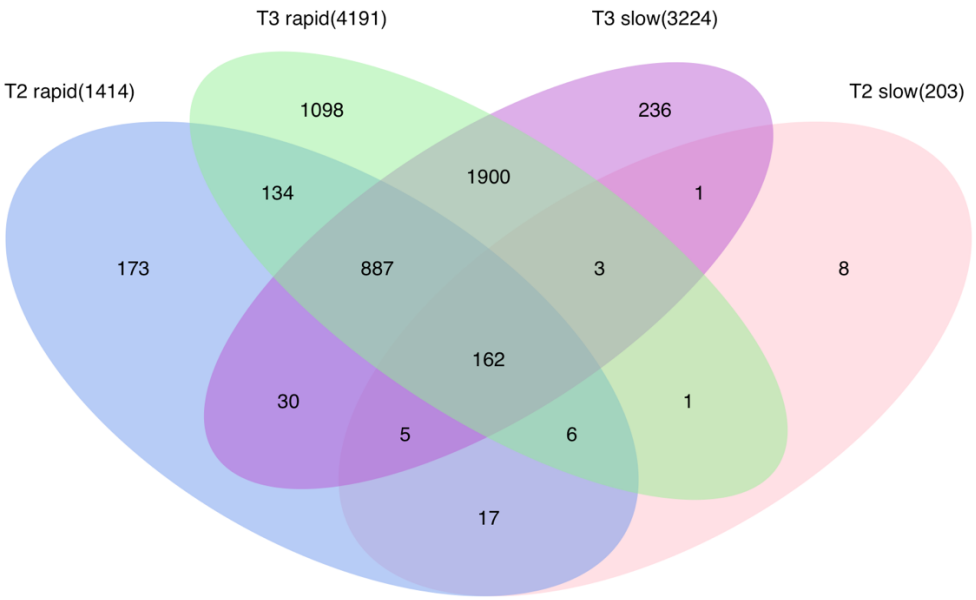

Figure 7. Overlapping DEGs in rapid and slow groups compared with control at T2 and T3. For each comparison, only genes with a q-value < 0.05 were considered as DEGs. The total number of DEGs found at each time point appears in parentheses.

Gene Ontology (GO) and pathway analysis of DEGs

To characterize the GO terms, including molecular functions, biological processes, cellular components, and functional pathways of DEGs, we conducted over-representation tests for all pairs of comparisons in PANTHER version 11.1 (released on October 24, 2016) (Figure 8 and Supplementary Table S10). We used the GO-Slim PANTHER annotation data set, which represents phylogenetically inferred annotations.[341]

Overlap of GO terms among comparisons was commonly seen in the current study. We will focus on "biological process" since it is the most characterized GO term. Within this category, the "immune system process" family was upregulated in all 10 comparisons presented in Figure 8, and the "immune response" family was upregulated in all except for the rapid versus slow comparison at T2 and the time course analysis. Both immune-related GO terms appeared to be more upregulated at T2 than T3. At T2, the "biological adhesion" family, especially the cell-cell adhesion subfamily, was expressed in the rapid group more than in the slow group (Supplementary Table S10).

The most common pathway represented by the DEGs within the various comparisons was the "integrin signaling pathway" (Figure 8). This was the only pathway identified in the comparison between rapid and slow groups. It was also the top upregulated pathway at T2 comparing rapid and control groups. Interestingly, analyzing the overlapping DEGs between T2 and T3, the integrin signaling pathway was identified as the top upregulated pathway within the rapid group, but not within the slow group, as compared with control.

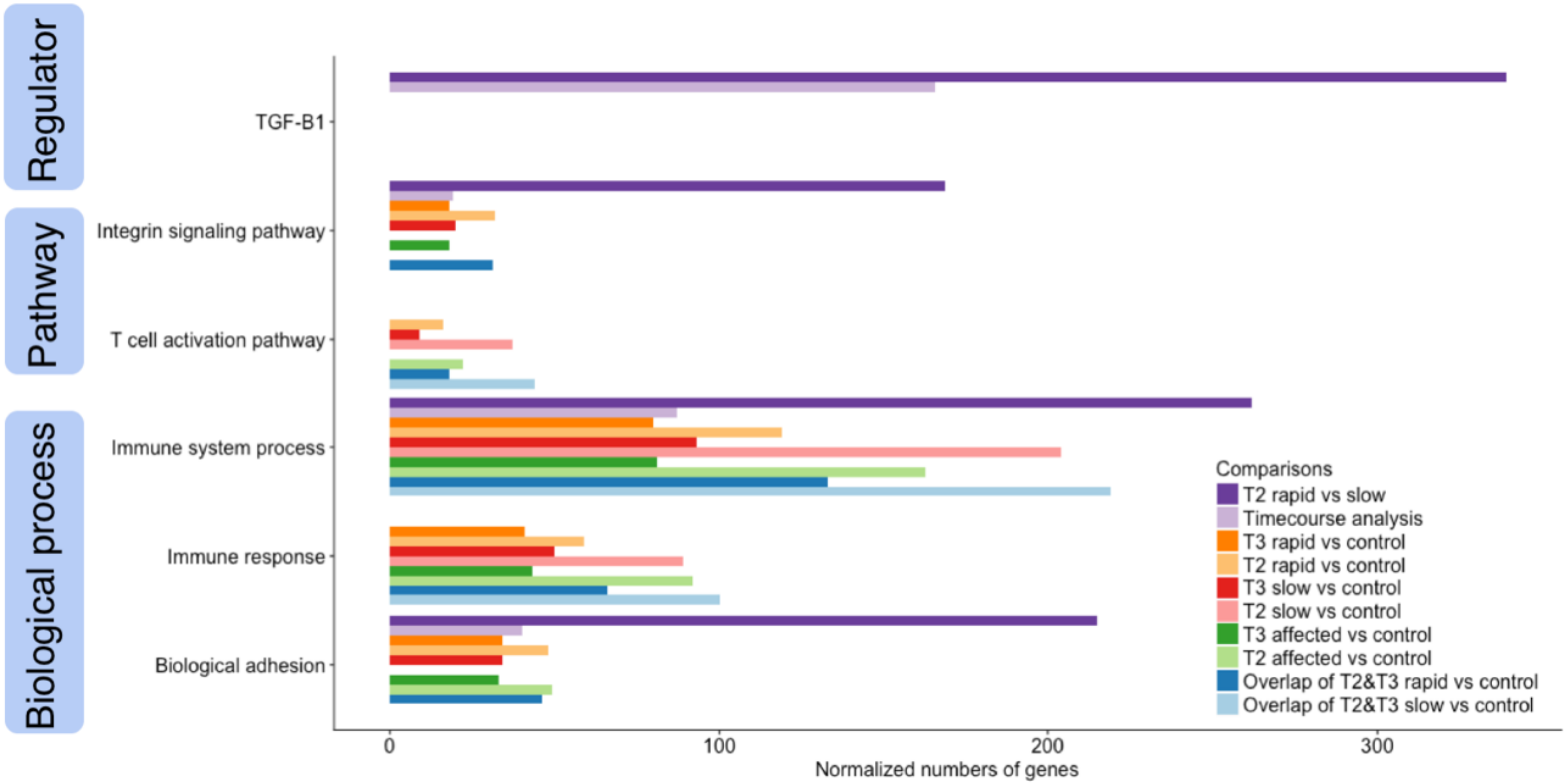

Figure 8. Enriched pathways and GO term analysis for 10 selected comparisons. Enriched pathways, biological processes, and regulator analysis for all DEGs are presented based on T2 and T3 comparisons as well as a time course analysis incorporating all time points for all groups. The number of genes was normalized to allow comparison between groups within the same pathway, and comparisons were color coded in pairs, with the darker color corresponding to the later time point or the rapid group.

The "T cell activation" pathway was another frequently detected pathway in our study (Figure 8). It was upregulated in all comparisons with control at T2 and in overlapping DEGs between T2 and T3 within both the rapid and the slow groups. Another upregulated pathway included the "inflammation mediated by chemokine and cytokine signaling pathway" that was identified only when comparing all affected dogs with controls at T2. Because only limited numbers of DEGs were discovered, no enriched pathways were identified at T1 with any comparison.

To further explore the possible biological interaction between orthologous genes in the human, mouse, and rat, we performed Ingenuity Pathway Analysis (IPA) to discover the most prevalent pathways and upstream regulators within each comparison. The "hepatic fibrosis/hepatic stellate cell activation pathway" was identified as the top pathway in multiple comparisons (Supplementary Table S11). Transforming growth factor beta 1 (TGF-β1) was the most activated upstream regulator when the rapid and slow groups were compared at T2 and in the time course analysis (Supplementary Table S11).

Immunohistochemistry (IHC) validation of inflammatory pathways

Lastly, we aimed to validate the overexpression of inflammatory pathways in kidney biopsies. We chose to identify the predominant lymphocyte subtype present (T versus B cell) since the identified inflammatory pathways are all closely related to the presence of T lymphocytes[342] and antibodies for CD3 (T cell) and CD20 (B cell) are validated for use in dogs.[343,344] As shown in Figure 9, we confirmed the lymphocyte infiltration in the affected dogs to be composed mostly of T cells rather than B cells. This result correlates with the previously assigned chronic inflammation scores based on the

histopathological evaluation (Supplementary Table S5 and Figure S2) and validates our RNA-seq data.

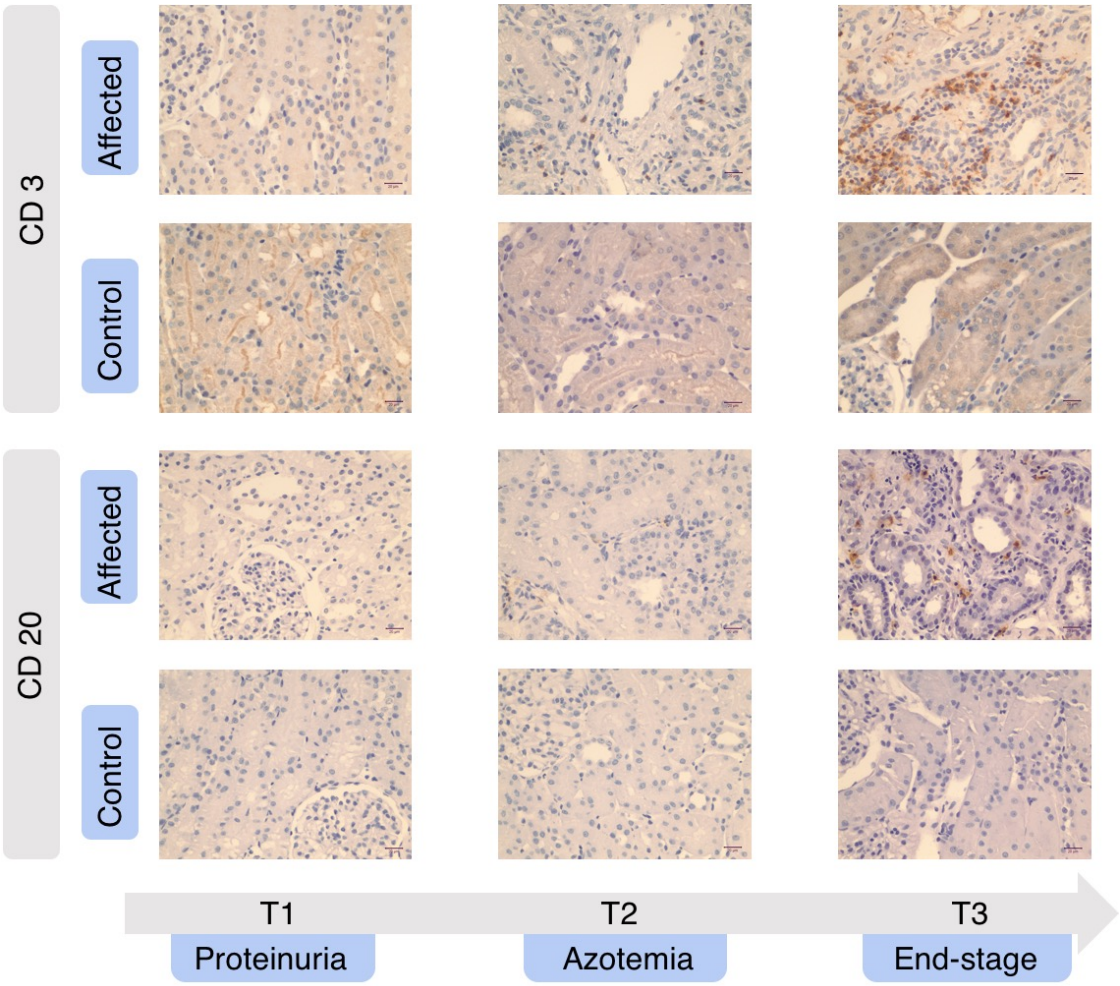

Figure 9. Expression of CD3 and CD20 using IHC in kidney biopsies from representative dogs. In affected dogs, lymphocyte infiltration presented at later time points consisted mostly of CD3-positive lymphocytes with few CD20-positive lymphocytes identified. Scale bar: 20 μm.

Discussion

Dogs with XLHN have been studied as both an example of progressive canine glomerular disease and an animal model of human AS, which has CKD as a major syndrome component.[20] The genetic cause is well characterized; however, the gene expression and molecular pathways influencing disease progression are incompletely known. In particular, the variable rate of disease progression in dogs with the same mutation and within families affected by AS is intriguing.[331] We, therefore, aimed to evaluate differential gene expression, overrepresented pathways, and upstream regulators by comparing RNA-seq data in dogs that displayed a rapid clinical progression of the disease to those with relatively slow disease progression.

In this study, we examined serial biopsies from rapid and slow groups as well as healthy age-matched littermates. To understand the biological changes during the pathogenesis of CKD, we included the earliest time point at which clinical disease could be detected in these dogs (onset of proteinuria, T1), with the onset of azotemia (T2) and the advent of end-stage disease (T3). By performing renal biopsies when animals reached specific clinical markers of disease progression, we could compare the same clinical stage in the rapid and slow groups. We believe this type of approach provides more confidence in identifying DEGs that are involved in the rate of disease progression than the traditional method of using age-driven time points, as differences detected are likely to be the driving force rather than the consequence of disease progression. Our data demonstrate the dynamic changes in gene expression at different stages of the disease. It also supports that the biological processes and pathways of fibrosis/adhesion and inflammation are the likely

driving forces producing different rates of disease progression in the rapid and slow groups.

While it is known that serum creatinine correlates strongly with tubulointerstitial fibrosis[335], one of the most intriguing findings when comparing the rapid and slow groups was the increase in fibrosis observed in the rapid group at the same clinical stage of disease (T2 and T3; Figure 3). This corresponds with many of the 70 DEGs identified using RNA-seq between the rapid and slow groups that are implicated in fibrosis, almost all of which were identified at T2. Several of these genes have been previously described as upregulated in XLHN dogs, Alport mice, and other kidney diseases.[21,23,345,346] Among these, one of the upregulated genes, *CD248* (endosialin or tumor endothelial marker 1, *TEM1*), has been found to mediate the adhesion and migration of cells through ligand interaction with the upregulated collagen-related genes: collagen type I, collagen type IV, and fibronectin-1(*FN1*).[347] CD248+ stromal cells bind extracellular matrix and have been implicated in kidney[348], liver[349], and lung fibrosis.[350] In non-inflamed kidneys, CD248 is expressed by mesangial cells located in glomeruli. In fibrotic kidneys, CD248 is additionally expressed by myofibroblasts and stromal fibroblasts, and the increased expression is closely related to prognostic indicators, such as albuminuria and renal scarring.[348] Of note, one of the downregulated genes in the rapid group, prolactin receptor (*PRLR*), decreased in association with the extent of interstitial collagen I deposition in kidney transplant rejection[351], suggesting that PRLR might be a protectant against renal fibrosis. In our study, the decrease in *PRLR* could be responsible for the more rapid development of fibrosis and consequential faster progression of disease in the rapid group.

Involvement of inflammatory components in the progression of CKD is another major finding of this study. Several inflammatory genes involved in fibrotic changes, such as biglycan (*BGN*), kielin/chordin-like protein (*KCP*), and *MMP2* were upregulated in the rapid versus slow groups. BGN plays a role in bone growth, muscle development and regeneration, and collagen fibril assembly in multiple tissues. *BGN* is upregulated in renal fibrosis[27], and BGN protein expression strongly correlated with chronic kidney progression in one study[345], which may suggest its role in regulating inflammation and innate immunity. KCP expression is stimulated by renal stress, and it enhances the antifibrotic function of BMP7 to attenuate the profibrotic stimulus of TGF-β and to suppress proinflammatory cytokines.[352] In Alport mice, the administration of recombinant BMP7 reduces glomerular and interstitial fibrosis but also upregulates MMP2.[353] This upregulation of MMP2 seems contradictory, as it is associated with renal fibrosis in several animal models, including XLHN dogs.[23] However, the function of MMP2 is specific to the temporal context of fibrosis. At the prefibrotic phase, increased MMP2 induces epithelial to mesenchymal transition, tubular atrophy, and fibrosis. For established fibrosis, inducing MMP2 synthesis by BMP7 promotes proteolytic removal of accumulated extracellular matrix, which is thought to be a potential therapeutic strategy.[354] Since both KCP and MMP2 are upregulated at T2, when fibrosis is already relatively well established in the rapid group, their downstream actions are likely skewed toward anti-fibrotic effects.

Mechanisms other than fibrosis and inflammation can also play roles in the rapid progression of CKD. *NAT8,* which is almost exclusively expressed by tubular cells in the

renal cortex[355], is a cysteine S-conjugate N-acetyltransferase that is responsible for glutathione-mediated detoxification of nephrotoxic substances. The downregulation of NAT8 in the rapid group suggests a more severe loss of normal renal function in the presence of similar serum creatinine concentrations compared with the slow group. Another downregulated gene, organic anion transporter 3 (*OAT3*, also known as *SLC22A8*), is decreased in kidney biopsies from human CKD patients[46] and in a nephrectomized rat model of CKD.[356,357] Reduced protein expression of Oat3 is associated with decreased excretion of an endogenous uremic toxin; meanwhile, the accumulation of this uremic toxin further inhibits Oat3-mediated transportation, accelerating toxin accumulation in serum.[356,357] Therefore, downregulation of *OAT3* in the rapid group may result in impaired urinary excretion that is not adequately represented by serum creatinine concentration.

Only 2 DEGs, SCD5 and TK1, were differentially expressed in the rapid group as compared with the slow group at T1. SCD5 was downregulated at both T1 and T2 in the rapid compared with the slow group. And, it was downregulated in the rapid versus control comparison throughout all 3 time points. SCD5 is an isoform of stearoyl-CoA desaturase that is responsible for the formation of monounsaturated fatty acids. Although SCD5 has not previously been described in the CKD literature, it has been proposed as a novel regulator of neural cell proliferation and differentiation, likely through β-catenin-independent (non-canonical) Wnt pathways.[358] In fibrotic kidneys, the canonical Wnt pathway induces myofibroblast differentiation, and the non-canonical Wnt pathway leads to cytoskeleton rearrangement, cell adhesion, and cell movement.[359] *TK1* is the only DEG

that was exclusively upregulated at T1. Thymidine kinase is responsible for producing dTMP that is later incorporated into DNA. The cytoplasmic isoform of TK1 is cell cycle-dependent, as it substantially increases in the S phase of the cell cycle. Given that unregulated proliferation is the hallmark of neoplasia, TK1 is a valuable serum marker for breast cancer, non-Hodgkin's lymphoma, plasmacytoma, and lung cancer.[360] Its upregulation in our study could indicate increased cell proliferation at T1 in the rapid group. However, further investigation of SCD5 and TK1 is needed to determine their roles in CKD progression.

In addition to abovementioned genes, many genes that are rarely described in CKD progression were found differentially expressed in the rapid versus slow groups at T2 (eg, *LOX, PAMR1, CDCA8, C1QTNF6, FNDC1, CCDC80, MFSD7, FMO2, SI, SLC26A4*). The protein product of the upregulated gene lysyl oxidase (*LOX*) is an extracellular enzyme that is essential for covalent cross-linking of collagen in irreversible extracellular matrix deposition.[361] Despite reports of its upregulation in liver fibrosis[362,363] and cardiomyopathy[364], the upregulation of LOX in CKD has only been described in one study using a glomerulonephritis mouse model.[365] Simtuzumab, a monoclonal antibody that inhibits one of the LOX family members, lysyl oxidase homologue 2 (LOXL2), has recently been a focus of research as a possible new treatment for lung, liver, and kidney fibrosis due to a similar pathogenesis.[366] Another gene minimally described in nephrology is the downregulated sucrase-isomaltase (*SI*). SI is an α-glucosidase that commonly appears on the brush border of small intestinal enterocytes and is involved in glucose digestion. SI is also present in small amounts in non-intestinal cells such as blood

leukocytes and kidney cells.[367] Little is known about the function and significance of SI in the renal tubule. However, the decreased expression of SI could indicate renal damage.

To characterize DEGs in functional groups, we performed GO terms and pathway analyses by comparing affected dog groups, both individually and collectively, with control dogs at each time point. GO terms showed that the functions of identified DEGs were associated with "biological adhesion," "immune system processes," and "immune response," representing a common mechanism of disease progression in the early stages of CKD.[368] Consistent with the GO terms, the "integrin signaling pathway" was the most upregulated pathway, and the "T cell activation pathway" and the "chemokine and cytokine signaling pathway" were also upregulated in multiple comparisons. The exclusive early expression of the "integrin signaling pathway" in the rapid group and universal expression at a later time point could indicate that it is an essential pathway driving rapid progression of disease in these dogs. The "integrin signaling pathway" consists mainly of collagen and integrin genes. The integrin subunit α 2 gene (*ITGA2*) was increased in the rapid versus control group at both T2 and T3. The COL4A3$^{-/-}$/ITGA2$^{-/-}$ double knockout Alport mouse model has delayed renal fibrosis compared with COL4A3$^{-/-}$/ITGA2$^{+/+}$ Alport mice, which express significantly higher levels of MMP2, MMP9, MMP12, and TIMP1.[369] Upregulation of *MMP2* is consistent with our Alport dog model, suggesting that the "integrin signaling pathway" is involved in matrix accumulation.

To verify the pathway analysis results, we used IHC to identify the infiltrating lymphocyte population. The "T cell activation," "integrin signaling," and the "inflammation mediated by chemokine and cytokine signaling" pathways are all closely

related to the presence of T lymphocytes.[342] Consistent with this, T lymphocytes were identified as the predominant inflammatory cell population present in the affected dogs, as well as in a study of canine end-stage renal disease.[370] Moreover, T cell infiltration inversely correlates with renal function at the time of renal biopsies in AS patients.[371] Overall, IHC validated the results of GO terms and pathway analyses, which showed that inflammatory pathways and corresponding biological processes are altered during the progression of CKD.

IPA allows for characterizing orthologous genes, and results identify possible mechanisms that have been validated in humans, mice, and rats. The top upregulated pathway identified in multiple comparisons was the "hepatic fibrosis/hepatic stellate cell activation pathway." The IPA identified enriched pathways based on the over-represented DEGs, and the principle is the same as that used in the Gene Ontology analysis via Panther. There was an extensive overlap between the DEGs we identified and the genes involved in the "hepatic fibrosis/hepatic stellate cell activation pathway" in the IPA, including collagen genes, cytokine-related genes, matrix metalloproteinases, tissue inhibitor of metalloproteinase, and the TNF receptor superfamily. Therefore, the upregulation of this pathway in our study supports common mechanisms involved in hepatic and renal fibrosis. It could also indicate contributing genes beyond those identified using known canine gene pathways.

The upstream regulator analysis of IPA identified the TGF-β group, especially TGF-β1, as the top upstream regulator, with both the highest activated z-score and the lowest *P*-value across multiple comparisons. Previous studies in canine[29] and murine[372]

models of AS demonstrated the expression of TGF-β mRNA in kidney tissue. However, TGF-β was not differentially expressed in our comparisons, and IHC staining for TGF-β did not demonstrate appreciable differences in XLHN dogs compared to controls in a previous study.[29] The IPA Upstream Regulator Analysis predicts the upstream regulator of gene expression changes based on the knowledge of this regulatory cascade in the literature compiled in the Ingenuity Knowledge Base. Thus, the identified upstream regulator may not be identified as a DEG despite its importance in gene regulation.

A limiting factor of this study is that the kidney biopsies were immediately placed into RNAlater to preserve RNA integrity, so microscopic evaluation could not be performed to determine whether the biopsy used for RNA isolation was representative of the cortex as a whole. Thus, one of the samples in the control group at T1 could have represented an area affected by a clinically insignificant insult. Another limiting factor is that expression data represents the mean expression by many cell types. Because the kidney has many cell types, all with different roles in CKD progression, it would be ideal to study gene expression changes in individual cells using laser-capture microdissection to further elucidate the progression of CKD. Last, extensive validation of the RNA-seq results was not performed; however, previous studies have shown RNA-seq to be a robust tool that highly correlates with qRT-PCR results.[32-37] RNA-seq may even be more reliable than qRT-PCR due to its higher sensitivity and lower probe bias.[34] We did perform IHC to further characterize the inflammatory population, which supported the pathways identified through the RNA-seq results.

In what appears to be the first RNA-seq study of a canine CKD model, we identified several previously described and novel genes and enriched pathways involved in the pathogenesis and development of CKD. The approach of acquiring biopsies at time points determined by the clinical stage of disease was an attempt to target causative gene expression starting at the clinical onset of proteinuria rather than secondary changes. Regardless of initial insult, CKD has common pathways that lead to end-stage kidney disease.[334] Therefore, many genes found in the current study may serve as predictive or diagnostic biomarkers for early detection of CKD in dogs and people. They may also be potential targets for drug development for this condition.

CHAPTER III

INVESTIGATION OF MICRORNAS AS NON-INVASIVE BIOMARKERS OF CHRONIC KIDNEY DISEASE IN DOGS

Introduction

Dogs with XLHN have been used as a model of canine CKD as well as an animal model of human AS.[20] XLHN dogs have a naturally-occurring, 10-base deletion in *COL4A5* gene located on the X chromosome. The genetic defect leads to inability to synthesize complete α5 chains[19], one of the main components in the GBM of the mature kidney in mammals[20], causing juvenile-onset, rapidly progressive CKD in affected (hemizygous) males and persistent proteinuria in carrier (heterozygous) female dogs.[20] In humans with AS, 85% are X-linked, with a mutation in *COL4A5*.[328] While male AS patients have juvenile-onset CKD, ocular abnormalities, and hearing loss[329], the renal abnormalities are the only documented feature in XLHN dogs.[20] The juvenile-onset CKD manifests as persistent proteinuria of glomerular origin as early as 3 months of age in the affected male dogs with XLHN, followed by progressive azotemia and decreased GFR, developing into end-stage renal failure between 6 months to 1 year of age.[18,20,373] Previously, our group used RNA-seq to characterize the gene expression in dogs with XLHN demonstrating rapid versus more slowly progressive disease. In that study, more than 1947 DEGs were identified in affected dogs, and TGF-β1 was identified as the top upstream regulator.[373] While we have described the gene expression related to CKD

progression, the driving force leading to such a distinct change has not been completely understood.

MiRNAs are small, non-coding RNAs that post-transcriptionally regulate gene expression through binding the 3' UTR of mRNAs.[39-41] The complex miRNA-mRNA interaction influences various physiological changes and pathological processes.[40] In the kidney, miRNAs play important roles in kidney development and progression of CKD in humans and animals.[374,375] While highly expressed renal miRNAs have been identified in healthy dogs[376,377], a comprehensive renal miRNA expression profile in dogs with CKD is lacking. Therefore, we aimed to use small RNA-seq to identify differentially expressed renal miRNAs that contribute to CKD progression in dogs.

A typical small RNA-seq workflow includes RNA isolation, library preparation, sequencing, data analysis, and qRT-PCR verification. Of these steps, data analysis remains the most intimidating step in sequencing projects.[30] Herein, we compared the performance of 3 different analysis tools: miRDeep2[378], Array Studio, and CPSS 2.0.[276] We subsequently used NormFinder[300] on the small RNA-seq data to explore promising miRNAs as internal controls for qRT-PCR normalization, followed by verification with geNorm[298] and qbase+.[299] The identified miRNA internal controls can be used for reliable normalization for the future studies.

In the current study, small RNA-seq was performed on RNA isolated from canine kidney biopsies to characterize and compare the miRNA expression between dogs with XLHN versus controls at 3 clinical time points. The performance of 3 alignment tools that use the canine genome and miRNA annotations were compared and verified by qRT-PCR.

The results obtained from the optimal alignment tool were used to find putative miRNA targets. We then conducted GO and pathway analyses to characterize the miRNAs targets among sample groups at specific time points. Our results deepen both the current understanding of the molecular mechanisms in AS as well as CKD progression in general. The DE miRs can be predictive biomarkers for the early detection of CKD and can represent potential therapeutic targets for CKD in both dogs and humans.

Material and methods

Animals

The dogs evaluated in this study were part of a colony with XLHN maintained at Texas A&M University.[18] XLHN is caused by a 10-base deletion in the gene encoding the α5 chain of type IV collagen. The affected males developed juvenile-onset CKD that progressed to end-stage renal disease as previously described.[18] Overall, 5 affected dogs and 4 age-matched, unaffected littermates were included in this study. All dogs were raised according to standardized protocols, and no treatments were given to these dogs. All protocols were approved by the Texas A&M University Institutional Animal Care and Use Committee.

Clinical phenotypes

Clinical progression in the affected dogs was determined by serial monitoring of serum and urine biomarkers of kidney diseases, which allowed for comparison of dogs at standardized clinical time points[335]: T1 (n = 5; onset of proteinuria: defined as the presence of microalbuminuria (E.R.D. HealthScreen Canine Urine Test strips, Loveland, CO, USA)

for 2 consecutive weeks); T2 (n = 3; onset of azotemia: serum creatinine ≥ 1.2 mg/dL); and T3 (n = 3; serum creatinine ≥ 2.4 mg/dL). On average, the affected dogs reached the first clinical time point (T1) at 13.2 weeks of age (range: 11-17 weeks), the second clinical time point (T2) at 23.3 weeks of age (range: 21-26 weeks), and the last clinical time point (T3) at 29.6 weeks of age (range: 24-33 weeks). (Supplementary Table S12).

Tissue collection and histopathological evaluation

Kidney cortex was collected by ultrasound-guided needle biopsy from each dog at the aforementioned 3 clinical time points (independent of age), and control dogs (n = 4 at all 3 time points) were biopsied to correspond with an affected littermate. Samples for pathology evaluation and immunohistochemistry were placed in formalin and embedded in paraffin, and they were processed and evaluated as previously described.[335,373] Samples for small RNA-seq were immediately placed in RNAlater Stabilization Solution (Life Technologies, Foster City, CA, USA) and stored at -80 °C until RNA isolation.

RNA isolation and sequencing

All samples (n = 23) were homogenized in RLT Buffer (Qiagen, Valencia, CA) using a Bead Ruptor Mill Homogenizer (Omni International, Kennesaw, GA). Total RNA, including small and miRNA, was isolated using the mirVana miRNA Isolation Kit (ThermoFisher Scientific, Waltham, MA) following the manufacturer's protocol. Total RNA concentration and the 260/280 absorbance ratio was determined by the NanoDrop 2000 (Thermo Fisher Scientific, Wilmington, DE, USA) (Supplementary Table S12). The samples were processed using the TruSeq Small RNA library prep kit

(Illumina, San Diego, CA, USA) according to the manufacturer's protocol. The steps of the library preparation included Small RNA filtration on PAGE gel, adapter ligation, reverse transcription, PCR product purification, and library quality testing by the Agilent 2100 Bioanalyzer (Agilent Technologies, Santa Clara, CA, USA) and the ABI StepOnePlus Real-Time PCR System. Samples were then sequenced using the Illumina HiSeq 4000 (50 bp single-end) at the sequencing facility (BGI) to reach the expected output of 10M reads per sample.

Data analysis

Small RNA-seq reads and quality control were reprocessed by the sequencing facility (BGI). Data analysis was carried out by using 3 different tools: (1) Array Studio (Version 10.0.1.48, Omicsoft lnc., Cary, NC), a commercial next-generation sequencing and -omic analysis software, (2) miRDeep2[378](version 2.0.0.8, Latest Update: May 2016), a popular algorithm for miRNA identification, and (3) CPSS 2.0 (http://114.214.166.79/cpss2.0/index.html), a web-based Small RNA-seq analysis tool.[276] For all 3 analyses, canine genome (CamFam 3.1) and miRBase (release 21) were used with default settings. MiRDeep2 was performed using the high performance research computing resources provided by Texas A&M University (http://hprc.tamu.edu) in the Linux operating system (version 2.6.32). For all 3 tools, un-normalized raw read counts were used to perform differential expression and statistical analysis with the identical script using DESeq2[272] (release 3.3) in R (version 3.3.2) as previously described.[373] We used the Benjamini-Hochberg procedure[340] to adjust *P*-values for multiple testing. An adjusted *P*-value < 0.05 was set for the selection of DE miRs.

Target prediction, gene ontology (GO), and pathway analysis

For DE miRs at each time point, we selected the top 10 up-regulated (fold change > 2) and down-regulated (fold change < 2) miRNAs as input for miRDB[379] (http://mirdb.org/. Last modified on May 3, 2016). MiRDB is an online database for miRNA target prediction that hosts predictive miRNA targets in 5 species: human, mouse, rat, dog and chicken. To date, there are 453 miRNAs targeting 128,703 genes in the database. All miRNA targets are assigned with a target score range from 50-100 determined by the MirTarget algorithm.[380] We used the target score of 90 as a cutoff value since higher scores represent more statistical confidence. The list of miRNA targets was passed onto Gene ontology and PANTHER pathway analysis using *Canis familiaris* reference list (20,141 genes in the database) and the Overrepresentation Test (released on December 5, 2017) in PANTHER[381] version 13.1 with the default setting (Protein ANalysis THrough Evolutionary Relationships, http://www.pantherdb.org/, released on February 3, 2018). Also, manually curated Reactome pathway analysis[382] version 58 (released on December 7, 2016) was used. The updated PANTHER Overrepresentation Test incorporates Fisher's Exact Test with false discovery rate multiple test correction, and adjusted P-value < 0.05 was set as the cutoff value.

qRT-PCR verification and normalization

Small RNA-seq data generated by the 3 alignment tools were analyzed using NormFinder[300] to identify suitable miRNAs as candidates for qRT-PCR internal controls. Ten RNA samples remain available after small RNA-seq were used for qRT-PCR. Additionally, 2 control samples used in a previous study[373] were recruited to make 2

affected dogs and 2 controls for each time point. The miRCURY LNA miRNA PCR Assays (Qiagen, Germany) were used for the miRNA targets: miR-142 (Cat. no. YP02102101), miR-147 (Cat. no. YP00204368), and miR-21 (Cat. no. YP00204230), and miRNA internal controls: miR-16 (Cat. no. YP00205702), miR-186 (Cat. no. YP00206053), miR-26b (Cat. no. YP00205953), and miR-99a (Cat. no. YP00204521). First, total RNA isolated from kidney biopsies was diluted to the concentration of 10 ng/μL. Next, the miRCURY LNA RT Kit (Qiagen, Germany) was used in a 10 μL reaction for RT consisting of 2 μl of 5X Reaction Buffer, 5 μL RNase-free water, 1 μL enzyme mix (omitted for no reverse transcriptase controls), and 2 μL diluted RNA (10 ng/μl). The RT reaction was performed using a T100 Thermal Cycler (Bio-Rad, UK) with the protocol of 60 minutes at 42°C (reverse transcription), 5 minutes at 95°C (inactivation), followed by storage at -20°C. While the cDNA is stable for up to 5 weeks, all PCRs were performed within 18 days from the RT reaction. For PCR, the miRCURY LNA SYBR Green PCR Kit (Qiagen, Germany) was used to make a 10 μL reaction consisting of 5 μL SYBR Green Master Mix, 1 μL PCR Primer Mix, 1 μL RNase-free water, and 3 μL 1:15 diluted cDNA (omitted for no template controls). Mater Mix and cDNA were distributed in Hard-Shell 384-Well Standard PCR Plates (Bio-Rad, UK) by the epMotion 5075 Automated Liquid Handling Systems (Eppendorf, Germany). The PCR was performed using a CFX384 Touch Real-Time PCR Detection System (Bio-Rad, UK) with the protocol of 2 minutes at 95°C (initial heat activation), 40 cycles of 10 seconds at 95°C (denaturation) and 60 seconds at 56°C (annealing), followed by a melting curve analysis at 60-95°C. Negative

controls included RNase-free water only, no reverse transcriptase (NRT), and no template controls (NTC) to ensure no genomic DNA contamination was present.

Once qRT-PCR was performed, the Cq values of these candidate miRNAs were further analyzed by geNorm[298] in the qbase+ software.[299] Candidate miRNAs for internal controls were ranked by geNorm[298] base on the stability (M value) and coefficient of variation. The algorithm of geNorm[298] then calculates the normalization factor (V value) and determines the optimal number of internal controls. Lastly, the consolidated candidate miRNAs were analyzed for reference target stability quality control in qbase+.[299] Data were normalized base on the $2^{-\Delta\Delta Cq}$ method[304], using miR-186 and miR-26b as reference miRNAs. One-way ANOVA was applied for mean comparison using the qbase+ software.[299] *P*-value less than 0.05 was set as cut-off value.

Results

Summary of histopathological evaluations

The interstitial fibrosis scores and the chronic inflammation scores of representative cortical fields of the kidney biopsies were recorded in Supplementary Table S12. In the current study, the clinical time points in affected dogs were defined as: T1 - onset of proteinuria (the earliest time point that clinical disease can be detected); T2 - onset of azotemia (sCr ≥ 1.2 mg/dL); and T3 – advanced CKD (sCr ≥ 2.4 mg/dL). At T2, the mean fibrosis and chronic inflammation scores were significantly higher in affected dogs than in controls (Supplementary Table S12). However, no statistically significant difference was observed between affected dogs and controls at T1 and T3.

Summary of canine RNA-sequencing data

We obtained an average RNA yield of 437.6 ng/μL with an average 260/280 absorbance ratio of 2.1 from 23 kidney biopsies collected at 3 clinical timepoints (Supplementary Table S12). For each sample, approximately 12 million single-end reads passed the quality control. Overall, 81-99% of reads were mapped to the canine genome (CanFam 3.1). The mean genome mapping rate of CPSS 2.0 (99.x%) was significantly higher than for Array Studio (90.0%) and miRDeep2 (88.7%) (Supplementary Figure S5). Both CPSS 2.0 (167 miRNAs) and Array Studio (170 miRNAs) detected a significantly higher number of miRNAs than miRDeep2 (124 miRNAs). The average miRNA mapping rates were high, ranging from 83 to 94% for each sample (Supplementary Table S12). The representative read length distribution and genome mapping results are illustrated in Figure 10.

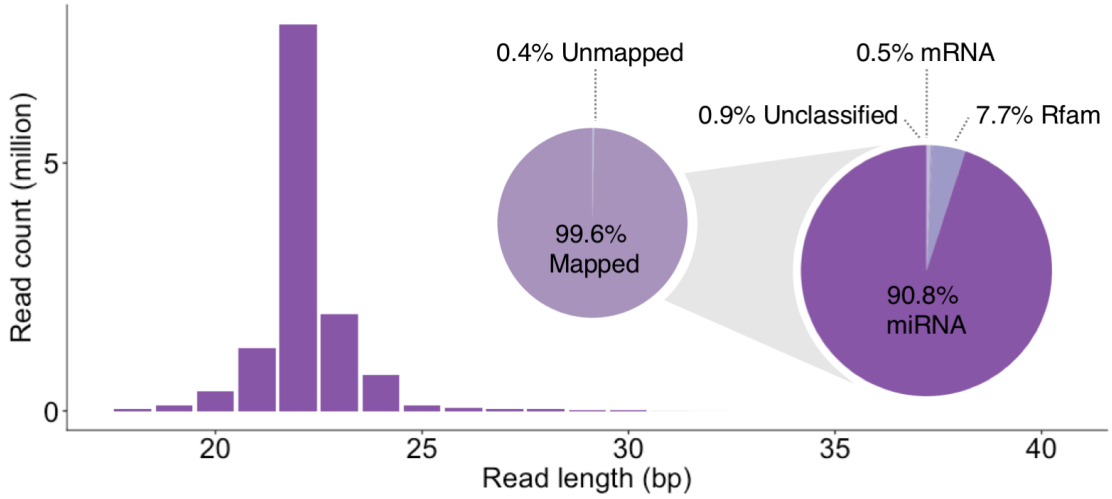

Figure 10. Averaged read length distribution (bar chart) and genome mapping results (pie charts). Bar chart: the majority of sequencing reads were between 21-25 nucleotides in length, consistent with miRNAs. Pie charts: the pie charts show almost all reads mapped to the dog genome. Among the mapped reads, the vast majority belong to miRNA (90.8%), with a small population mapped to non-coding RNA (Rfam database; 7.7%) and mRNA (0.5%). The results of CPSS 2.0 analysis were used.

Exploratory principal component analysis (PCA)

PCA was performed to assess the clustering between samples at each clinical time point (T1, T2, and T3). The PCA of read count tables obtained from all 3 alignment tools showed similar patterns, and representative PCA plots for each clinical time point are shown in Figure 11. Two samples from affected dogs showed a distinct miRNA expression pattern at T1 (Figure 11A). At T2, samples were further separated out except for one affected dog (Figure 11B). When dogs developed advanced azotemia at T3, a clear separation between affected and control dogs was seen (Figure 11C). At each clinical time point, the principal components 1 (PC1) and 2 (PC2) accounted for 62-76% of the total variation in miRNA expression.

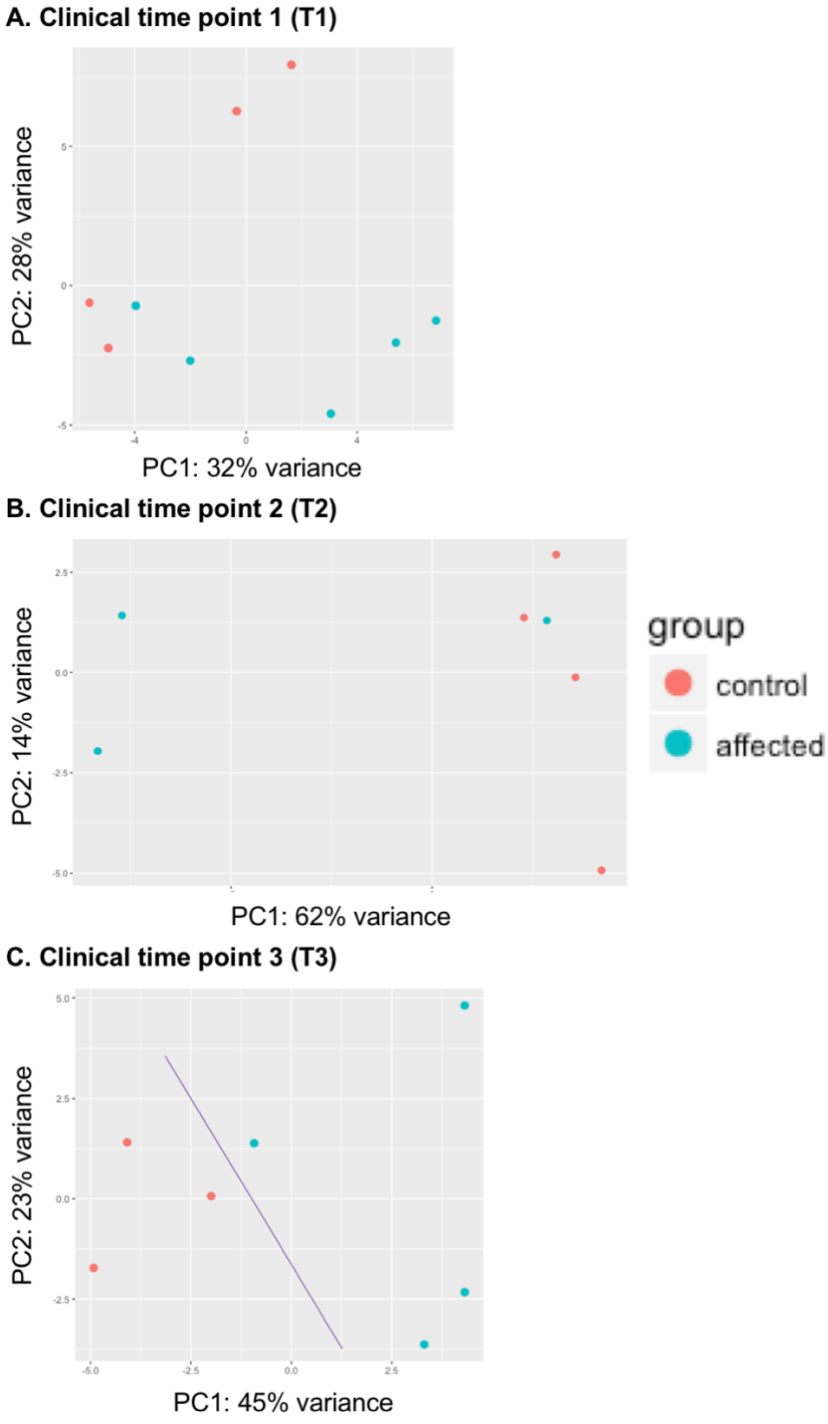

Figure 11. PCA plots for all samples at 3 clinical time points. The percentage of variance in principal component 1 (PC1) and 2 (PC2) indicates how much variance in miRNA expression was explained by PC1 and PC2. The result of CPSS 2.0 were used. (Red: control group; Green: affected group).

Differentially expressed miRNAs (DE miRs)

Overall, up to 25 miRNAs (adjusted *P*-value < 0.05) differentially expressed between affected and control dogs were found at each clinical time point as shown in the Venn diagrams (Figure 12 and Supplementary Table S13). The number of DE miRs detected at each time point by all 3 alignment tools were similar to each other. Of note, miR-147 was identified as upregulated with a more than 3.78-fold change at all time points in both CPSS 2.0 and Array Studio but not in miRDeep2. Similarly, both CPSS 2.0 and miRDeep2 found miR-142 upregulated with a more than 2.14-fold change at all time points, whereas Array Studio did not identify miR-142 as differentially expressed.

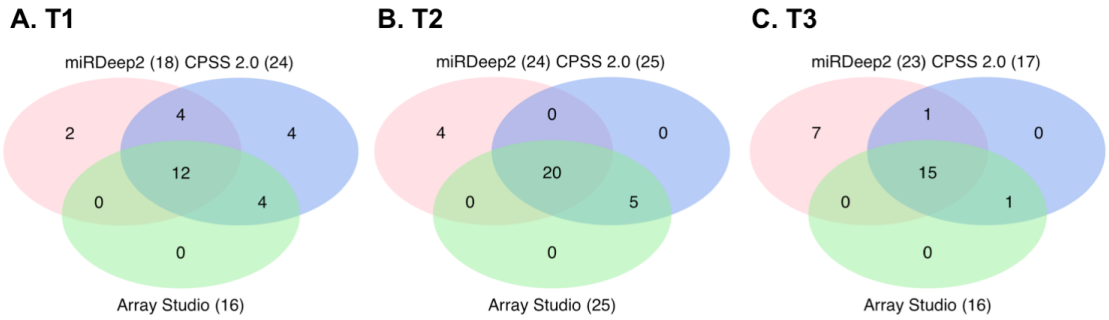

Figure 12. DE miRs identified by each alignment tool at the 3 time points (T1, T2, and T3). Comparing the affected dogs with sex- and age-matched controls, up to 25 DE miRs were found at each clinical time point. Only miRNAs with an adjust *P*-value < 0.05 were considered as DE miRs. The total number of DE miRs found at each time point appears in parentheses.

The miRNAs repetitively identified as differentially expressed in all 3 tools at each time point are listed in Table 5 (adjusted *P*-value < 0.05, absolute fold change > 2). MiR-802, miR-146b, and miR-21 were upregulated in kidney tissues of affected dogs

throughout all time points. Hierarchical clustering analysis and heatmap of miR-802, miR-146b, and miR-21 in all samples show almost all affected dogs clustered together (Cluster 1 in Figure 13). The hierarchical clustering results (Cluster 2 in Figure 13) agree with PCA plots in that affected dogs were distinctly separated from the controls for all but 2 T1 dogs (Figure 11A) and 1 T2 affected dogs (Figure 11B).

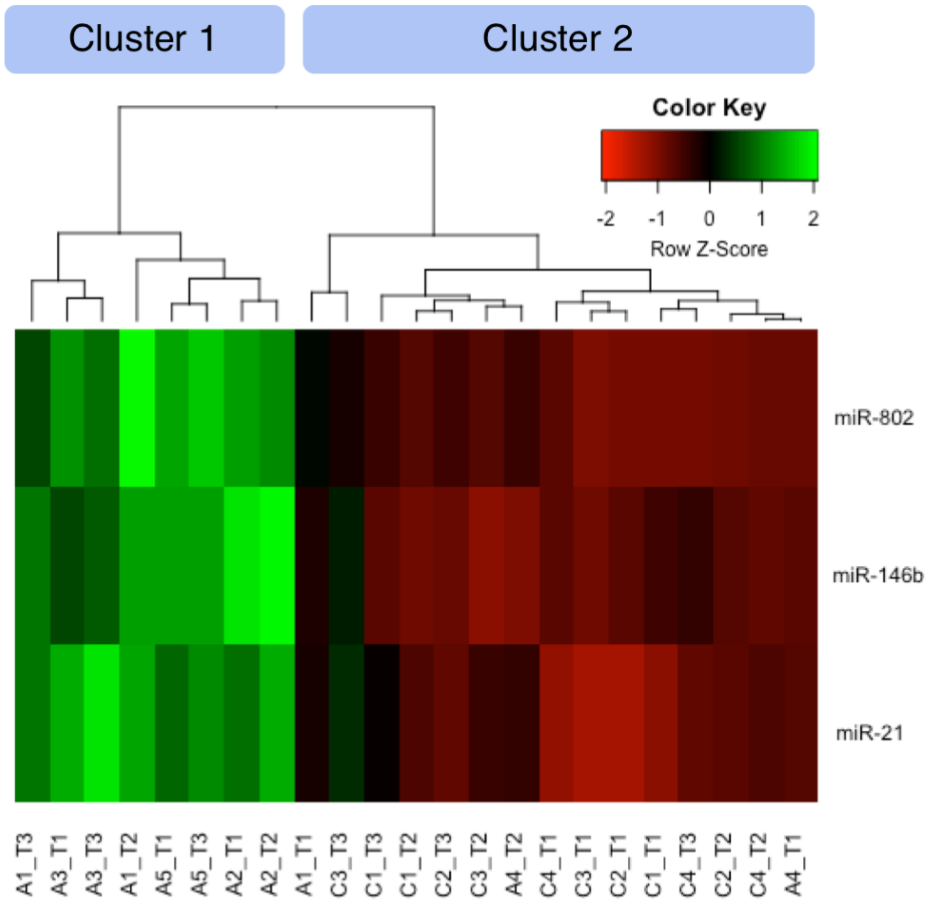

Figure 13. Hierarchical clustering analysis and heatmap of miR-802, miR-146b, and miR-21. MiR-802, miR-146b, and miR-21 were upregulated throughout all time points in affected dogs compared with controls. (Column names: A and C designate affected dogs and controls; Arabic numerals represent individual dogs in each group; T1, T2, and T3 designate 3 clinical time points). The result from CPSS 2.0 analysis were used.

Table 5. Top DE miRs identified in affected dogs versus controls at 3 time points.

Time points	Regulation	miRNAs	Fold Change	Adjusted *P*-value
T1	Up	miR-802*	10.34	6.07E-05
		miR-146b*	5.04	1.84E-03
		miR-21*	4.92	4.66E-05
		miR-150	3.76	1.14E-02
		miR-142	3.18	2.35E-03
		miR-101	2.78	1.76E-02
		miR-31	2.70	2.39E-02
		miR-19a	2.59	4.32E-02
		miR-29a	2.30	7.68E-04
		miR-340	2.21	3.80E-04
T2	Up	miR-802*	18.33	4.09E-06
		miR-146b*	9.16	1.08E-04
		miR-183	8.18	1.08E-04
		miR-150	6.33	3.06E-04
		miR-182	4.99	8.25E-04
		miR-142	4.65	8.25E-04
		miR-96	4.18	2.10E-02
		miR-21*	3.75	1.25E-03
		miR-146a	3.59	1.02E-02
		miR-380	3.57	9.17E-03
		miR-410	3.35	9.37E-03
		miR-155	3.03	3.70E-02
		miR-335	2.77	3.37E-02
		miR-31	2.49	9.70E-03
		miR-451	2.29	4.63E-02
		miR-29a	2.29	3.35E-03
	Down	miR-196a	-2.13	8.25E-04
		miR-215	-2.28	1.84E-02
T3	Up	miR-802*	6.99	8.03E-05
		miR-146b*	4.03	5.47E-04
		miR-18a	3.35	1.30E-02
		miR-21*	3.29	3.48E-03
		miR-155	2.89	3.23E-02
		miR-34a	2.89	3.23E-02
		miR-708	2.08	4.07E-02
	Down	miR-486	-2.40	2.62E-02

All listed miRs have an absolute fold change > 2 and adjusted *P*-value < 0.05 in the CPSS 2.0 analysis.
* miRNAs were DE miRs identified in all 3 time points.

qRT-PCR validation of DE miRs

To verify the sequencing results, we performed qRT-PCR for 3 miRNAs (miR-142, miR-147, and miR-21) that were found to be upregulated at all time points using at least 2 alignment tools. Also, NormFinder analysis was performed on the sequencing data, and 4 miRNAs were identified as promising internal controls (miR-16, miR-186, miR-26b, and miR-99a). We examined the expression of these 7 miRNAs using 10 samples sequenced in the current study and 2 control samples used in a previously study[373] to make 2 samples from each group at each respective time points. The geNorm analysis showed stable expression for 3 of the 4 promising internal controls (miR-16, miR-186, and miR-26b), and the use of the 2 most stable miRNAs (miR-186 and miR-26b) were indicated (Supplementary Figure S6). In the reference target stability quality control of qbase+, we further verified the stability of miR-186 and miR-26b and confirmed that they are reliable for normalization (Supplementary Figure S6C).

Using qRT-PCR, we verified the upregulation of miR-142, miR-147, and miR-21 in the kidney tissues of affected dogs at T2 and T3, as detected by small RNA-seq (Figure 14). This finding supports that CPSS 2.0 outperformed Array Studio and miRDeep2 in capturing the expression of miR-142 and miR-147. Moreover, the qRT-PCR data showed a time-dependent increase in the degree of upregulation that was not discernable from the small RNA-seq data. As shown in Figure 14, the expression of miR-142, miR-147, and miR-21 gradually increased as the kidney disease progressed in the affected dogs while expression in the control dogs was similar throughout each time point. The complete pair-wise comparison results are available in Supplementary Table S14.

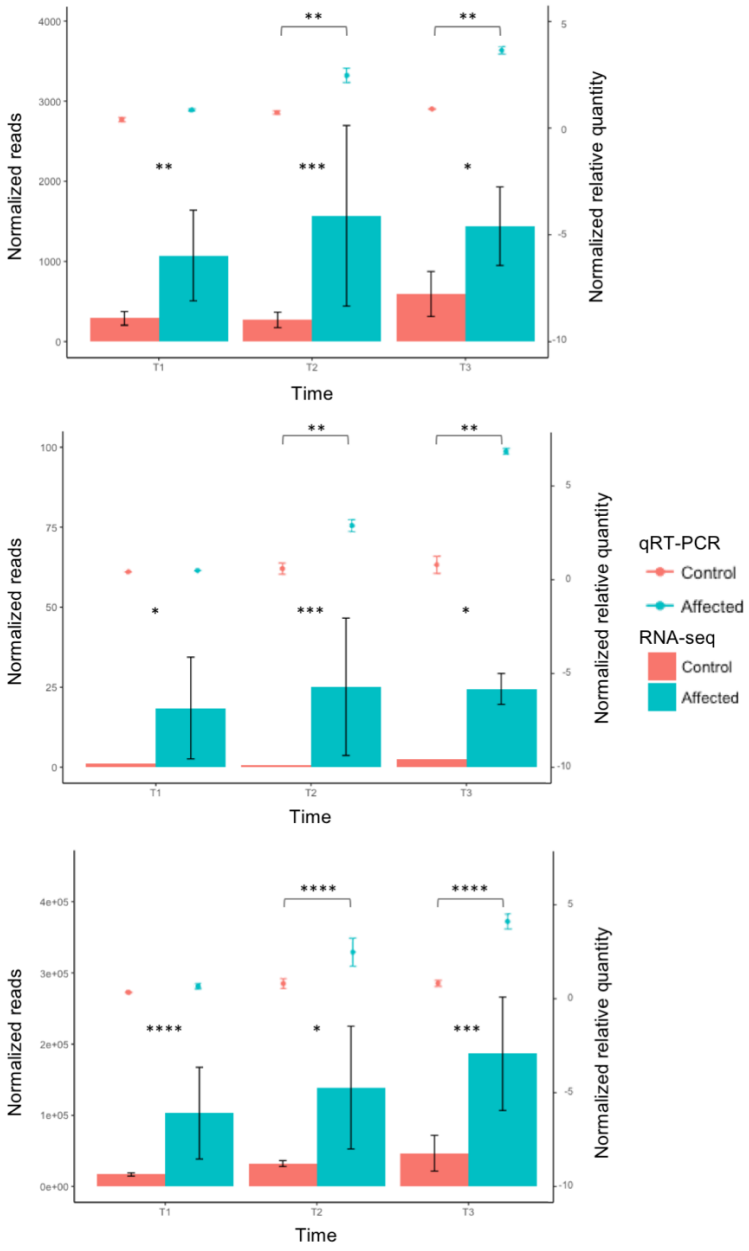

Figure 14. Expression of selected upregulated miRNAs in affected dogs and controls detected by qRT-PCR and small RNA-seq at 3 time points. (A) Expression of miR-142, (B) Expression of miR-147, (C) Expression of miR-21. The expression of miRNAs detected using qRT-PCR is represented in lines on the top of each figure with the corresponding normalized relative quantity on the right vertical axis. The bars on the bottom of each figure represent the small RNA-seq data with the corresponding normalized reads on the left vertical axis. Data are presented as mean value ± standard deviation. (*: *P*-value < 0.05; **: *P*-value < 0.01;***: *P*-value < 0.001; ****: *P*-value < 0.0001).

Target prediction, Gene Ontology (GO), and pathway analysis for DE miRs

Based on the qRT-PCR results, data obtained from CPSS 2.0 were used to proceed with the remaining analysis. The top 10 DE miRs with an absolute fold change more than 2 were selected as inputs for miRDB.[379] To better characterize the changes in target genes, upregulated and downregulated DE miRs were used as 2 separate inputs. In miRDB, only putative target genes with a target score higher than 90 were considered satisfactory for the subsequent overrepresentation test in the PANTHER Gene Ontology and pathway analyses[381,382] (Supplementary Table S15).

Due to the low number of downregulated miRNAs and the consequently insufficient miRNA targets, no Gene Ontology and pathway analyses results were obtained for downregulated miRNAs at all time points. In contrast, 319 to 729 putative targets of upregulated miRNAs were mapped in PANTHER, identifying 12 biological process GO terms, 3 Reactome pathways, and 12 PANTHER pathways (Supplementary Table S16). Cellular process and RNA metabolic process were the main GO terms enriched in the current study. Specifically, "regulation of transcription from RNA polymerase II promoter" was upregulated at T1 and T3 while "intracellular signal transduction" and "regulation of phosphate metabolic process" were upregulated at T2 and T3.

For Reactome pathway analysis, the signal transduction pathway was enriched in affected dogs throughout the progression of kidney disease, and its subfamily pathway, the "signaling by TGF-β receptor complex" pathway was also enriched approximately 5-fold at T1. The PANTHER pathways, such as gonadotropin-releasing hormone receptor pathway and Wnt signaling pathway, were enriched in affected dogs at T1 and T2. Ten

other enriched PANTHER pathways were identified at T2, but no PANTHER pathway was identified at T3, presumptively due to fewer miRNA targets (Supplementary Table S16).

Discussion

Dogs with XLHN haven been studied as an example of canine CKD as well as an animal model for human AS. The gene expression in XLHN dogs has been partially characterized using qRT-PCR[29] and microarray.[21] Recently, our group used RNA-seq to investigate the gene expression linked to rapid CKD progression in dogs with XLHN.[373] In the current study, we performed small RNA-seq on 23 kidney specimens collected during serial renal biopsies from affected dogs and healthy littermates to characterize the miRNA expression during CKD progression. Up to 25 miRNAs were differentially expressed at specific clinical time points comparing affected dogs with controls, including 3 miRNAs (miR-146b, miR-21, and miR-802) that were upregulated throughout all 3 time points. Meanwhile, we compared 3 miRNA alignment tools to optimize the data analysis in small RNA-seq and identified promising miRNA internal controls (miR-186 and miR-26b) for qRT-PCR normalization.

Table 5 lists DE miRs with more than a 2-fold change during the progression of CKD, including 22 unique upregulated miRNAs and 3 downregulated miRNAs. The majority of DE miRs were upregulated in the kidney tissue of affected animals as in previous studies using CKD mouse models.[383,384] Among them, miR-146b, miR-21, and miR-802 were consistently upregulated in affected dogs before the presence of azotemia. Both miR-146b and miR-21 were previously described in the context of CKD. In one

study, miR-146b and miR-21 were among the top 3 upregulated miRNAs in the kidney tissue of 12-month-old mice with spontaneous CKD (B6.MRLc1) compared to healthy controls (C57BL/6).[383] The upregulation of renal miR-146b was also noted in 4 other kidney injury mouse models (folic acid-induced, unilateral ureteral obstruction, bilateral renal ischemia/reperfusion, and cisplatin-induced)[384,385] with peak expression associated with fibrosis. In our study, miR-146b reached peak expression at T2 based on sequencing data, which was the time that XLHN dogs became azotemic and had visible fibrotic change on histopathological evaluation.[373] MiR-21 is regulated by TGF-β1/Smad3[386,387] and contributes to renal fibrosis by silencing metabolic pathways[388]; however, it also possesses a protective effect against ischemic injury in the kidney.[389] Several studies have documented an increase in renal miR-21 during CKD.[383,387,390-392] In the current study, qRT-PCR verified upregulation of renal miR-21 at T2 and T3 in affected dogs, corresponding with our previous finding that TGF-β1 is the top up-stream regulator of CKD progression in XLHN dogs.[373] Recently, we have identified the same miR-21 upregulation pattern in a larger group of XLHN dogs. The expression of renal miR-21 did not increase significantly until affected dogs became azotemic (unpublished observations). Similarly, the expression of renal miR-21 did not differ between T2 and T3 in the current study (Supplementary Table S13).

In addition to abovementioned DE miRs, renal miR-146b, miR-150, and miR-29a that have been described in CKD progression were also upregulated in affected dogs at various time points. MiR-146a is highly homologous to miR-146b, and they differ by only 2 nucleotides in dogs, mice, and humans. In dogs with XLHN, renal miR-146 was

upregulated at T2 in the affected dogs. The upregulation of miR-146a was seen in the kidney tissues of IgAN patients[393], a CKD mouse model[383], a DN rat model[394], dogs with CKD[100], and in the glomeruli of LN[395] and membranoproliferative GN.[396] Renal miR-150 is upregulated at T1 and T2 in affected dogs. It was also upregulated in 24-month-old rats compared to young rats[397] and in LN patients.[398] Mir-29a was upregulated at T1 and T3 in affected dogs. In contrast, decreased renal miR-29a expression was seen in streptozotocin-induced DN mice and in an adenine-induced renal fibrosis mouse model.[399] Some studies showed the inhibition of miR-29 was caused by TGF-β1[399] and likely mediated by Smad3 during DN progression.[400] However, the reduction of miR-29 could also be regulated by hyperglycemia, given the changes seen in podocytes and mesangial cells of DN mice.[401,402] We speculated that the discrepancies in the directions and time points of miRNA expression could be caused by the difference in the enriched location of miRNAs (TI versus glomerular) and different subtypes of CKD.

Several miRNAs identified in our study have only been rarely described in the context of CKD, including miR-802, miR-142, and miR-147. The expression of renal miRNA-802 was upregulated in the dogs with XLHN throughout all 3 time points. The increased expression of miR-802 was observed in the kidney, specifically in the cortical collecting duct, of mice exposed to high potassium diets.[403] *In vitro*, miR-802 targets caveolin-1 and decreases caveolin-1 expression, which in turn increases the surface expression of the renal outer medullary potassium channel and facilitates potassium excretion.[403] We have reported the caveolin-1 gene (*CAV1*) being differentially expressed in dogs with XLHN at T2 and T3[373]; however, we would expect the putative target for

miR-802 to be downregulated, whereas it was upregulated in that study. More studies are needed to resolve the discrepancy. The upregulation of renal miR-142 in XLHN dogs was verified by qRT-PCR at T2 and T3. The canine miR-142 (cfa-miR-142) differs from miR-142-3p in humans, mice, and rats by 2 nucleotides. The human miR-142-3p (hsa-miR-142-3p) was upregulated in patients with acute rejection of a renal allograft[404], most likely due to an influx of lymphoid cells as in acute T-cell mediated rejection.[405] We have demonstrated T cells were the predominant lymphoid cells that infiltrate the kidneys of dogs with XLHN[373]; therefore, the source of upregulated miR-142 would likely be T cells. The upregulated miR-147 in XLHN dogs at T2 and T3 was also verified by qRT-PCR. However, research on human miR-147b-3p and its role in the development of CKD is lacking.

We identified DE miR target genes and performed GO terms and pathway analyses at each time point. The biological process GO terms were mainly "Cellular process" and "RNA metabolic process," with subfamilies indicating "MAPK cascade" and "regulation of transcription from RNA polymerase II promoter," respectively. We incorporated the peer-reviewed, manually curated Reactome pathways to characterize the miRNA targets presented in our study.[381] The Reactome pathway analysis results are consistent with the GO terms that show involvement of the "signal transduction" pathway. Particularly, the "signaling by TGF-β receptor complex" is consistent with our previous finding that TGF-β1 was the top upstream regulator of CKD progression in XLHN dogs.[373] Other PANTHER pathways were also related to signaling transduction, such as "gonadotropin-releasing hormone receptor" and "Wnt signaling" pathways. Indeed, several genes in these

2 pathways were downregulated in dogs with XLHN used in a previous mRNA-seq study (eg, *ACTG2*, *ADCYAP1R1*, and *CACNA1C* at T1; *MAP3K3*, *FZD4*, *ACVR1B*, *PER1*, *GATA2*, *MYH15*, and *GATA4* at T2).[373]

The raw sequencing reads were aligned to the same version of the canine genome and miRNA annotations with 3 alignment tools using the default settings. CPSS 2.0 had a significantly higher genome mapping rate than Array Studio and miRDeep2. For the number of miRNAs detected, no difference was found between CPSS 2.0 and Array Studio, but both detected more miRNAs than miRDeep2. CPSS 2.0 and miRDeep2 employ the same alignment algorithm, Bowtie[406], for genome mapping; however, Bowtie is operated under different default settings. For example, CPSS allows up to 3 mismatches in genome alignment, but miRDeep2 by default only retains perfect mappings.[378] The difference could impact the genome mapping rate and the number of miRNAs detected, as we observed. Array Studio uses OSA[407], a different alignment algorithm from Bowtie, to achieve genome mapping. Although the performance of OSA and Bowtie have not been directly compared using small RNA-seq data, OSA has been reported to align more reads in a shorter time than the other alignment tool for RNA-seq that incorporates Bowtie.[407]

Further, we incorporated qRT-PCR to verify the sequencing results for 3 miRs: miR-21, miR-142, and miR-147. miR-21 was repetitively detected in all 3 alignment tools throughout all time points, whereas both miR-142 and miR-147 were detected by only 2 of the 3 all alignment tools. qRT-PCR verified the upregulation of all 3 miRNAs in affected dogs at T2 and T3. Given that Array studio and miRDeep2 did not identify upregulated miR-142 or miR-147, CPSS 2.0 was the only alignment tool that accurately

captured the changes in miR-142 and miR-147. To our surprise, despite all 3 miRNAs showing upregulation in affected dogs at T1 based on the small RNA-seq data, no statistically significant change at T1 was observed based on the qRT-PCR data (Figure 14). Although RNA-seq has been argued to be more sensitive and have lower probe bias than qRT-PCR[34], we speculate that using 2 samples for each group at respective time points might lead to the indifferent expression in qRT-PCR as those verified by qRT-PCR may not represent all sequenced samples.

In qRT-PCR, the expression levels of miRNAs are closely tied to the normalization method used. In theory, the high concentration of RNA isolated from tissue samples would permit reliable quantification and the subsequent use of a fixed RNA quantity for qRT-PCR input. However, normalization is still required since the miRNA proportion in the isolated total RNA could fluctuate between samples.[384] Although snRNAU6 is frequently used for qRT-PCR normalization, snRNAs are structurally and functionally different from miRNAs. The difference in nucleic acid composition, length, and secondary structure could potentially introduce variation between a snRNAs control and miRNAs of interest. We used NormFinder[300] on small RNA-seq data to select 4 miRNAs (miR-16, miR-26b, miR-99a, and miR-186) for further assessment by qRT-PCR. All miRNAs except miR-99a had a similarly low M value in the geNorm analysis (Supplementary Figure S6). The stably expressed miR-16[377], miR-186[377], and miR-26b[408] have all been proposed as internal controls in renal studies. In particular, miR-16 and miR-186 were identified as 2 of the most stably and ubiquitously expressed miRNAs across 16 types of canine tissues, including kidney.[377] MiR-26b has also been described as a suitable internal control for

glomerular miRNA quantification in IgA nephropathy patients.[408]

One of the limiting factors of this study is the inability to perform microscopic evaluation and RNA isolation on the same kidney biopsy. Given that the biopsied renal tissues were immediately placed into RNAlater to preserve RNA integrity, we could not determine whether the biopsy used for RNA isolation was representative of the cortex. Two affected samples at T1 and 1 affected sample at T2 had similar miRNA expression patterns as control samples, which could indicate that the biopsy used for RNA isolation were from more slowly progressing dogs. Indeed, affected dog A1 and A4 reached the end-point of the experiment at the age of 36 to 37 weeks while the end-point happened at the age of 27 to 37 weeks in the other 3 affected dogs. Laser-capture microdissection could help narrow down the cell types of interests to achieve a more homogenous miRNA expression that more accurately represents each clinical time point.

In the current study, we have identified several previously described and novel miRNAs that were differentially expressed in the presence of CKD. Along with our previous RNA-seq study in the same canine CKD model[373], the putative targets of DE miRs and the enriched pathways further characterize the development and the progression of CKD. Both studies took the approach of acquiring biopsies at defined clinical stages of disease in an attempt to more accurately compare gene expression among different dogs throughout progression of disease. Since common pathways in CKD lead to end-stage kidney disease regardless of the initial insult[334], miRNAs found in the current study may be predictive biomarkers for the early detection of CKD and can represent potential therapeutic targets for CKD in both dogs and humans.

CHAPTER IV

COMPARISON OF RNA ISOLATION AND LIBRARY PREPARATION METHODS FOR SMALL RNA SEQUENCING IN CANINE BIOFLUIDS

Introduction

MicroRNAs (miRNAs) are highly-conserved, small (21–25 nucleotides in length), non-coding RNAs that are present in different types of biofluids such as serum, plasma, and urine.[53] Through the post-transcriptional regulation of mRNA expression, miRNAs control diverse physiological activities.[40] Recently, it has been reported that biofluid-derived miRNAs can serve as novel non-invasive biomarkers for early detection of cancers and degenerative and metabolic diseases as well as therapeutic targets for such conditions.[91,409,410] Several veterinary studies have profiled biofluid-derived miRNAs, mainly in serum and plasma.[52,101,111,123,139]

To date, there is no gold standard for isolating miRNA from biofluids, in part due to lack of a gold standard method for evaluation.[87,207,218,219,221,223,225,227] The quantitative real-time PCR (qRT-PCR) is the most commonly used method for evaluating the performance of miRNA isolation methods. While qRT-PCR is a sensitive and specific tool that allows absolute quantification of miRNAs[308], it is a low-throughput technique and requires pre-selection of miRNAs of interest. Thus, qRT-PCR limits the complete understanding of miRNA expression and the discovery of novel miRNAs. In contrast, small RNA sequencing [30] allows comprehensive miRNA profiling (ie, miRNome). This

technique not only provides high accuracy in distinguishing similar miRNAs but also can detect novel miRNAs.[308]

However, the relative scarcity of miRNAs in biofluids compared to tissue combined with the high requirement for RNA input for the library preparation poses a challenge for small RNA-seq in biofluids.[288] For instance, the TruSeq Small RNA Library Preparation Kit (Illumina), which is most commonly used, requires 200 ng/μL total RNA or 2-10 ng/μL purified small RNA in 5 μl nuclease-free water. In contrast, miRNA isolated from 200 μL human serum was reported to be as low as 14-184 pg/μL.[219] Although using a large volume of biofluid could boost the RNA yield, such volumes often are unavailable in retrospective veterinary studies.

The objective of this study was to test 6 commonly used commercial miRNA isolation kits using canine serum and urine. Using small RNA-seq, we compared the performance of selective miRNA isolation kits and 2 library preparation kits. We hypothesized that small RNA-seq would reveal differences in miRNA isolation and library preparation kits regarding the global miRNA profile such as the total number of reads, genome mapping rate, miRNA mapping rate, miRNA reads, and the species and numbers of unique and overlapping miRNAs. The results provide a comprehensive assessment for choosing the optimal miRNA isolation and library preparation methods for small RNA-seq research in canine biofluids.

Material and methods

Serum and urine collection and processing

Pooled serum and urine were collected as part of routine medical evaluations of 7 proteinuric but non-azotemic female dogs that were carriers for X-linked hereditary nephropathy (XLHN) and housed at Texas A&M University.[18] For serum, blood samples were allowed to clot at room temperature for 30-60 minutes and then centrifuged at 1500 x g for 10 minutes at room temperature. Once separated, 2.5 to 5 mL serum that was obtained from each dog was pooled together then aliquoted into individual cryotubes to ensure equal comparison among methods. Urine was collected via cystocentesis, and urine remaining after urinalysis was centrifuged at 1000 x g for 10 minutes at 4°C. Supernatant was pooled and aliquoted into separate 15 ml tubes. All serum and urine samples were processed within 2 hours of collection and immediately frozen after processing and stored at -80 °C until RNA isolation. All protocols were approved by the Texas A&M University Institutional Animal Care and Use Committee.

RNA isolation

Six miRNA isolation methods were evaluated in the current study. Serum miRNA isolation kits included Zymo Direct-zol RNA MiniPrep Kit (Zymo Research, Irvine, CA, USA), mirVana PARIS Kit (Ambion, Austin, TX, USA), and miRCURY RNA Isolation Kit-Biofluids (Qiagen, Germany). Urine miRNA isolation kits included Norgen Urine Exosome RNA Isolation Kit (Norgen Biotek, Thorold, ON, Canada), Qiagen exoRNeasy Serum/Plasma Maxi Kit (Qiagen, Germany), and miRCURY Exosome Isolation Kit -

Cells, urine and CSF (Qiagen, Germany). RNA isolation was performed in triplicate for each method. Furthermore, RNA was isolated from serum and urine by the same person (CPC), and each sample underwent a single freeze-thaw cycle. A fixed amount of serum (2ml) and urine (10ml) was used for each isolation. The volume of reagents used was adjusted based on input volume as needed, according to the manufacturers' protocols. For Zymo Direct-zol, however, the isolation protocol was modified (Supplementary File S1). For each isolation, the elution volume was fixed to 100 µl to facilitate inter-method comparisons. For each sample type, the NanoDrop 2000 (Thermo Fisher Scientific, Wilmington, DE, USA), Qubit microRNA Assay Kit (Invitrogen Corporation, Carlsbad, CA, USA), and Fragment Analyzer High Sensitivity RNA Analysis Kit (Advanced Analytical Technologies, Inc., Ankeny, IA, USA) were used to identify the methods with the highest RNA yield for subsequent sequencing.

Library preparation and sequencing

We compared 2 library preparation kits: TruSeq Small RNA Library Preparation Kit (Illumina, San Diego, CA, USA) and NEXTflex Small RNA Library Prep Kit (Bioo Scientific Corp, Austin, TX, USA). According to the manufacturer, the NEXTflex kit requires only 95 pg/µL - 190 ng/µL total RNA in up to 10.5 µL nuclease-free water.[248] For TruSeq, 15 PCR amplification cycles were performed. The libraries were run in a PippinHT system (Sage Science, Beverly, MA, USA) with a 3% gel cassette to achieve size selection of 120 bp to 180 bp. For NEXTflex, 24 PCR amplification cycles were performed according to the manufacturer protocol for low RNA input. The libraries were run in a PippinHT system (Sage Science, Beverly, MA, USA) with a 3% gel cassette to

select 115 bp to 170 bp as dictated by the manufacturer protocol. Following size selection, there was a bead purification step in which the final library was eluted in 25 μL of the included resuspension buffer.

To minimize technical variation, samples were sequenced using the 50 base-pair, single-end setting of the Illumina Genome Analyzer (HiSeq 2500v4 Rapid Mode) in a single lane of the flow cell. The library preparation, sequencing, and initial quality check were performed by the Texas A&M AgriLife Genomics and Bioinformatics Service (http://www.txgen.tamu.edu/).

Data analysis

The small RNA-seq data was analyzed using CPSS 2.0 (http://114.214.166.79/cpss2.0/index.html), a newly updated computational platform for species-specific small RNA-seq data analysis.[276] The canine genome (*Canis familiaris*) and default setting were used. The statistical significance of the sequencing results was tested using the Wilcoxon rank sum test using the stats package in R, and the continuity correction was applied if required. Once the read count table was generated, the differential expression and statistical analysis on the raw unnormalized miRNA read counts were done using the DESeq2 package in R.[272] For multiple testing, we used the Benjamini-Hochberg procedure to adjust *P*-values. A false discovery rate (FDR) < 0.05 was set to select DE miRs. Novel miRNAs were identified using miRDeep2.[378] Predictive novel miRNAs were deemed significant and selected for further analysis based on a miRDeep2 score ≥ 2 as suggested in a previous study.[249] Novel miRNAs of interest was

search against miRBase(release 22) to establish the evidence of homology (*E*-value < 0.05) between novel and existing sequence.[48]

Results

RNA quantification

A summary of the RNA quantification results for each isolation method is presented in Table 6. For each sample type, the 2 highest-yield isolation methods based on the Fragment analyzer and Qubit miRNA Assay results were selected to proceed with library preparation. For serum, these were the modified Zymo Direct-zol and miRCURY-Biofluids kits; for urine, they were the Qiagen exoRNeasy and Norgen Urine Exosome kits. Based on our selection of isolation and library preparation kits, we expected to compare 4 sequencing results each for serum and urine. However, only the modified Zymo Direct-zol isolation method in combination with the NEXTflex library preparation passed quality control. Therefore, only one serum sequencing result was available.

Table 6. Total RNA/miRNA concentration in serum and urine samples isolated using different kits.

		NanoDrop		Qubit miRNA Assay		
Sample (volume)	Isolation kits	Mean RNA concentration (ng/μL)	SD (ng/μL)	Mean RNA concentration(ng/μL)	SD (ng/μL)	Proceed to library preparation
Serum (2ml)	Modified Zymo Direct-zol	10.8	2.61	1.31	0.635	Yes
	miRCURY - Biofluids	49.0	39.5	2.82	0.360	Yes
	mirVana PARIS	4.67	1.45	1.22	0.553	No
Urine (10 ml)	Qiagen exoRNeasy	11.6	1.13	5.443	0.794	Yes
	Norgen Urine Exosome	6.53	1.14	0.474	0.012	Yes
	miRCURY Exosome	3.07	0.115	<0.25*	N/A*	No
*The miRNA concentration is below the detection limit of the Qubit miRNA Assay.						

Small RNA-seq statistics

Both urine miRNA isolation kits, Qiagen exoRNeasy and Norgen Urine Exosome, produced similar total reads and genome mapping rates (Table 7). However, Qiagen exoRNeasy produced significantly higher miRNA mapping rates ($P < 0.005$) and miRNA reads ($P < 0.005$), and it detected more miRNAs ($P < 0.05$), irrespective of the library preparation used. Similarly, the NEXTflex library preparation produced more total reads ($P < 0.005$) and higher genome mapping rates ($P < 0.005$) compared to TruSeq. Our sequencing results indicate 89-95% mapping of the genome (Table 7). Also, 198 miRNAs were found in the serum sample while up to 115 miRNAs were found in the urine sample.

Table 7. Sequencing results of serum and urine samples from different combinations of isolation and library preparation kits.

			Total reads		Genome mapping (%)		miRNA mapping (%)		miRNA reads	Number of detected miRNAs*	
Sample	Isolation kits	Library prep	Mean	SD	Mean	SD	Mean	SD	Mean	SD	Mean
Serum (2ml)	Modified Zymo Direct-zol	NEXTflex	9570811	512651	95.64	0.14	10.19	1.35	935949	159778	198
Urine (10ml)	Qiagen exoRNeasy	NEXTflex	8785349[a]	751807	95.00[a]	0.07	0.34[a]	0.03	28089[a]	2284	115[a]
		TruSeq	6521116[b]	371876	89.78[b]	0.33	0.54[a]	0.06	31550[a]	1708	96[a]
	Norgen Urine Exosome	NEXTflex	8221119[a]	669080	95.77[a]	0.64	0.07[b]	0.05	5357[b]	3736	73[b]
		TruSeq	5845279[b]	550725	91.12[b]	0.41	0.03[b]	0.01	1538[b]	330	45[b]

* Number of detected miRNAs for each combination was determined based on the sum of reads mapped to miRNA from triplicates.
[a,b] Within each column, different superscripts indicate a statistically significant difference in mean values using the Wilcoxon rank sum test ($P < 0.05$, unless specified in the main text). Only urine samples were teste.

MiRNA expression

We used principal component analysis (PCA) to explore the variation in miRNA expression among different sample types and combinations of isolation and library preparation kits. The PCA plot shows distinct miRNA expression in serum compared to urine (Figure 15A). For urine samples, principal component 1 (PC1) accounts for most of the variance, and samples prepared by different library preparation kits separated horizontally (Figure 15B). To a lesser degree, samples isolated by different isolation kits were also separated vertically based on principal component 2 (PC2). Thus, the PCA results indicated that library preparation introduced a higher degree of variation in miRNA expression than miRNA isolation method.

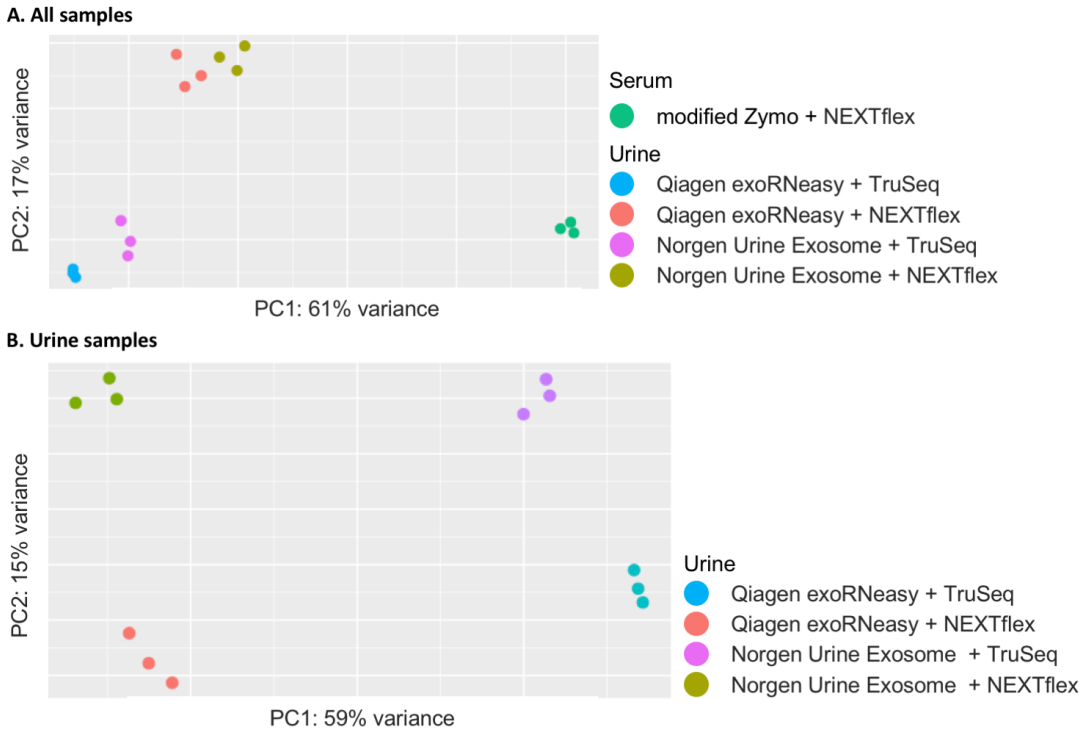

Figure 15. PCA plots for all sequenced samples. (A) all samples (B) urine samples only. PCA reduced the dimension of the data to multiple principal components (only PC1 and PC2 were shown here) while preserving the differences between samples. The percentage of variance indicates how much variance could be explained by PC1 and PC2.

To further compare the miRNA expression among samples, Venn diagrams were created, where each oval represents miRNA detected under a specific combination. Comparing the 2 urine results and the single serum result using the NEXTflex library preparation, more mature and novel miRNAs were detected in serum compared to urine (Figure 16 and S1). For serum, many mature and novel miRNAs were serum-specific. Among those serum-specific novel miRNAs, one has the highest miRDeep2 score (528.3) and approximately 1000 mapped reads that bears a sequence (aggacuguccaaccugagagug) almost identical to miR-1388 in multiple species (Supplementary File S2). Similarly, 3

other sequences were identified as potential homologs sequences to miR-502, miR-324, and miR-1224. While urine mature miRNAs were mostly detectable in serum, only 2 novel miRNAs overlap between urine and serum with borderline miRDeep2 scores (2.8 and 3.1) (Supplementary File S3).

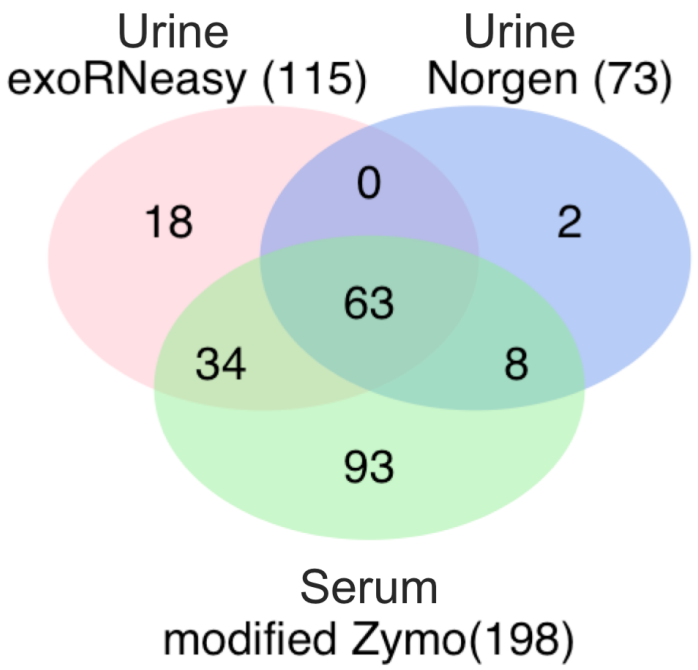

Figure 16. Serum and urine mature miRNA detected using different isolation methods. All samples were prepared with NEXTflex library preparation. For each method, only the miRNAs that have more than one mapped read across triplicates were counted. The total number of miRNAs detected is indicated in parentheses.

Next, we compared urine miRNA expression among all 4 method combinations of isolation and library preparation kits (Figure 17 and Supplementary File S4). Overall, the combination of Qiagen exoRNeasy and NEXTflex identified most of the mature and novel miRNA presented in our studies. None of the novel miRNAs was consistently presented,

and the only 2 overlapping novel miRNAs were seen in samples isolated with Qiagen exoRNeasy with borderline miRDeep2 scores (Supplementary File S4). On the other hand, 39 mature miRNAs were consistently detected in all combinations (Figure 17), and all 39 are highly expressed miRNAs in canine kidney tissues based on 2 recent studies.[376,377]

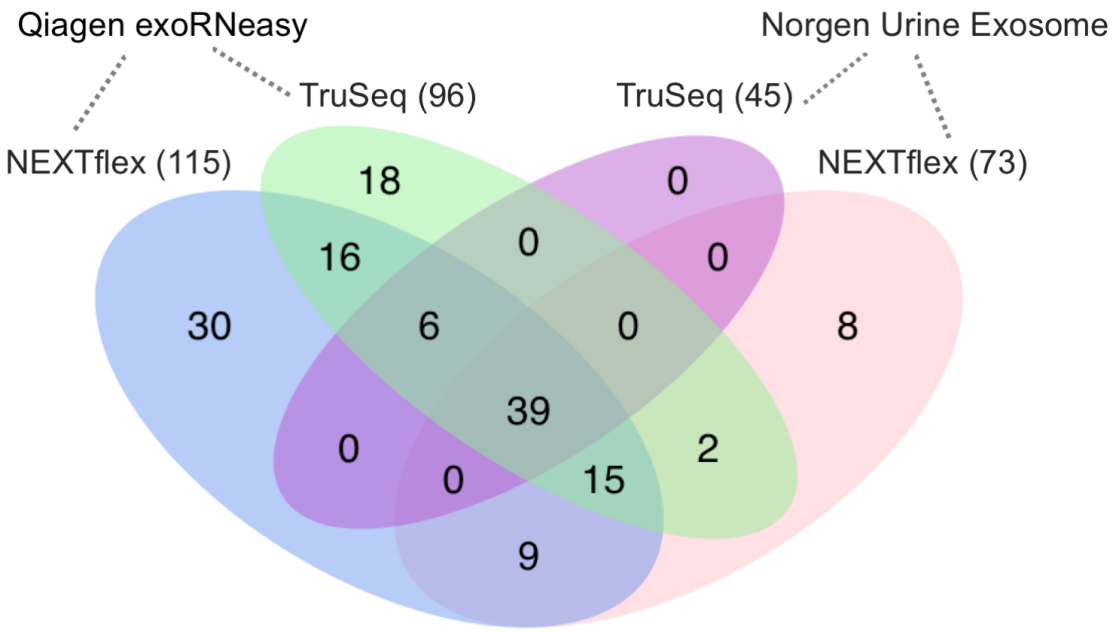

Figure 17. Urine mature miRNAs detected using different combinations of isolation and library preparation methods. For each combination, only the miRNAs that have more than one mapped read across triplicates were counted. The total number of miRNAs detected is indicated in parentheses.

Further, we compared the read count distribution pattern for these 39 miRNAs, comparing different miRNA isolation kits using the same library preparation, and comparing different library preparations for the miRNA isolation kit identified as most optimal in this study (Figure 18). Despite using different miRNA isolation methods, nearly identical normalized read count distribution patterns were observed when the same library

preparation was used (Figure 18A, B). In contrast, using the same miRNA isolation method (Qiagen exoRNeasy) but different library preparations, substantial discrepancies in miRNA expression was observed (Figure 18C). Moreover, the differential expression for NEXTflex compared with TruSeq was as high as ~20-fold upregulation in let-7b and ~29-fold downregulation in miR-126 (Supplementary Table S17).

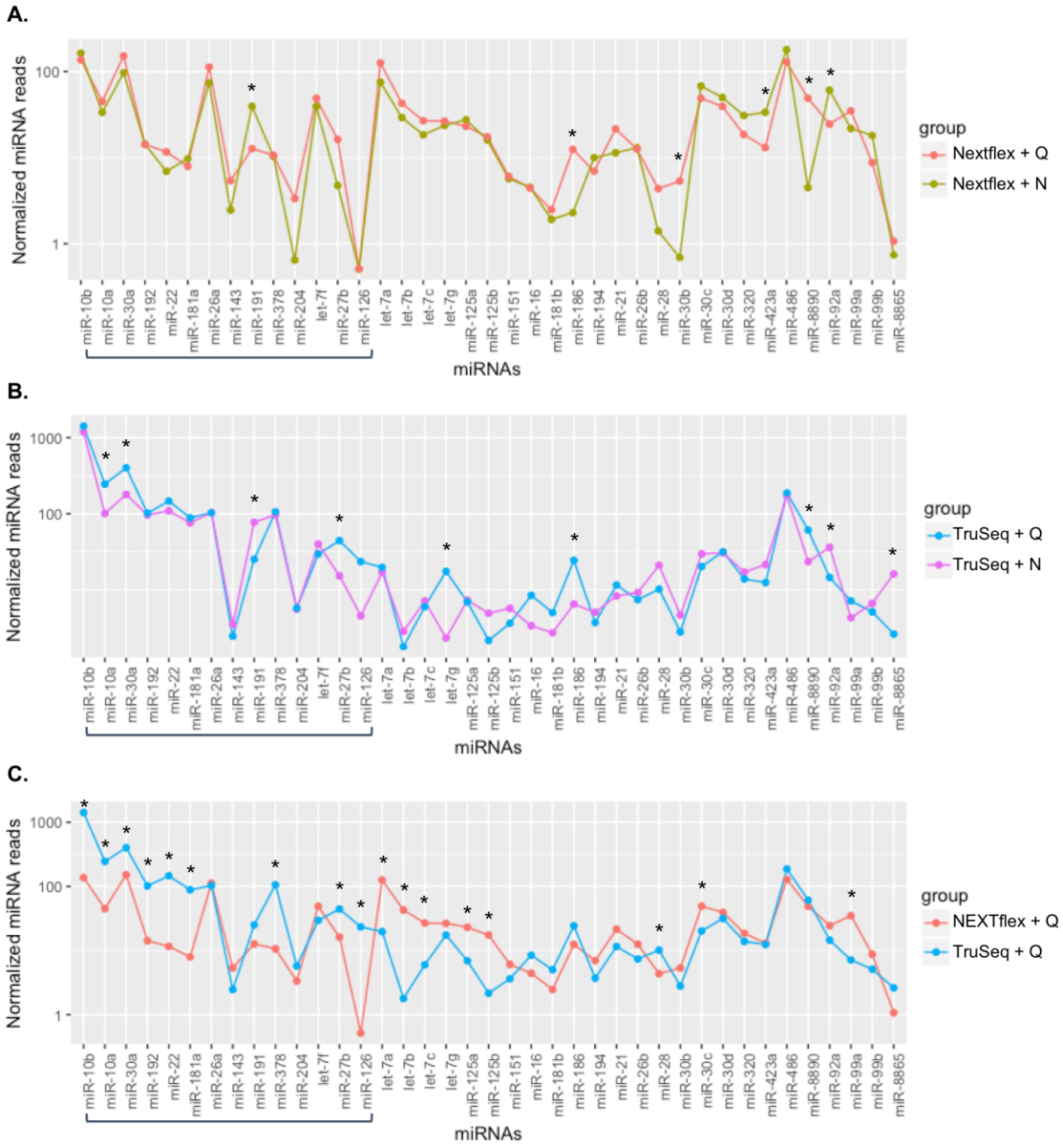

Figure 18. Comparisons of normalized miRNAs reads sequenced from urine samples that were processed by different RNA isolation and library preparation kits. (A) NEXTflex + Q versus NEXTflex + N. (B) TruSeq + Q versus TruSeq + N. (C) NEXTflex + Q versus TruSeq + Q. The most abundantly expressed miRNAs in canine kidney were sorted on the left side of the plot in a descending order as indicated by the bracket. Q: Qiagen exoRNeasy; N: Norgen Urine Exosome. (*: DE miRs between the 2 methods being compared) (false discovery rate < 0.05 and absolute fold change ≥ 2).

Discussion

To date, there is no gold standard for isolating miRNA from biofluids. Several studies have compared commercial miRNA isolation kits for serum[227], plasma[207,221-223,225,226], and urine[71,87] using samples from human and non-human primates. In addition, various kit modifications[207,221,223,225-227] and measurements (eg, NanoDrop[218,224,226] and Agilent Bioanalyzer[226,227]) have been used for comparing methods. However, most of these studies used qRT-PCR to determine the optimal miRNA isolation methods[87,207,218,219,221,223,225,227], and conclusions were often reached based on the expression levels of only a few miRNAs. In our current study, we tested 6 commercial miRNA isolation kits and used small RNA-seq to compare the performance of 2 urinary miRNA isolation kits along with 2 library preparation kits. Thus, we provide a more comprehensive approach to identifying optimal preparations for miRNA from canine serum and urine.

We first used RNA concentration to compare the performance of miRNA isolation kits. NanoDrop is a spectrophotometer commonly used for measuring tissue- and cell-derived total RNA. Given that total RNA concentration in biofluids often falls below its detection limit (4-10 ng/μL)[207], NanoDrop was of limited use in our case.[171] Unlike the NanoDrop, the Agilent Bioanalyzer Small RNA Kit can quantify small RNAs at lower concentrations (50-2,000 pg/μL). In an isolation method comparison study, the Agilent Bioanalyzer results corresponded to microarray results while NanoDrop failed to distinguish the performance between isolation kits.[224] Due to the lack of access to the Agilent Bioanalyzer, we used the Fragment Analyzer to measure the total RNA

concentration (50-5000 pg/μL). Both machines employ capillary gel electrophoresis to analyze nucleic acids. Our sequencing facility uses a cutoff value of 0.8 ng/μL for total RNA concentration to anticipate successful library preparation using NEXTflex (personal communication). Indeed, the miRCURY-Biofluids kit yielded a mean RNA concentration of 0.659 ng/μL, and the sample consequently failed in both library preparations.

Since the NanoDrop and the Fragment Analyzer only measured total RNAs, we incorporated the Qubit microRNA Assay to measure small RNAs. The Qubit microRNA Assay uses specific fluorescent dyes that selectively bind to small RNAs (detection range: 50-10,000 pg/μL). Garcia-Elias et al. have reported that the Qubit microRNA Assay is better than the NanoDrop and the Agilent Bioanalyzer to evaluate low miRNA concentration in human plasma.[411] Indeed, the Qiagen exoRNeasy kit yielded the highest RNA concentration in the urine sample as determined by the Qubit microRNA Assay (Table 6). Based on sequencing data, RNA isolated with this kit also had higher miRNA reads and number of miRNAs as compared with the Norgen kit (Table 7). Surprisingly, for serum miRNA isolation methods, we were unable to generate libraries for the RNA isolated by the miRCURY-Biofluids kit, even though this kit had the highest RNA concentration based on the Qubit microRNA Assay. Since the Qubit microRNA Assay detects all forms of small RNAs[411], this discrepancy might have been caused by the presence of other types of small RNAs isolated by the miRCURY-Biofluids kit.

Regarding correlation between RNA quantification methods and small RNA-seq, previous studies have shown that RNA concentration and miRNA percentage determined by the Agilent Bioanalyzer did not translate into the number of miRNA reads and the

percentage of miRNAs found using small RNA-seq.[238,239] Since the Agilent Bioanalyzer could misclassify degraded mRNAs as miRNAs, small RNA-seq is a better tool for comparing isolation performance. In our study, we also noticed that an increase in the number of reads mapped to miRNAs did not translate into a higher number of detected miRNAs. This supports that certain library preparations might be selective for certain miRNAs as demonstrated by recent studies compared multiple commercially available library preparation kits.[244]

Compared to RNA quantification methods, small RNA-seq provides a more comprehensive assessment of miRNA isolation and library preparations regarding miRNA mapping rate, the number of miRNAs detected, and novel miRNAs. In our study, we found that the miRNA mapping rate varied between serum and urine, ranging from approximately 10% in serum to less than 0.5% in urine (Table 7). Our results are similar to previous human and canine studies in which wide ranges of miRNA mapping rates have been reported for serum (10-25%) and urine (0.42-11%).[100,239,412,413] Although miRNA mapping rates could vary due to different preprocessing steps of raw reads in different studies, the number of miRNA reads and miRNAs detected in human serum and plasma are consistently higher than urine[53,412], as in our canine samples (Figure 16). Of note, we found extensive overlapping of miRNAs between serum and urine samples. While these dogs have inherited protein-losing nephropathy, studies in healthy people also shown substantial overlaps between circulating and urinary miRNAs.[412,413] For novel miRNAs, more were detected in canine serum than urine samples. While none of the urine-specific novel miRNAs was deemed homologous sequence in analysis, we identified 4 promising

serum-derived novel miRNA that could be homologous to miR-1388, miR-502, miR-324, and miR-1224 in other species.

Moreover, we observed that the library preparation method introduced more variation in miRNA detection than the method of miRNA isolation (Figure 15). Several studies have found that the adapter ligation step was the main cause of bias during library preparation.[248,414] Bias-contributing factors in adapter ligation, such as ligation efficiency, secondary structure, and adapter sequences, have been reviewed by Raabe et al.[246] TruSeq and NEXTflex use different types of adapters (fixed versus degenerate), different ligases (T4 versus AIR ligase), and different strategies to prevent adapter dimers (none versus removal of extra 3' adapters). Therefore, we anticipated different miRNA profiles and differential expression of the overlapping miRNAs between these 2 library preparations. Similar to previous studies used high[243,244,248] and low RNA inputs[244] isolated from tissues[248], cells[243], and plasma[244], we found that NEXTflex can detect miRNAs that evade capture by TruSeq. To our surprise, however, the expression levels of certain miRNAs, including some that are highly expressed in canine kidney tissues[376,377], were markedly different between the 2 library preparations (Figure 18). These highly expressed miRNAs in kidney tissues have a great potential to be biomarkers for kidney diseases.[377] For example, several miRNAs for which expression differed considerably between the 2 preparations have been described as promising biomarkers in kidney diseases (for example, serum let-7b in IgA nephropathy[415] and urinary miR-126 in DN[416]). Our results support the conclusion that library preparation method can greatly influence the identification and selection of biomarkers if based on sequencing data alone.

There are several limitations of this study. Pooled serum and urine samples from dogs with a single cause of protein-losing nephropathy were used to ensure equal comparison among methods. Although disease-specific bias in miRNA isolation methods has not been reported, we cannot rule out the possibility that this single sample source could introduce bias in the performance of the miRNA isolation kits. To measure the isolated RNA, we used the Fragment Analyzer and the Qubit miRNA Assay but did not incorporate the Agilent Bioanalyzer because of limited access. Also, we did not test one of the commonly used library preparation kits, NEBNext (New England BioLabs). However, a recent study shown no significant difference in the number of miRNA detected by TruSeq and NEBNext.[244] Finally, we sequenced our samples using one Illumina platform at a single sequencing facility since the study was designed to be a pilot study for a larger sequencing project. While one study demonstrated that sequencing platform and sequencing facility were not major contributors to variation in miRNA expression profiles[248], a recent study has shown increased impact of library preparation location on the percentage of RNA mapped reads when using low input RNA, particularly with the NEXTflex kit.[244] Therefore, including more sequencing platforms and locations could potentially expand the scope of the current study.

In conclusion, we successfully performed small RNA sequencing with total RNA isolated from 2 ml serum and 10 ml urine in dogs. We found that the optimal isolation method tested for canine serum was the modified Zymo Direct-zol kit and that for canine urine was the Qiagen exoRNeasy RNA isolation kit. The NEXTflex library preparation kit was the optimal library preparation method tested in this study for canine serum and

urine. Knowledge of the performance of these isolation and library preparation methods might be helpful for planning future studies in which a limited volume of biofluids is available. Also, different isolation and library preparation methods demonstrated significant differences in miRNA expression. Notably, library preparation method introduced a much higher variation in miRNA expression than miRNA isolation method. The library preparation-dependent bias could be significant in miRNA profiling for biomarker discovery.

CHAPTER V

MICRORNA PROFILING IN DOGS WITH CHRONIC KIDNEY DISEASE CAUSED BY GLOMERULAR DISEASES

Introduction

CKD is a significant cause of morbidity and mortality in all breeds of dogs, and it is commonly caused by underlying glomerular diseases. Our recent data indicate that an overwhelming majority (>80%) of proteinuric dogs with CKD have immune complex-mediated glomerulonephritis (ICGN), glomerulosclerosis (GS), or amyloidosis (AMYL).[15] While dogs with AMYL tend to have higher urine protein to urine creatinine ratio (UPC) values than dogs with other types of glomerular diseases, extensive overlap in UPC values exists among all groups.[417] Renal biopsy and comprehensive histopathologic examination are currently indispensable to the diagnosis of specific glomerular diseases and to guide proper treatments.[16] Patients deemed unsuitable to undergo anesthesia for a renal biopsy can be empirically managed with immunosuppressive treatment; however, immunosuppressive therapy is considered contraindicated in non-ICGN glomerular diseases.[418]

MiRNAs are small, non-coding, highly-conserved RNAs that post-transcriptionally regulate gene expression and play important roles in governing biological activity in both health and disease. To date, more than 2,600 mature miRNA sequences have been identified in humans (miRBase 22 release). These miRNAs not only exist in

cells, but they are also present in cell-free biofluids, including serum, plasma, and urine.[53] For CKD, biofluid miRNAs could serve as promising non-invasive biomarkers of disease onset, progression (including monitoring of therapeutic interventions), the degree of kidney damage, and categorization (ie, histologic diagnosis).

Several studies have identified circulating and urinary miRNAs in human patients with glomerular diseases. The subjects were either grouped as CKD patients[89,311] or studied within individual glomerular disease categories, such as FSGS[319,320], LN[325,326], and IgA nephropathy.[88,327] Since tissue-specific miRNA expression patterns have been described in patients with DN, FSGS, IgA nephropathy, and membranoproliferative GN[396], it is reasonable to expect that biofluid-derived miRNA could exhibit similar patterns of expression and might even differentiate categories of glomerular diseases.

Using next-generation small RNA-seq technology, we aimed to globally characterize miRNAs in urine and serum from clinically healthy dogs and dogs with CKD caused by the 3 most common glomerular diseases (ICGN, GS, and AMYL) at 2 different stages of disease progression. We hypothesized that unique miRNA signatures would be found in the serum and urine of dogs with each of these glomerular diseases and that these miRNAs might serve as non-invasive diagnostic markers or targets for novel therapies that contribute to both canine health and human health.

Material and methods

Animal specimens

Samples from 18 dogs, 6 from each glomerular disease category (ICGN, GS, and AMYL), were selected from archived serum and urine samples previously submitted to the International Veterinary Renal Pathology Service (IVRPS) for diagnostic purposes. Additionally, samples from 6 clinically healthy dogs were used as controls. Signalment and clinical information for all 24 dogs are summarized in Supplementary Table S18.

Dogs with kidney disease were assigned a glomerular disease category based on a comprehensive kidney biopsy evaluation including light microscopy, transmission electron microscopy, and immunofluorescence.[419] Membranous glomerulonephropathy, a form of ICGN where the immune deposits are subepithelial in location, was selected to represent ICGN in this study. Urine and serum samples were obtained at the time of renal biopsy. A standard protocol was provided to clinicians for centrifugation and separation of supernatant. Samples were then shipped overnight on wet ice and stored at -80°C for 1 to 6 years until analysis. Dogs with CKD were retrospectively selected based on (1) age (≥1-year-old), (2) category of glomerular disease (confirmed by biopsy)[285], (3) inactive urine sediment (within 2 weeks of biopsy defined as absence of discoloration or cloudiness on gross examination, <5 WBCs/high-power field, <100 RBCs/high-power field, and no bacteriuria), (4) adequate sample volume (serum: ≥ 1 ml and urine: ≥ 3 ml), and (5) non-hemolyzed serum base on a hemolysis score (see "RNA isolation" section). Serum and urine from the same dog were required for inclusion in the study. Within each disease category, CKD dogs were further divided into stage 1 and stage 2. Stage 1 was defined as

dogs with proteinuria but not azotemia (sCr < 1.4 mg/dl or appropriately low for the breed) and with biopsy findings limited to minimal to mild tubulointerstitial (TI) damage. Stage 2 was defined as dogs with proteinuria and mild to moderate azotemia (1.4 ≤ sCr ≤ 5 mg/dl) or sCr < 1.4 mg/dl but inappropriately high for the breed and biopsy results demonstrating significant TI damage. All stage 1 GS dogs exhibited FSGS while stage 2 GS dogs had advanced segmental to global glomerulosclerosis.

For the clinically healthy dogs used as controls, a physical examination, complete blood count, chemistry panel, urinalysis, and UPC were performed. After collection, uncoagulated blood was allowed to sit at room temperature for 30 minutes to 1 hour then centrifuged at 1500 g for 10 minutes at room temperature to separate serum. Urine was collected via cystocentesis, and urine remaining after the urinalysis was centrifuged at 1000 g for 10 minutes at 4°C. Serum and urine were aliquoted into cryotubes and stored at -80°C for approximately 3 years until RNA isolation. The protocol was approved by the Texas A&M University Institutional Animal Care and Use Committee and client consent was obtained.

RNA isolation

All serum samples were screened for hemolysis by measuring the A385 and A414 using the NanoDrop 2000 (Thermo Fisher Scientific, Wilmington, DE, USA) and the following formula: hemolysis score = A414 - A385 + lipemia correlation factor*A385.[197] Incorporating A385 in the calculation of the hemolysis score was done to minimize the interference of lipemia when measuring A414.[197] Scores were compared with an in-house hemolysis score cutoff value generated from a set of 28 grossly non-hemolyzed leftover

from clinical samples submitted to the Texas A&M University Veterinary Medical Teaching Hospital.

Circulating RNA was isolated from serum by a modified protocol using the Direct-zol RNA MiniPrep Kit (Zymo Research, Irvine, CA, USA). For each dog, 1 mL of serum was first homogenized with 5 ml QIAzol Lysis Reagent (Qiagen, Germany). The mixture was vortexed then incubated at room temperature for 5 minutes. Next, 1.2 ml chloroform was added, and lysates were vortexed then incubated at room temperature again, for 5 minutes, followed by 4°C centrifugation at 13400 g for 15 minutes. After centrifugation, the upper aqueous phase was mixed with 4.8 ml 100% ethanol, added to the Zymo-Spin Column (Zymo Research, Irvine, CA, USA), and centrifuged for 30 seconds at 12000 g at room temperature. The spin column was then washed 4 times: twice with Zymo RNA pre-wash buffer (Zymo Research, Irvine, CA, USA), once with Zymo RNA wash buffer (Zymo Research, Irvine, CA, USA), and last with 500 μL 80% ethanol. Finally, 25 μL 50°C RNase-free water was used to elute RNA.

For each dog, urinary RNA was isolated from 3 mL urine using the Qiagen exoRNeasy Serum/Plasma Maxi Kit (Qiagen, Germany). The manufacture's protocol was followed up to the point of adding QIAzol Lysis Reagent (Qiagen, Germany). The subsequent steps were identical to the serum isolation protocol, except that the RNeasy MinElute Spin Columns (Qiagen, Germany) were washed 3 times: Once with Buffer RWT (Qiagen, Germany) and twice with Buffer RPE (Qiagen, Germany). RNA was also eluted with 25 μL 50°C RNase-free water.

Small RNA sequencing and data analysis

RNA samples were measured using the Fragment Analyzer High Sensitivity RNA Analysis Kit (Advanced Analytical Technologies, Inc., Ankeny, IA, USA). Laboratory personnel at the Texas A&M University Genomics and Bioinformatics service generated a cDNA library using the NEXTflex Small RNA Library Prep Kit (Bioo Scientific Corp, Austin, TX, USA). Under a 50 base-pair, single-end setting, all 48 cDNA libraries were multiplexed and sequenced in parallel on 3 lanes of a flow cell in an Illumina Genome Analyzer (HiSeq 2500v4) to minimize technical variation and ensure sufficient data output.

Pre-processing of raw reads (fastq files) included (1) removal of the 3' adapter sequence (TGGAATTCTCGGGTGCCAAGG), (2) trimming of the first and last 4 bases from the adapter-clipped reads (as recommended by the manufacturer)[285], (3) filtering out reads less than 16 base-pair to prevent false degraded RNA or adapter dimers[264], and (4) removal of low quality reads (quality score < 30). Untrimmed raw reads were discarded as they were unlikely to be miRNAs based on read lengths. FASTX-Toolkit (version 0.0.14) was used to transform the fastq format into collapsed fasta files as proper inputs for CPSS 2.0 (http://114.214.166.79/cpss2.0/index.html).[276] Default settings along with the canine genome (*Canis familiaris,* CanFam 3.1) and microRNA annotation in miRBase (release 21) were used for analysis. To identify candidate miRNAs for internal controls, NormFinder (updated January 2015) was applied to the read count table.[300] The DESeq2 package in R was used for miRNA differential expression.[272] For multiple testing, Wald test *P*-values were corrected to the false discovery rate (adjusted *P*-values) by the

Benjamini-Hochberg procedure. An adjusted *P*-value < 0.05 was set to robustly select DE miRs.

Results

Circulating and urinary DE miRs expression

Figure 19 shows the clinical parameters of dogs in the current study. The difference in mean age between different disease groups is noted while no overall difference in sCr is seen among the disease groups. As expected based on our study design, sCr is significantly higher in stage 2 CKD dogs than stage 1 CKD dogs and controls. No UPC difference was seen among dogs with different types of glomerular diseases, but dogs with stage 2 CKD had higher UPC values than stage 1 dogs and controls.

Forty-eight RNA samples were used for small RNA-seq, 24 samples isolated from serum and 24 samples isolated from urine. One serum sample representing stage 2 ICGN was excluded for having less than 5 million reads (Supplementary Table S19). Sequenced serum samples had an average of 6.5 million reads and a 97.6% genome mapping rate, with 1.6 million reads mapped to miRNAs whereas urine samples had an average of 6.9 million reads and a 90.1% genome mapping rate, with 79019 reads mapped to miRNAs. On average, 167 and 88 miRNAs with at least 10 mapped reads were detected in serum and urine samples, respectively.

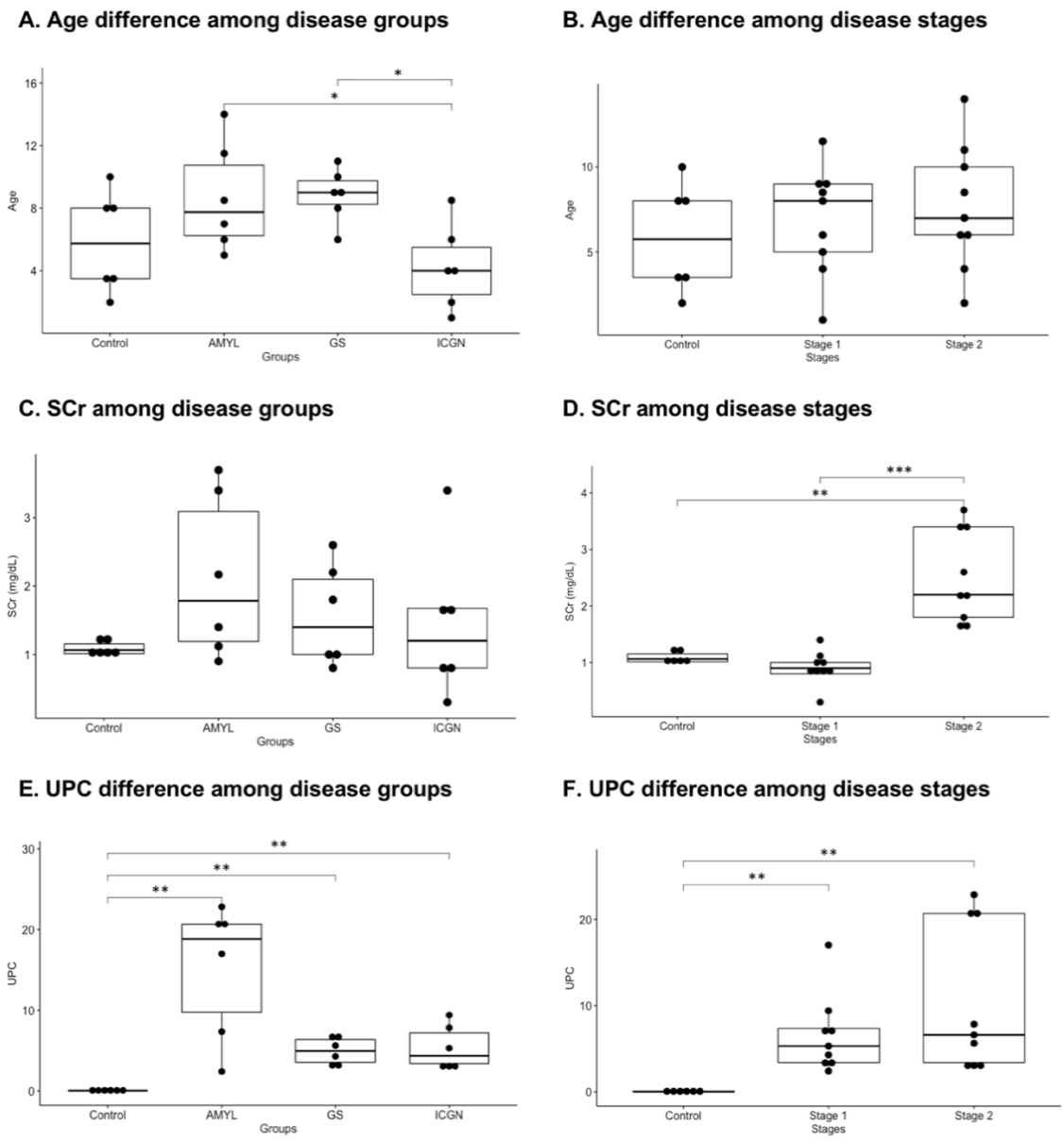

Figure 19. Boxplots of age, sCr, and UPC distribution. (A, B) Age difference among different disease groups and stages. (C, D) SCr difference among different disease groups and stages. (E, F) UPC difference among different disease groups and stages. Wilcoxon test was performed in a pair-wise manner with Benjamini-Hochberg Procedure for multiple testing. *P*-values < 0.05 was shown in the plots. (*: *P*-value < 0.05; **: *P*-value < 0.01; ***: *P*-value < 0.001).

For each sample type, we compared DE miRs in dogs with CKD to clinically healthy controls. Overall, 47 circulating miRNAs and 18 urinary miRNAs were DE in CKD dogs versus controls. Comparing stage 1 CKD dogs (non-azotemic and minimal TI damage) with controls, 9 circulating and 13 urinary DE miRNA were detected while 46 circulating and 24 urinary DE miRs were discovered comparing stage 2 CKD dogs (azotemic and advanced TI damage) with controls. For DE miRs identified in specific glomerular diseases (ICGN, GS, and AMYL), only those with an absolute fold change > 2 that were also differentially expressed in CKD dogs compared to controls were listed (Figure 20). In each category, CKD dogs were compared to controls regardless of disease stage (Figure 20A, D) or were further divided into stage 1 (Figure 20B, E) and stage 2 (Figure 20C, F). Regardless of disease stage, 5 circulating miRNAs (miR-107, miR-129, miR-186, miR-365, and miR-371) and 5 urinary miRNAs (miR-7, miR-9, miR-22, miR-203, and miR-423a) were DE in dogs with all 3 glomerular diseases when compared to controls. Downregulated circulating miR-186 was also one of the 6 common DE miRs among all 3 disease categories comparing stage 2 CKD dogs with controls (Fig 20C). Downregulated urinary miR-7 and miR-22 were the only 2 common DE miRs among all 3 disease categories identified in stage 1 dogs compared with controls, and they also comprised 2 of the 5 DE miRs in stage 2 dogs compared with controls (Fig 20E-F). In general, more DE miRs were discovered in samples from dogs with stage 2 disease than were discovered in samples from dogs with stage 1 disease. A list of circulating and urinary DE miR is provided in Supplementary Tables S20 and S21. For DE miRs in

specific disease categories, only those DE miRs that were also differentially expressed when comparing all dogs with CKD with controls at the respective stage are included.

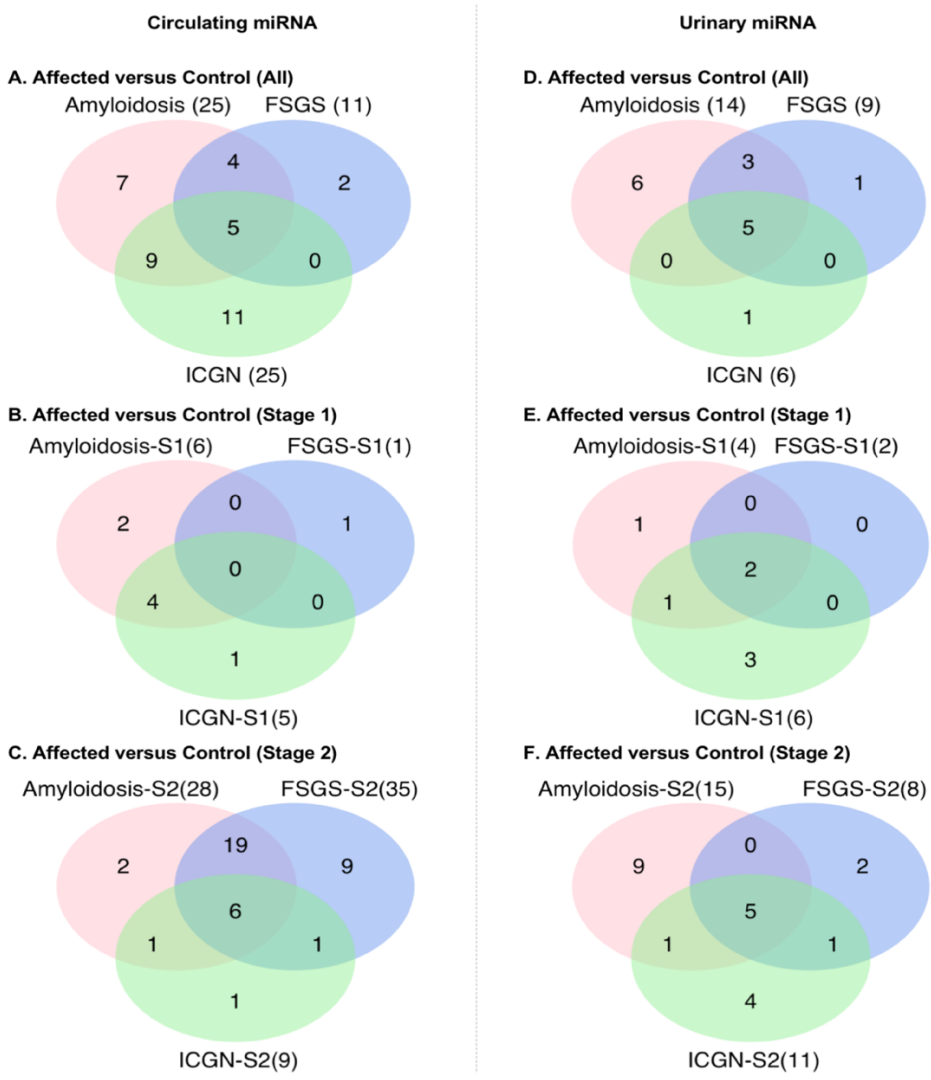

Figure 20. DE circulating and urinary miRNAs identified in CKD dogs (based on glomerular disease category) versus controls. Dogs with CKD were compared to controls regardless of disease stage (A, D), at stage 1 (B, E), and at stage 2 (C, F). The total number of DE miRs are shown in parenthesis. Only those DE miRs that were also differentially expressed when comparing all dogs with CKD with controls at the respective stage are included. Differential expression was based on an absolute fold change > 2 and an adjusted *P*-value < 0.05. (S1: stage 1 CKD; S2: stage 2 CKD).

DE miRs associated with disease progression

We further examined miRNAs that were differentially expressed in CKD dogs at stage 2 compared to stage 1. When all CKD dogs were combined together regardless of glomerular disease category, no circulating DE miRs were identified between stage 2 CKD dogs and stage 1 CKD dogs. However, 3 urinary DE miRs were identified comparing stage 2 versus stage 1 CKD dogs, including 2 upregulated DE miRs (miR-182, and miR-21) and 1 downregulated DE miRs (miR-486) (Figure 21). Notably, the expression of urinary miR-486 is significantly decreased in stage 2 CKD compared to both stage 1 and controls (Figure 21).

Comparing the glomerular disease categories, no DE miRs were found when comparing stage 2 to stage 1 AMYL. However, 22 circulating DE miRs and 1 downregulated urinary (miR-486) miRNAs were found comparing stage 2 to stage 1 GS. The high number of circulating DE miRs in stage 1 versus stage 2 GS were caused by the indistinguishable miRNA expression of 2 stage 1 GS samples from the controls (Supplementary Figure S7). For ICGN, 1 downregulated circulating (miR-485) and 1 downregulated urinary (miR-128) miRNA were found comparing stage 2 to stage 1 CKD dogs. A complete list of circulating and urinary DE miRs comparing stage 1 and stage 2 is provided in Supplementary Table S22.

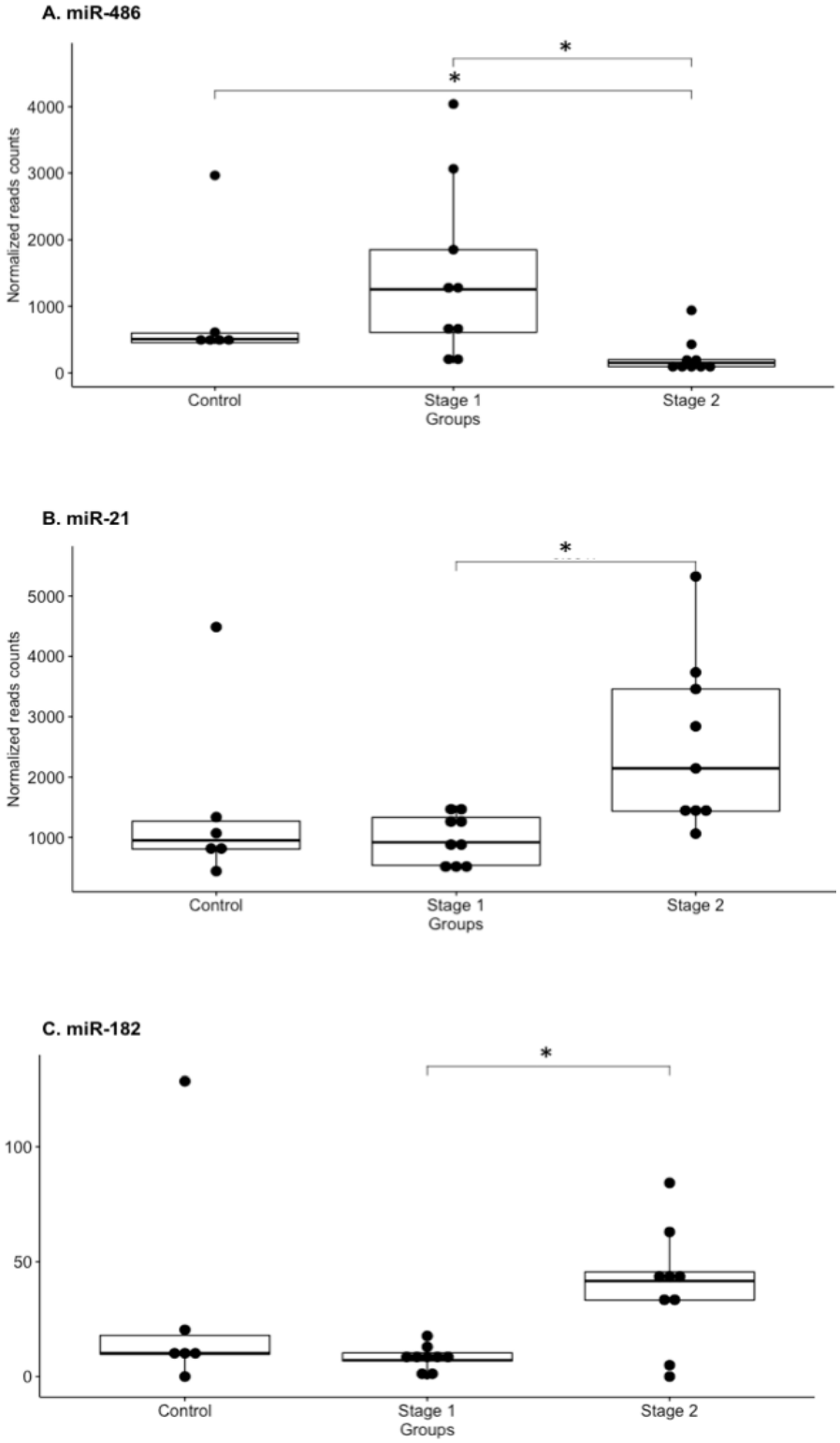

Figure 21. Normalized read counts for urinary DE miRs identified between stage 2 and stage 1 CKD dogs. (A) miR-486, (B) miR-21 (C) miR-182. (*: *P*-value < 0.05).

Disease-specific urinary miRNAs

We aimed to identify biofluid-derived miRNAs that are exclusively differentially expressed in certain types of canine glomerular diseases. No circulating miRNAs were found to be differentially expressed among the different glomerular diseases. For urinary miRNAs, the expression of level of miR-335 was significantly higher in dogs with GS than in other categories, including controls (Figure 22).

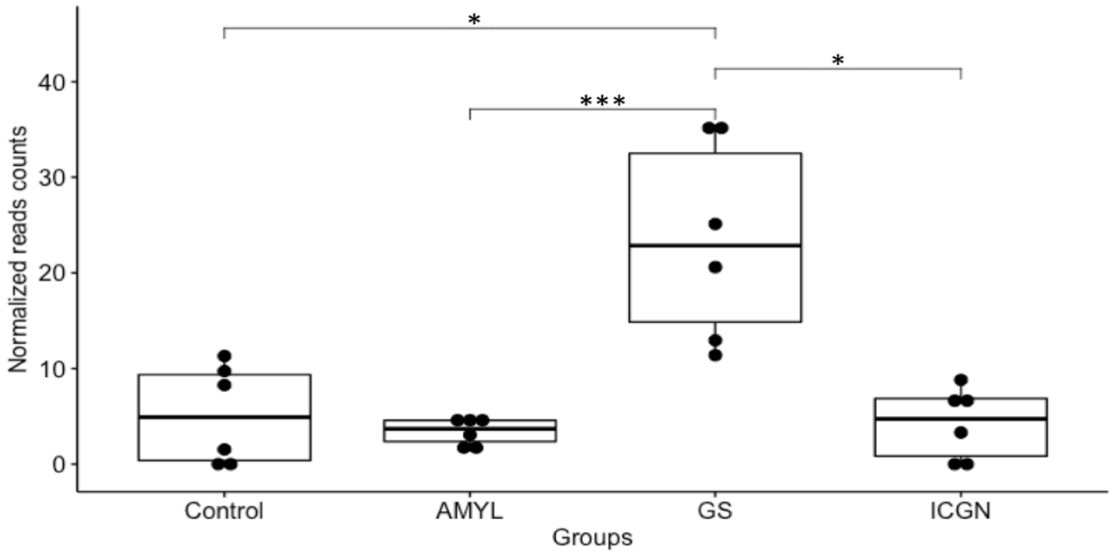

Figure 22. Normalized read counts for urinary miR-335 in all 4 categories. (*: *P*-value < 0.05; ***: *P*-value < 0.001).

We also compared each glomerular disease category within each disease stage to examine the DE miRs in early vs. later disease. In Table 8, we first noticed the unlikely enormous upregulation of canine miR-1836 (cfa-miR-1836). Literature search confirmed that the annotation of cfa-miR-1836 overlaps with snoRNA 20 (SNORA20) with high

confidence (probability = 0.99).[420] Therefore, we will exclude miR-1836 in our analysis. At stage 1, 3 circulating miRNAs (miR-335, miR-101, and miR-32) and 5 circulating miRNAs (miR-320, miR-99b, miR-218, miR-335, and miR-485) were differentially expressed in ICGN compared with AMYL and GS, respectively. No urinary DE miRs were identified among stage 1 samples. At the later stage, urinary miR-350 were differentially expressed comparing AMYL and GS. No circulating DE miR was found for ICGN versus AMYL, and circulating miR-374a was differentially expressed in ICGN versus AMYL. At the later stage, 5 urinary DE miRs were discovered in at least one pair of comparisons among the 3 glomerular diseases. Notably, the distinctive expression of urinary miR-126, miR-335, and miR-128 could correctly group azotemic, proteinuric dogs into ICGN, GS, or AMYL (Figure 23). This unique finding supports that urinary miRNAs might help establish a diagnosis in azotemic dogs with suspected glomerular disease.

Table 8. DE miRs identified in each glomerular disease category in early versus later disease.

		Serum			Urine		
	Comparisons	miRNA	Fold change	Adjusted *P*-value	miRNA	Fold change	Adjusted *P*-value
Stage 1	AMYL vs GS	N/A	N/A	N/A	N/A	N/A	N/A
	AMYL vs ICGN	miR-335	86.7	1.10E-02	N/A	N/A	N/A
		miR-101	3.67	4.70E-02			
		miR-1836*	23852	4.70E-02			
		miR-32	14.9	4.70E-02			
	GS vs ICGN	miR-320	-4.30	3.00E-03	N/A	N/A	N/A
		miR-99b	-3.18	4.30E-02			
		miR-218	6.23	4.70E-02			
		miR-335	42.0	4.70E-02			
		miR-485	-19.0	4.70E-02			
Stage 2	AMYL vs GS	miR-1836*	-3726076	2.30E-05	miR-335	-9.61	1.28E-02
		miR-350	91.6	2.90E-02	miR-8904b	20.8	1.28E-02
	AMYL vs ICGN	miR-1836*	-5769001	1.80E-04	miR-126	-10.9	1.25E-02
					miR-128	4.15	1.25E-02
					miR-143	-7.02	4.45E-02
	GS vs ICGN	miR-374a	-5.86	2.03E-02	miR-8904b	-24.3	6.80E-03
					miR-126	-26.3	4.74E-02
* miR-1836: See main text for the description of cfa-miR-1836.							

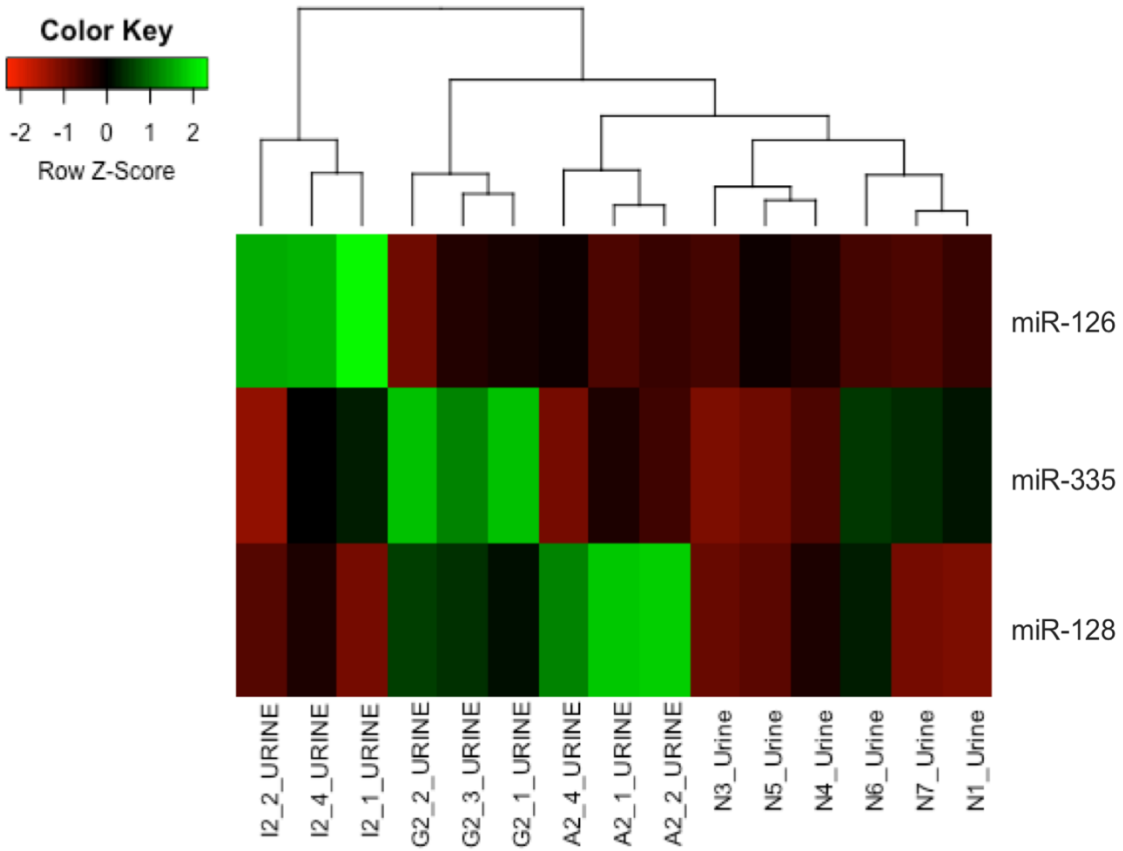

Figure 23. Heatmap and clustering analysis of urinary miR-126, miR-335, and miR-128 in dogs with stage 2 glomerular diseases and controls. The expression levels of miR-126, miR-335, and miR-128 are significantly higher in azotemic dogs diagnosed with I (ICGN), G (GS), and A (AMYL), respectively.

Endogenous controls for biofluid-derived miRNAs in dogs with CKD

Lastly, to identify appropriate endogenous reference miRNAs as controls, NormFinder[300] was performed on sequencing data. Small RNA-seq data were grouped according to disease stage and category, then NormFinder[300] was applied to rank candidate genes based on their expression stability in the given experimental design. The stability score is a direct measurement of estimated expression variation. Therefore, miRNAs that

are good candidates for being an internal control should have lower stability scores. The miRNAs with the lowest stability scores are presented in Table 9. It is worth noticing that these candidate miRNAs were not identified as DE miRs in any given pair of comparisons in the current study.

Table 9. Top 3 endogenous reference miRNAs identified in serum and urine by NormFinder.

	Serum			Urine			
miRNA	Group difference	Group standard deviation	Stability	miRNA	Group difference	Group standard deviation	Stability
let-7d	2561.65	366.64	115.71	miR-151	215.27	77.48	100.42
miR-192	2900.57	530.42	131.38	miR-28	93.81	138.49	108.06
miR-15b	1703.19	670.56	275.62	miR-8859a	235.13	98.79	109.99

Discussion

Canine CKD is commonly caused by glomerular diseases. A 2013 study found that more than 80 percent of dogs biopsied for suspicion of glomerular disease have ICGN (48.1%), GS (20.6%), or AMYL (15.2%).[15] Renal biopsies are the gold standard method for diagnosing glomerular diseases, and patients that are unable to have a kidney biopsy obtained due to cost or anesthetic risk are empirically managed.[418] Therefore, our aim was to identify miRNA biomarkers in serum and urine in dogs with CKD compared with clinically healthy dogs. In particularly, we aimed to identify miRNAs that indicate disease progression and might distinguish between the most common types of glomerular diseases (ICGN, GS, and AMYL).

Several studies have investigated the expression of biofluid-derived miRNAs in human CKD patients. Early studies provided limited information due to the low numbers of miRNAs screened[89,311], or identification of miRNAs with low fold changes (< 2 fold).[179] With the development of next-generation sequencing, more recent studies have sequenced urinary miRNAs in CKD patients, providing more extensive and robust data.[316] In one study, the miRNA expression in 15 CKD patients was compared with 10 healthy controls using small RNA-seq. In this study, 16 urinary miRNAs were found to be consistently differentially expressed throughout all 4 stages of CKD.[316] Comparing those urinary miRNAs with the DE miRs discovered in the current study, miR-222 is the only overlapping miRNA that was also upregulated in dogs with CKD compared to controls (Supplementary Table S21). While not extensively studied in the context of kidney disease, miR-222 was identified in the exosomes derived from melanoma cells. Its upregulation promotes tumorigenesis by activating the PI3K/AKT pathway.[421]

At this point in time, only one canine study has used small RNA-seq for investigating urinary miRNAs in dogs with kidney disease. In this study, 2 urine samples were sequenced: one pooled sample from dogs with kidney disease and one pooled sample from healthy controls. The sample obtained from dogs with kidney diseases had more reads mapped to miR-10a, miR-10b, miR-21, and miR-486 than the control sample while the number of reads mapped to miR-191, miR-192, miR-22, and miR-30a were reported to be similar between the 2 samples.[100] However, since no statistical analysis was performed due to the lack of biological replicates[100], the reproducibility is questionable. Among the 4 miRNAs reported in that study to have higher expression in diseased dogs[100],

miR-486 was the only urinary DE miR identified in our study. Moreover, miR-22, one of the miRNAs previously determined to be similarly expressed between dogs with kidney diseases and controls[100], was one of the top urinary DE miRs across all pairs of comparisons between CKD dogs and controls in our study.

In addition to identifying DE miRs in dogs with CKD, we also explored biofluid-derived miRNAs that could potentially indicate disease progression. The expression levels of miR-182, miR-21, and miR-486 in the urine of azotemic, proteinuric dogs are significantly different from those of non-azotemic, proteinuric dogs. In a rat renal proximal tubular cell line (NRK-52E), miR-182 targets the transcription factor 7-like-2 (TCF7L2) mRNA expression. In hypoxic NRK-52E cells, TCF7L2 suppresses hypoxia-induced apoptosis by activating the Wnt/β-catenin signaling pathway to promote cell repair. Increased miR-182 inhibits TCF7L2, resulting in increased apoptosis and exacerbating acute kidney injury (AKI).[422] Furthermore, the knockdown of miR-182 results in decreased blood urea nitrogen (BUN) and sCr in an AKI rat model[422], indicating that miR-182 could be involved in the molecular mechanisms resulting in TI damage. The expression level of miR-182 was found to be increased in the kidney tissue from patients with post-transplant AKI compared to allographs without pathology.[423] In the current study, the expression level of miR-182 in urine is significantly higher in azotemic CKD dogs than non-azotemic CKD dogs and controls. Taken together, urinary miR-182 could be a potential biomarker for kidney injury.

Urinary miR-21 was also found to be increased in azotemic CKD dogs in our study, similar to other studies in dogs with azotemic kidney disease. In dogs with X-linked

hereditary nephropathy, urinary miR-21 increased upon the development of azotemia based upon qRT-PCR and normalization with miR-16 (unpublished observations). Based on a small RNA-seq study, more reads were mapped to miR-21 in dogs with azotemic kidney disease due to a variety of causes compared with controls.[100] In humans, urinary miR-21 is higher in AKI patients compared to healthy controls.[424,425] Also, it has been proposed as a potential biomarker for hypertensive kidney injury and fibrosis in a study using a murine model[426]; however, additional studies using validated endogenous controls other than snRNAU6 are needed.[315]

The expression level of miR-486 was significantly lower in the urine of azotemic CKD dogs than both non-azotemic CKD dogs and the healthy controls. MiR-486 results in inhibition of transcription factor FoxO1. While FoxO1 has many proposed actions, it appears to be a dominant mediator of muscle wasting in CKD.[427] Exosomes derived from human endothelial colony-forming cells (ECFC) that were enriched with miR-486 were protective against AKI in mice, inhibiting endothelial cell apoptosis caused by hypoxia and reperfusion, and inhibition of miR-486 obviated these protective effects.[428] Although they originate from endothelial cells, it has been shown that ECFC-derived exosomes could be delivered to the kidney via renal capillaries and renal tubules.[429] Therefore, it is possible that a portion of the protective miR-486 could be detected in urine, and the downregulation of miR-486 in CKD dogs may play a role in the progression of kidney disease.

In azotemic dogs, the upregulation of urinary miR-126, miR-355, and miR-128 were exclusively seen in those diagnosed with ICGN, GS, and AMYL, respectively

(Figure 23). Given that not all of them were significantly increased in one disease category compared with the others, simply measuring just 1 miRNA would likely be insufficient for distinguishing different glomerular diseases in azotemic dogs. ICGN was the most common cause of glomerular disease in dogs biopsied for suspicion of glomerular disease.[15] Our study demonstrated a significant increase in miR-126 in azotemic dogs with ICGN compared with GS and AMYL. While no published literature currently exists regarding the expression of miR-126 in ICGN, increased expression of urinary miR-126 was found in patients with type 2 diabetes mellitus and DN compared with patients without DN.[416] Similarly, in a recent meta-analysis including 14 studies on miRNA expression in blood and urine from DN patients, urinary miR-126 expression was significantly upregulated compared to healthy controls and patients with no evidence of DN.[430] In contrast, both our data and previous studies on DN patients documented a significant decrease in circulating miR-126 expression in dogs and people with kidney disease (Supplementary Table S20).[7,430] MiRNA-126 was shown to be enriched in endothelial progenitor cell-derived extracellular vesicles and was thought to be responsible, in part, for their protective effect against ischemic AKI.[429] Given the opposite findings in the serum vs. urine, more studies regarding the originations of circulating and urinary miR-126 are needed to understand the discrepancy in its detection and its potential role in disease.

In the current study, urinary miR-335 was upregulated in azotemic dogs diagnosed with GS when compared to azotemic dogs with AMYL. Similarly, miR-335 was upregulated in the kidney tissue of old rats (24 months old) compared to young rats (3

months old).[431] In aging mesangial cells, significant upregulation of miR-335 was seen, and the expression of superoxide dismutase 2 (SOD2), a putative target of miR-335, was markedly downregulated.[431] Based on knockout and over expression studies, miR-335 contributes to the accumulation of reactive oxygen species (ROS) and consequent renal aging by suppressing the antioxidant effect of SOD2 in mitochondria.[431] While the pathophysiological mechanism of FSGS is not entirely understood, putative pathways involving ROS have been postulated.[432] Several studies found that agents that lower ROS levels[433,434] or stimulate SOD activity[435] could attenuate GS in murine models. Therefore, miR-335 is likely involved in the pathogenesis of GS in dogs.

Urinary miR-128 is upregulated in azotemic dogs with AMYL when compared to azotemic dogs with ICGN. Currently, miRNA studies in renal amyloidosis are lacking; however, the function of miR-128 in renal cells has been characterized. The overexpression of miR-128 induces apoptosis in human embryonic kidney cells (HEK293T) by regulating the pro-apoptotic protein Bax.[436] In normal rat kidney cells (NRT) in which miR-128 was overexpressed, the expression of pro-inflammatory genes such as *CCL5*, *CX3CL1*, and *CXCL7* was also upregulated.[417] The MAPK pathway appears to be the top enriched pathway of miR-128 target genes.[417]

Future directions

The highlighted miRNAs that were differentially present among the disease groups and disease stages in this small RNA-seq study will be validated using qRT-PCR in a second cohort of similarly-obtained and stored samples from dogs with a variety of glomerular diseases. This will help to establish a miRNA profile for CKD and different

glomerular diseases in dogs. Our small RNA-seq data has provided a foundation for selecting promising endogenous miRNAs as controls for this qRT-PCR. However, spike-in synthetic miRNA will be introduced during RNA isolation and analyzed along with the internal control candidates using the geNorm[298] algorithm for normalization. The validated results will be correlated with clinical and pathologic data, such as histopathologic scoring of kidney biopsies, routine tests of renal function, and survival data. Results will provide valuable information for discovering non-invasive, novel microRNA biomarkers in dogs with glomerular diseases.

CHAPTER VI

CONCLUSIONS

CKD is a significant cause of morbidity and mortality in dogs. The majority of proteinuric CKD dogs have glomerular diseases, including FSGS, ICGN, and AMYL. These glomerular diseases have distinct therapeutic strategies, and a renal biopsy is needed for an accurate diagnosis. In this report, our ultimate goal was to use small RNA-seq to investigate miRNAs as biomarkers for early detection and progression of CKD. To achieve our goal, we first explored the genes and miRNA expression in kidney biopsies from male dogs with XLHN using RNA-seq and small RNA-seq. Next, samples from female dogs that were carriers for XLHN were used to optimize RNA isolation and library preparation for small RNA-seq. Finally, the established protocol was applied to dogs with 3 types of glomerular diseases (FSGS, ICGN, and AMYL). The knowledge acquired from naturally occurring, progressive CKD establishes the basis for future studies.

In the first RNA-seq study in a canine model of CKD, Chapter II described a study that profiled the gene expression in kidney biopsies obtained from male dogs with XLHN that have different speeds of disease progression. For these dogs born with the same gene mutation, lifespan until end-stage renal disease varied from as rapid as 6 months to as slow as one year. The results identified up to 70 DEGs when rapid and slow groups were compared at specific clinical time points. When using the time-course analysis to identify genes with group-specific changes over time, 1947 DEGs were identified. The

upregulation of inflammatory pathways was verified by T cell infiltration via IHC, and TGF-β1 was identified as the top upstream regulator. Before this study, the gene expression in dogs with XLHN was partially characterized by low-throughput methods, and progression-related genes were unknown. Hence, the study provides new insights into the underlying molecular mechanisms of disease progression in XLHN, and the identified DEGs are translatable to all CKDs.

In Chapter III, we further explored the driving force leading to the distinct gene expression seen in Chapter II. We used small RNA-seq to profile miRNA expression in kidney biopsies from affected dogs with XLHN versus controls. We also compared the performance of 3 alignment tools for the analysis of the data. We identified miR-186 and miR-26b as suitable internal controls for canine kidney tissues. Up to 25 miRNAs were differentially expressed at specific clinical time points, including miR-146b, miR-21, and miR-802 that were constantly upregulated throughout progression of CKD. These DE miRs target genes involved in the signal transduction pathway, particularly the "signaling by TGF-β receptor complex" pathway. In what appears to be the first small RNA-seq study in a canine model of CKD, the DE miRs found in the current study may be predictive biomarkers for the early detection of CKD and can represent potential therapeutic targets for CKD in both dogs and humans.

With the ultimate goal being to profile miRNAs in canine biofluids, the previously used methods in Chapter III required modification to accommodate the limited sample volume and scarcity of miRNAs in biofluids. In Chapter IV, we compared the performance of 6 commercial RNA isolation kits and 2 library preparation methods for small RNA-seq

using canine serum and urine collected and pooled from female dogs that are carrier for XLHN. For serum, Zymo Direct-zol combined with NEXTflex was the only combination that enabled successful library preparation, while for urine, Qiagen exoRNeasy combined with NEXTflex outperformed other combinations in detecting miRNAs. The total number of miRNAs detected in serum and urine was 198 and up to 115, respectively. MiRNA expression in serum was distinct from urine. Furthermore, we found that the library preparation method introduced a higher variation in urine results than RNA isolation method. Small RNA-seq provides an unbiased, global assessment for comparing these methods in canine biofluids, and we concluded that different isolation and library preparation methods show significant differences in miRNA results that could affect biomarker discovery.

Developed upon the foundation provided in the previous discoveries, we used small RNA-seq to profile miRNA expression in serum and urine of dogs with different types of glomerular diseases. In Chapter V, archived IVRPS serum and urine samples obtained from 24 dogs with ICGN, GS, AMYL, and healthy controls were divided into azotemic and non-azotemic groups. Comparing CKD dogs with controls, 47 circulating miRNAs and 18 urinary miRNAs were differentially expressed. Regardless of disease stage, 5 circulating miRNAs (miR-107, miR-129, miR-186, miR-365, and miR-371) and 5 urinary miRNAs (miR-7, miR-9, miR-22, miR-203, and miR-423a) were differentially expressed in dogs with all 3 glomerular diseases when compared to controls. The differential expression of urinary miR-182, miR-21, and miR-486 was related to the

progression of CKD. The distinctive expression of urinary miR-126, miR-335, and miR-128 could correctly group azotemic dogs into ICGN, GS, and AMYL, respectively.

This report is the first sequencing-based investigation in dogs with glomerular diseases. Future evaluation will use qRT-PCR to validate the DE miRs present among the disease groups and disease stages in a second cohort of dogs with glomerular disease, as in Chapter V. The validated results will be correlated with clinical and pathologic data, such as histopathologic scoring of kidney biopsies, routine tests of renal function, and survival data. In summary, the results provide valuable information for the discovery of non-invasive, novel miRNA biomarkers in dogs with glomerular diseases.

REFERENCES

1. Polzin DJ. Chronic kidney disease in small animals. *Vet Clin North Am Small Anim Pract.* 2011;41:15-30.

2. O'Neill DG, Elliott J, Church DB, et al. Chronic Kidney Disease in Dogs in UK Veterinary Practices: Prevalence, Risk Factors, and Survival. *J Vet Intern Med.* 2013;27:814-821.

3. Bartges JW. Chronic kidney disease in dogs and cats. *Vet Clin North Am Small Anim Pract.* 2012;42:669-692.

4. Lees GE. Early diagnosis of renal disease and renal failure. *Vet Clin North Am Small Anim Pract.* 2004;34:867-885.

5. Grauer GF. Early detection of renal damage and disease in dogs and cats. *Vet Clin North Am Small Anim Pract.* 2005;35:581-596.

6. Polzin DJ. Evidence-based step-wise approach to managing chronic kidney disease in dogs and cats. *J Vet Emerg Crit Care (San Antonio).* 2013;23:205-215.

7. Zampetaki A, Kiechl S, Drozdov I, et al. Plasma microRNA profiling reveals loss of endothelial miR-126 and other microRNAs in type 2 diabetes. *Circ Res.* 2010;107:810-817.

8. Von Hendy-Willson VE, Pressler BM. An overview of glomerular filtration rate testing in dogs and cats. *Vet J.* 2011;188:156-165.

9. Finco DR, Brown SA, Vaden SL, Ferguson DC. Relationship between plasma creatinine concentration and glomerular filtration rate in dogs. *J Vet Pharmacol Ther.* 1995;18:418-421.

10. Braun J-P, Lefebvre HP. Kidney Function and Damage. In: Kaneko JJ, Harvey JW, Bruss ML, eds. *Clinical Biochemistry of Domestic Animals.* 6th ed. San Diego, CA: Academic Press; 2008: 485-528.

11. Hall JA, Yerramilli M, Obare E, et al. Serum concentrations of symmetric dimethylarginine and creatinine in dogs with naturally occurring chronic kidney disease. *J Vet Intern Med.* 2016;30:794-802.

12. Nabity MB, Lees GE, Boggess MM, et al. Symmetric dimethylarginine assay validation, stability, and evaluation as a marker for the early detection of chronic kidney disease in dogs. *J Vet Intern Med.* 2015;29:1036-1044.

13. Hall JA, Yerramilli M, Obare E, et al. Relationship between lean body mass and serum renal biomarkers in healthy dogs. *J Vet Intern Med.* 2015;29:808-814.

14. Martinez J, Kellogg C, Iazbik MC, et al. The renin-angiotensin-aldosterone system in Greyhounds and non-Greyhound dogs. *J Vet Intern Med.* 2017;31:988-993.

15. Schneider SM, Cianciolo RE, Nabity MB, et al. Prevalence of immune-complex glomerulonephritides in dogs biopsied for suspected glomerular disease: 501 cases (2007-2012). *J Vet Intern Med.* 2013;27 Suppl 1:S67-75.

16. Subgroup ICGSGEP, Segev G, Cowgill LD, et al. Consensus recommendations for immunosuppressive treatment of dogs with glomerular disease based on established pathology. *J Vet Intern Med.* 2013;27 Suppl 1:S44-54.

17. Yamada T, Okuda Y, Takasugi K, Itoh K, Igari J. Relative serum amyloid A (SAA) values: the influence of SAA1 genotypes and corticosteroid treatment in Japanese patients with rheumatoid arthritis. *Ann Rheum Dis.* 2001;60:124-127.

18. Lees GE, Helman RG, Kashtan CE, et al. New form of X-linked dominant hereditary nephritis in dogs. *Am J Vet Res.* 1999;60:373-383.

19. Cox ML, Lees GE, Kashtan CE, Murphy KE. Genetic cause of X-linked Alport syndrome in a family of domestic dogs. *Mamm Genome.* 2003;14:396-403.

20. Lees GE. Kidney diseases caused by glomerular basement membrane type IV collagen defects in dogs. *J Vet Emerg Crit Care (San Antonio).* 2013;23:184-193.

21. Greer KA, Higgins MA, Cox ML, et al. Gene expression analysis in a canine model of X-linked Alport syndrome. *Mamm Genome.* 2006;17:976-990.

22. Kashtan CE. Familial hematuria due to type IV collagen mutations: Alport syndrome and thin basement membrane nephropathy. *Curr Opin Pediatr.* 2004;16:177-181.

23. Rao VH, Lees GE, Kashtan CE, et al. Increased expression of MMP-2, MMP-9 (type IV collagenases/gelatinases), and MT1-MMP in canine X-linked Alport syndrome (XLAS). *Kidney Int.* 2003;63:1736-1748.

24. Rao VH, Lees GE, Kashtan CE, et al. Dysregulation of renal MMP-3 and MMP-7 in canine X-linked Alport syndrome. *Pediatr Nephrol.* 2005;20:732-739.

25. Zeisberg M, Khurana M, Rao VH, et al. Stage-specific action of matrix metalloproteinases influences progressive hereditary kidney disease. *PLoS Med.* 2006;3:e100.

26. Ke B, Fan C, Yang L, Fang X. Matrix Metalloproteinases-7 and Kidney Fibrosis. *Front Physiol.* 2017;8:21.

27. LeBleu VS, Teng Y, O'Connell JT, et al. Identification of human epididymis protein-4 as a fibroblast-derived mediator of fibrosis. *Nat Med.* 2013;19:227-231.

28. Noone D, Licht C. An update on the pathomechanisms and future therapies of Alport syndrome. *Pediatr Nephrol.* 2013;28:1025-1036.

29. Benali SL, Lees GE, Nabity MB, et al. X-Linked hereditary nephropathy in Navasota dogs: clinical pathology, morphology, and gene expression during disease progression. *Vet Pathol.* 2016;53:803-812.

30. RNA-Seq Blog – Poll Results. RNA-Seq Blog. 2017. Available at: http://www.rna-seqblog.com/rna-seq-blog-poll-results-25/. Accessed May 17, 2018.

31. Byron SA, Van Keuren-Jensen KR, Engelthaler DM, Carpten JD, Craig DW. Translating RNA sequencing into clinical diagnostics: opportunities and challenges. *Nat Rev Genet.* 2016;17:257-271.

32. Marioni JC, Mason CE, Mane SM, Stephens M, Gilad Y. RNA-seq: an assessment of technical reproducibility and comparison with gene expression arrays. *Genome Res.* 2008;18:1509-1517.

33. Mortazavi A, Williams BA, McCue K, Schaeffer L, Wold B. Mapping and quantifying mammalian transcriptomes by RNA-Seq. *Nat Methods.* 2008;5:621-628.

34. Wang Z, Gerstein M, Snyder M. RNA-Seq: a revolutionary tool for transcriptomics. *Nat Rev Genet.* 2009;10:57-63.

35. Griffith M, Griffith OL, Mwenifumbo J, et al. Alternative expression analysis by RNA sequencing. *Nat Methods.* 2010;7:843-847.

36. Nagalakshmi U, Wang Z, Waern K, et al. The transcriptional landscape of the yeast genome defined by RNA sequencing. *Science.* 2008;320:1344-1349.

37. Camarena L, Bruno V, Euskirchen G, Poggio S, Snyder M. Molecular mechanisms of ethanol-induced pathogenesis revealed by RNA-sequencing. *PLoS Pathog.* 2010;6:e1000834.

38. Mutryn MF, Brannick EM, Fu W, Lee WR, Abasht B. Characterization of a novel chicken muscle disorder through differential gene expression and pathway analysis using RNA-sequencing. *BMC Genomics.* 2015;16:399.

39. He L, Hannon GJ. MicroRNAs: small RNAs with a big role in gene regulation. *Nat Rev Genet.* 2004;5:522-531.

40. Ambros V. The functions of animal microRNAs. *Nature.* 2004;431:350-355.

41. Bartel DP. MicroRNAs: target recognition and regulatory functions. *Cell.* 2009;136:215-233.

42. Kim YK, Kim VN. Processing of intronic microRNAs. *EMBO J.* 2007;26:775-783.

43. Rodriguez A, Griffiths-Jones S, Ashurst JL, Bradley A. Identification of mammalian microRNA host genes and transcription units. *Genome Res.* 2004;14:1902-1910.

44. Han J, Lee Y, Yeom KH, et al. The Drosha-DGCR8 complex in primary microRNA processing. *Genes Dev.* 2004;18:3016-3027.

45. Yi R, Qin Y, Macara IG, Cullen BR. Exportin-5 mediates the nuclear export of pre-microRNAs and short hairpin RNAs. *Genes Dev.* 2003;17:3011-3016.

46. Hutvagner G, McLachlan J, Pasquinelli AE, et al. A cellular function for the RNA-interference enzyme Dicer in the maturation of the let-7 small temporal RNA. *Science.* 2001;293:834-838.

47. Iwasaki S, Kobayashi M, Yoda M, et al. Hsc70/Hsp90 chaperone machinery mediates ATP-dependent RISC loading of small RNA duplexes. *Mol Cell.* 2010;39:292-299.

48. Kozomara A, Griffiths-Jones S. miRBase: annotating high confidence microRNAs using deep sequencing data. *Nucleic Acids Res.* 2014;42:D68-73.

49. Ha M, Kim VN. Regulation of microRNA biogenesis. *Nat Rev Mol Cell Biol.* 2014;15:509-524.

50. Saetrom P, Snove O, Nedland M, et al. Conserved microRNA characteristics in mammals. *Oligonucleotides.* 2006;16:115-144.

51. Boggs RM, Moody JA, Long CR, Tsai KL, Murphy KE. Identification, amplification and characterization of miR-17-92 from canine tissue. *Gene.* 2007;404:25-30.

52. Fleischhacker SN, Bauersachs S, Wehner A, Hartmann K, Weber K. Differential expression of circulating microRNAs in diabetic and healthy lean cats. *Vet J.* 2013;197:688-693.

53. Weber JA, Baxter DH, Zhang S, et al. The microRNA spectrum in 12 body fluids. *Clin Chem.* 2010;56:1733-1741.

54. Arroyo JD, Chevillet JR, Kroh EM, et al. Argonaute2 complexes carry a population of circulating microRNAs independent of vesicles in human plasma. *Proc Natl Acad Sci USA.* 2011;108:5003-5008.

55. Vickers KC, Palmisano BT, Shoucri BM, Shamburek RD, Remaley AT. MicroRNAs are transported in plasma and delivered to recipient cells by high-density lipoproteins. *Nat Cell Biol.* 2011;13:423-433.

56. Wang K, Zhang S, Weber J, Baxter D, Galas DJ. Export of microRNAs and microRNA-protective protein by mammalian cells. *Nucleic Acids Res.* 2010;38:7248-7259.

57. Wagner J, Riwanto M, Besler C, et al. Characterization of levels and cellular transfer of circulating lipoprotein-bound microRNAs. *Arterioscler Thromb Vasc Biol.* 2013;33:1392-1400.

58. Turchinovich A, Weiz L, Langheinz A, Burwinkel B. Characterization of extracellular circulating microRNA. *Nucleic Acids Res.* 2011;39:7223-7233.

59. Hunter MP, Ismail N, Zhang X, et al. Detection of microRNA expression in human peripheral blood microvesicles. *PLoS One.* 2008;3:e3694.

60. Etheridge A, Lee I, Hood L, Galas D, Wang K. Extracellular microRNA: a new source of biomarkers. *Mutat Res.* 2011;717:85-90.

61. Valadi H, Ekstrom K, Bossios A, et al. Exosome-mediated transfer of mRNAs and microRNAs is a novel mechanism of genetic exchange between cells. *Nat Cell Biol.* 2007;9:654-659.

62. Hill AF, Pegtel DM, Lambertz U, et al. ISEV position paper: extracellular vesicle RNA analysis and bioinformatics. *J Extracell Vesicles.* 2013;2.

63. Miranda KC, Bond DT, McKee M, et al. Nucleic acids within urinary exosomes/microvesicles are potential biomarkers for renal disease. *Kidney Int.* 2010;78:191-199.

64. Ratajczak J, Miekus K, Kucia M, et al. Embryonic stem cell-derived microvesicles reprogram hematopoietic progenitors: evidence for horizontal transfer of mRNA and protein delivery. *Leukemia.* 2006;20:847-856.

65. Nolte-'t Hoen EN, Buermans HP, Waasdorp M, et al. Deep sequencing of RNA from immune cell-derived vesicles uncovers the selective incorporation of small non-coding RNA biotypes with potential regulatory functions. *Nucleic Acids Res.* 2012;40:9272-9285.

66. Akers JC, Ramakrishnan V, Kim R, et al. MiR-21 in the extracellular vesicles (EVs) of cerebrospinal fluid (CSF): a platform for glioblastoma biomarker development. *PLoS One.* 2013;8:e78115.

67. Semenov DV, Baryakin DN, Brenner EV, et al. Unbiased approach to profile the variety of small non-coding RNA of human blood plasma with massively parallel sequencing technology. *Expert Opin Biol Ther.* 2012;12:S43-S51.

68. Cheng L, Sharples RA, Scicluna BJ, Hill AF. Exosomes provide a protective and enriched source of miRNA for biomarker profiling compared to intracellular and cell-free blood. *J Extracell Vesicles.* 2014;3.

69. Chevillet JR, Kang Q, Ruf IK, et al. Quantitative and stoichiometric analysis of the microRNA content of exosomes. *Proc Natl Acad Sci USA.* 2014;111:14888-14893.

70. McDonald JS, Milosevic D, Reddi HV, Grebe SK, Algeciras-Schimnich A. Analysis of circulating microRNA: preanalytical and analytical challenges. *Clin Chem.* 2011;57:833-840.

71. Cheng L, Sun X, Scicluna BJ, Coleman BM, Hill AF. Characterization and deep sequencing analysis of exosomal and non-exosomal miRNA in human urine. *Kidney Int.* 2014;86:433-444.

72. Fritz JV, Heintz-Buschart A, Ghosal A, et al. Sources and Functions of Extracellular Small RNAs in Human Circulation. *Annu Rev Nutr.* 2016;36:301-336.

73. Takeshita N, Hoshino I, Mori M, et al. Serum microRNA expression profile: miR-1246 as a novel diagnostic and prognostic biomarker for oesophageal squamous cell carcinoma. *Br J Cancer.* 2013;108:644-652.

74. Pigati L, Yaddanapudi SC, Iyengar R, et al. Selective release of microRNA species from normal and malignant mammary epithelial cells. *PLoS One.* 2010;5:e13515.

75. Guduric-Fuchs J, O'Connor A, Camp B, et al. Selective extracellular vesicle-mediated export of an overlapping set of microRNAs from multiple cell types. *BMC Genomics.* 2012;13:357.

76. Bail S, Swerdel M, Liu H, et al. Differential regulation of microRNA stability. *RNA*. 2010;16:1032-1039.

77. Krol J, Loedige I, Filipowicz W. The widespread regulation of microRNA biogenesis, function and decay. *Nat Rev Genet.* 2010;11:597-610.

78. Kim YK, Yeo J, Kim B, Ha M, Kim VN. Short structured RNAs with low GC content are selectively lost during extraction from a small number of cells. *Mol Cell.* 2012;46:893-895.

79. Janas T, Janas MM, Sapon K, Janas T. Mechanisms of RNA loading into exosomes. *FEBS Lett.* 2015;589:1391-1398.

80. Turchinovich A, Tonevitsky AG, Burwinkel B. Extracellular miRNA: a collision of two paradigms. *Trends Biochem Sci.* 2016;41:883-892.

81. Schratt GM, Tuebing F, Nigh EA, et al. A brain-specific microRNA regulates dendritic spine development. *Nature.* 2006;439:283-289.

82. Hornstein E, Mansfield JH, Yekta S, et al. The microRNA miR-196 acts upstream of Hoxb8 and Shh in limb development. *Nature.* 2005;438:671-674.

83. Croce CM. Causes and consequences of microRNA dysregulation in cancer. *Nat Rev Genet.* 2009;10:704-714.

84. Esteller M. Non-coding RNAs in human disease. *Nat Rev Genet.* 2011;12:861-874.

85. Chen X, Ba Y, Ma L, et al. Characterization of microRNAs in serum: a novel class of biomarkers for diagnosis of cancer and other diseases. *Cell Res.* 2008;18:997-1006.

86. Wang K, Zhang S, Marzolf B, et al. Circulating microRNAs, potential biomarkers for drug-induced liver injury. *Proc Natl Acad Sci USA.* 2009;106:4402-4407.

87. Alvarez ML, Khosroheidari M, Kanchi Ravi R, DiStefano JK. Comparison of protein, microRNA, and mRNA yields using different methods of urinary exosome isolation for the discovery of kidney disease biomarkers. *Kidney Int.* 2012;82:1024-1032.

88. Min QH, Chen XM, Zou YQ, et al. Differential expression of urinary exosomal microRNAs in IgA nephropathy. *J Clin Lab Anal.* 2018;32.

89. Lv LL, Cao YH, Ni HF, et al. MicroRNA-29c in urinary exosome/microvesicle as a biomarker of renal fibrosis. *Am J Physiol Renal Physiol.* 2013;305:F1220-1227.

90. Solé C, Cortés-Hernández J, Felip ML, Vidal M, Ordi-Ros J. miR-29c in urinary exosomes as predictor of early renal fibrosis in lupus nephritis. *Nephrol Dial Transplant.* 2015;30:1488-1496.

91. Fendler A, Stephan C, Yousef GM, Kristiansen G, Jung K. The translational potential of microRNAs as biofluid markers of urological tumours. *Nat Rev Urol.* 2016;13:734-752.

92. Butz H, Nofech-Mozes R, Ding Q, et al. Exosomal microRNAs are diagnostic biomarkers and can mediate cell–cell communication in renal cell carcinoma. *Eur Urol Focus.* 2016;2:210-218.

93. Koppers-Lalic D, Hackenberg M, de Menezes R, et al. Noninvasive prostate cancer detection by measuring miRNA variants (isomiRs) in urine extracellular vesicles. *Oncotarget.* 2016;7:22566-22578.

94. Endzelins E, Melne V, Kalnina Z, et al. Diagnostic, prognostic and predictive value of cell-free miRNAs in prostate cancer: a systematic review. *Mol Cancer.* 2016;15:41.

95. Zhang HG, Grizzle WE. Exosomes: a novel pathway of local and distant intercellular communication that facilitates the growth and metastasis of neoplastic lesions. *Am J Pathol.* 2014;184:28-41.

96. Gracia T, Wang X, Su Y, et al. Urinary exosomes contain microRNAs capable of paracrine modulation of tubular transporters in kidney. *Sci Rep.* 2017;7:40601.

97. Camussi G, Deregibus MC, Bruno S, Cantaluppi V, Biancone L. Exosomes/microvesicles as a mechanism of cell-to-cell communication. *Kidney Int.* 2010;78:838-848.

98. Singh R, Pochampally R, Watabe K, Lu Z, Mo YY. Exosome-mediated transfer of miR-10b promotes cell invasion in breast cancer. *Mol Cancer.* 2014;13:256.

99. Xin H, Li Y, Buller B, et al. Exosome-mediated transfer of miR-133b from multipotent mesenchymal stromal cells to neural cells contributes to neurite outgrowth. *Stem Cells.* 2012;30:1556-1564.

100. Ichii O, Ohta H, Horino T, et al. Urinary exosome-derived microRNAs reflecting the changes of renal function and histopathology in dogs. *Sci Rep.* 2017;7:40340.

101. Dirksen K, Verzijl T, Grinwis GC, et al. Use of serum microRNAs as biomarker for hepatobiliary diseases in dogs. *J Vet Intern Med.* 2016;30:1816-1823.

102. Dirksen K, Verzijl T, van den Ingh TS, et al. Hepatocyte-derived microRNAs as sensitive serum biomarkers of hepatocellular injury in Labrador retrievers. *Vet J.* 2016;211:75-81.

103. Li Q, Freeman LM, Rush JE, Laflamme DP. Expression profiling of circulating microRNAs in canine myxomatous mitral valve disease. *Int J Mol Sci.* 2015;16:14098-14108.

104. Gidlof O, Andersson P, van der Pals J, Gotberg M, Erlinge D. Cardiospecific microRNA plasma levels correlate with troponin and cardiac function in patients with ST elevation myocardial infarction, are selectively dependent on renal elimination, and can be detected in urine samples. *Cardiology.* 2011;118:217-226.

105. Steudemann C, Bauersachs S, Weber K, Wess G. Detection and comparison of microRNA expression in the serum of Doberman Pinschers with dilated cardiomyopathy and healthy controls. *BMC Vet Res.* 2013;9:12.

106. Tritten L, Burkman E, Moorhead A, et al. Detection of circulating parasite-derived microRNAs in filarial infections. *PLoS Negl Trop Dis.* 2014;8:e2971.

107. Stenfeldt C, Arzt J, Smoliga G, et al. Proof-of-concept study: profile of circulating microRNAs in Bovine serum harvested during acute and persistent FMDV infection. *Virol J.* 2017;14:71.

108. Casas E, Cai G, Kuehn LA, et al. Association of microRNAs with antibody response to Mycoplasma bovis in beef cattle. *PLoS One.* 2016;11:e0161651.

109. Shaughnessy RG, Farrell D, Riepema K, Bakker D, Gordon SV. Analysis of biobanked serum from a Mycobacterium avium subsp paratuberculosis bovine infection model confirms the remarkable stability of circulating miRNA profiles and defines a bovine serum miRNA repertoire. *PLoS One.* 2015;10:e0145089.

110. Farrell D, Shaughnessy RG, Britton L, et al. The identification of circulating miRNA in bovine serum and their potential as novel biomarkers of early Mycobacterium avium subsp paratuberculosis infection. *PLoS One.* 2015;10:e0134310.

111. Hansen EP, Kringel H, Thamsborg SM, Jex A, Nejsum P. Profiling circulating miRNAs in serum from pigs infected with the porcine whipworm, Trichuris suis. *Vet Parasitol.* 2016;223:30-33.

112. Fujiwara-Igarashi A, Igarashi H, Mizutani N, et al. Expression profile of circulating serum microRNAs in dogs with lymphoma. *Vet J.* 2015;205:317-321.

113. Mizuno H, Nakamura A, Aoki Y, et al. Identification of muscle-specific microRNAs in serum of muscular dystrophy animal models: promising novel blood-based markers for muscular dystrophy. *PLoS One.* 2011;6:e18388.

114. Jeanson-Leh L, Lameth J, Krimi S, et al. Serum profiling identifies novel muscle miRNA and cardiomyopathy-related miRNA biomarkers in Golden Retriever muscular dystrophy dogs and Duchenne muscular dystrophy patients. *Am J Pathol.* 2014;184:2885-2898.

115. Tigchelaar S, Streijger F, Sinha S, et al. Serum microRNAs reflect injury severity in a large animal model of thoracic spinal cord injury. *Sci Rep.* 2017;7:1376.

116. Ioannidis J, Donadeu FX. Circulating microRNA profiles during the bovine oestrous cycle. *PLoS One.* 2016;11:e0158160.

117. Ioannidis J, Donadeu FX. Circulating miRNA signatures of early pregnancy in cattle. *BMC Genomics.* 2016;17:184.

118. Spornraft M, Kirchner B, Haase B, et al. Optimization of extraction of circulating RNAs from plasma--enabling small RNA sequencing. *PLoS One.* 2014;9:e107259.

119. Sanz Rubio D, Lopez-Perez O, de Andres Pablo A, et al. Increased circulating microRNAs miR-342-3p and miR-21-5p in natural sheep prion disease. *J Gen Virol.* 2017;98:305-310.

120. Balaraman S, Lunde ER, Sawant O, et al. Maternal and neonatal plasma microRNA biomarkers for fetal alcohol exposure in an ovine model. *Alcohol Clin Exp Res.* 2014;38:1390-1400.

121. Baker LA, Lee KC, Palacios Jimenez C, et al. Circulating microRNAs reveal time course of organ injury in a porcine model of acetaminophen-induced acute liver failure. *PLoS One.* 2015;10:e0128076.

122. Basagoudanavar SH, Hosamani M, Tamil Selvan RP, et al. Host serum microRNA profiling during the early stage of foot-and-mouth disease virus infection. *Arch Virol.* 2018.

123. Taxis TM, Bauermann FV, Ridpath JF, Casas E. Circulating microRNAs in serum from cattle challenged with bovine viral diarrhea virus. *Front Genet.* 2017;8:91.

124. Guelfi G, Stefanetti V, De Luca S, et al. Serum microRNAs in buffalo cows: Potential biomarkers of pregnancy. *Res Vet Sci.* 2017;115:294-300.

125. Ioannidis J, Donadeu FX. Changes in circulating microRNA levels can be identified as early as day 8 of pregnancy in cattle. *PLoS One.* 2017;12:e0174892.

126. Kasimanickam V, Kastelic J. Circulating cell-free mature microRNAs and their target gene prediction in bovine metritis. *Sci Rep.* 2016;6:29509.

127. Zhao K, Liang G, Sun X, Guan le L. Comparative miRNAome analysis revealed different miRNA expression profiles in bovine sera and exosomes. *BMC Genomics.* 2016;17:630.

128. Bae IS, Chung KY, Yi J, et al. Identification of reference genes for relative quantification of circulating microRNAs in bovine serum. *PLoS One.* 2015;10:e0122554.

129. Noferesti SS, Sohel MM, Hoelker M, et al. Controlled ovarian hyperstimulation induced changes in the expression of circulatory miRNA in bovine follicular fluid and blood plasma. *J Ovarian Res.* 2015;8:81.

130. Kent MS, Zwingenberger A, Westropp JL, et al. MicroRNA profiling of dogs with transitional cell carcinoma of the bladder using blood and urine samples. *BMC Vet Res.* 2017;13:339.

131. Yang VK, Loughran KA, Meola DM, et al. Circulating exosome microRNA associated with heart failure secondary to myxomatous mitral valve disease in a naturally occurring canine model. *J Extracell Vesicles.* 2017;6:1350088.

132. Rouse R, Rosenzweig B, Shea K, et al. MicroRNA biomarkers of pancreatic injury in a canine model. *Exp Toxicol Pathol.* 2017;69:33-43.

133. Gaitero L, Russell SJ, Monteith G, LaMarre J. Expression of microRNAs miR-21 and miR-181c in cerebrospinal fluid and serum in canine meningoencephalomyelitis of unknown origin. *Vet J.* 2016;216:122-124.

134. Smith A, Calley J, Mathur S, et al. The Rat microRNA body atlas; Evaluation of the microRNA content of rat organs through deep sequencing and characterization of pancreas enriched miRNAs as biomarkers of pancreatic toxicity in the rat and dog. *BMC Genomics.* 2016;17:694.

135. Hulanicka M, Garncarz M, Parzeniecka-Jaworska M, Jank M. Plasma miRNAs as potential biomarkers of chronic degenerative valvular disease in Dachshunds. *BMC Vet Res.* 2014;10:205.

136. Cappelli K, Capomaccio S, Viglino A, et al. Circulating miRNAs as putative biomarkers of exercise adaptation in endurance horses. *Front Physiol.* 2018;9:429.

137. da Costa Santos H, Hess T, Bruemmer J, Splan R. Possible role of microRNA in equine insulin resistance: a pilot study. *J Equine Vet Sci.* 2017.

138. Cowled C, Foo CH, Deffrasnes C, et al. Circulating microRNA profiles of Hendra virus infection in horses. *Sci Rep.* 2017;7:7431.

139. Mach N, Plancade S, Pacholewska A, et al. Integrated mRNA and miRNA expression profiling in blood reveals candidate biomarkers associated with endurance exercise in the horse. *Sci Rep.* 2016;6:22932.

140. Unger L, Fouche N, Leeb T, Gerber V, Pacholewska A. Optimized methods for extracting circulating small RNAs from long-term stored equine samples. *Acta Vet Scand.* 2016;58:44.

141. Pacholewska A, Mach N, Mata X, et al. Novel equine tissue miRNAs and breed-related miRNA expressed in serum. *BMC Genomics.* 2016;17:831.

142. Lee S, Hwang S, Yu HJ, et al. Expression of microRNAs in horse plasma and their characteristic nucleotide composition. *PLoS One.* 2016;11:e0146374.

143. Longpre KM, Kinstlinger NS, Mead EA, et al. Seasonal variation of urinary microRNA expression in male goats (Capra hircus) as assessed by next generation sequencing. *Gen Comp Endocrinol.* 2014;199:1-15.

144. Andersson P, Gidlof O, Braun OO, et al. Plasma levels of liver-specific miR-122 is massively increased in a porcine cardiogenic shock model and attenuated by hypothermia. *Shock.* 2012;37:234-238.

145. Braun JP, Bourges-Abella N, Geffre A, Concordet D, Trumel C. The preanalytic phase in veterinary clinical pathology. *Vet Clin Pathol.* 2015;44:8-25.

146. Mitchell PS, Parkin RK, Kroh EM, et al. Circulating microRNAs as stable blood-based markers for cancer detection. *Proc Natl Acad Sci USA.* 2008;105:10513-10518.

147. Ding M, Wang C, Lu X, et al. Comparison of commercial exosome isolation kits for circulating exosomal microRNA profiling. *Anal Bioanal Chem.* 2018:1-10.

148. Wang K, Yuan Y, Cho JH, et al. Comparing the MicroRNA spectrum between serum and plasma. *PLoS One.* 2012;7:e41561.

149. Yamada A, Cox MA, Gaffney KA, et al. Technical factors involved in the measurement of circulating microRNA biomarkers for the detection of colorectal neoplasia. *PLoS One.* 2014;9:e112481.

150. Heegaard NH, Schetter AJ, Welsh JA, et al. Circulating micro-RNA expression profiles in early stage nonsmall cell lung cancer. *Int J Cancer.* 2012;130:1378-1386.

151. Bai X, Fischer S, Keshavjee S, Liu M. Heparin interference with reverse transcriptase polymerase chain reaction of RNA extracted from lungs after ischemia-reperfusion. *Transpl Int.* 2000;13:146-150.

152. Plieskatt JL, Feng Y, Rinaldi G, et al. Circumventing qPCR inhibition to amplify miRNAs in plasma. *Biomark Res.* 2014;2:13.

153. Garcia ME, Blanco JL, Caballero J, Gargallo-Viola D. Anticoagulants interfere with PCR used to diagnose invasive aspergillosis. *J Clin Microbiol.* 2002;40:1567-1568.

154. Laurent LC, Abdel-Mageed AB, Adelson PD, et al. Meeting report: discussions and preliminary findings on extracellular RNA measurement methods from laboratories in the NIH Extracellular RNA Communication Consortium. *J Extracell Vesicles.* 2015;4:26533.

155. Boeckel J-N, Thomé CE, Leistner D, et al. Heparin selectively affects the quantification of microRNAs in human blood samples. *Clin Chem.* 2013;59:1125-1127.

156. Kim DJ, Linnstaedt S, Palma J, et al. Plasma components affect accuracy of circulating cancer-related microRNA quantitation. *J Mol Diagn.* 2012;14:71-80.

157. Gilad S, Meiri E, Yogev Y, et al. Serum microRNAs are promising novel biomarkers. *PLoS One.* 2008;3:e3148.

158. Kroh EM, Parkin RK, Mitchell PS, Tewari M. Analysis of circulating microRNA biomarkers in plasma and serum using quantitative reverse transcription-PCR (qRT-PCR). *Methods.* 2010;50:298-301.

159. MacLellan SA, MacAulay C, Lam S, Garnis C. Pre-profiling factors influencing serum microRNA levels. *BMC Clin Pathol.* 2014;14:27.

160. Karere GM, Glenn JP, VandeBerg JL, Cox LA. Differential microRNA response to a high-cholesterol, high-fat diet in livers of low and high LDL-C baboons. *BMC Genomics.* 2012;13:320.

161. Tarallo S, Pardini B, Mancuso G, et al. MicroRNA expression in relation to different dietary habits: a comparison in stool and plasma samples. *Mutagenesis.* 2014;29:385-391.

162. Baggish AL, Hale A, Weiner RB, et al. Dynamic regulation of circulating microRNA during acute exhaustive exercise and sustained aerobic exercise training. *J Physiol.* 2011;589:3983-3994.

163. Mooren FC, Viereck J, Kruger K, Thum T. Circulating microRNAs as potential biomarkers of aerobic exercise capacity. *Am J Physiol Heart Circ Physiol.* 2014;306:H557-563.

164. Bye A, Rosjo H, Aspenes ST, et al. Circulating microRNAs and aerobic fitness--the HUNT-Study. *PLoS One.* 2013;8:e57496.

165. Rome S. Use of miRNAs in biofluids as biomarkers in dietary and lifestyle intervention studies. *Genes Nutr.* 2015;10:483.

166. Rekker K, Saare M, Roost AM, et al. Circulating miR-200-family micro-RNAs have altered plasma levels in patients with endometriosis and vary with blood collection time. *Fertil Steril.* 2015;104:938-946 e932.

167. Mehta N, Cheng HY. Micro-managing the circadian clock: The role of microRNAs in biological timekeeping. *J Mol Biol.* 2013;425:3609-3624.

168. Danielson KM, Estanislau J, Tigges J, et al. Diurnal variations of circulating extracellular vesicles measured by nano flow cytometry. *PLoS One.* 2016;11:e0144678.

169. Heegaard NH, Carlsen AL, Lilje B, et al. Diurnal variations of human circulating cell-free micro-RNA. *PLoS One.* 2016;11:e0160577.

170. Mooney C, Raoof R, El-Naggar H, et al. High throughput qPCR expression profiling of circulating microRNAs reveals minimal sex-and sample timing-related variation in plasma of healthy volunteers. *PLoS One.* 2015;10:e0145316.

171. Tataruch-Weinert D, Musante L, Kretz O, Holthofer H. Urinary extracellular vesicles for RNA extraction: optimization of a protocol devoid of prokaryote contamination. *J Extracell Vesicles.* 2016;5:30281.

172. Zhou H, Yuen PS, Pisitkun T, et al. Collection, storage, preservation, and normalization of human urinary exosomes for biomarker discovery. *Kidney Int.* 2006;69:1471-1476.

173. Witwer KW, Buzas EI, Bemis LT, et al. Standardization of sample collection, isolation and analysis methods in extracellular vesicle research. *J Extracell Vesicles.* 2013;2.

174. Jia Y, Guan M, Zheng Z, et al. MiRNAs in Urine Extracellular Vesicles as Predictors of Early-Stage Diabetic Nephropathy. *J Diabetes Res.* 2016;2016:7932765.

175. Eissa S, Matboli M, Aboushahba R, Bekhet MM, Soliman Y. Urinary exosomal microRNA panel unravels novel biomarkers for diagnosis of type 2 diabetic kidney disease. *J Diabetes Complications.* 2016;30:1585-1592.

176. Andreu Z, Otta Oshiro R, Redruello A, et al. Extracellular vesicles as a source for non-invasive biomarkers in bladder cancer progression. *Eur J Pharm Sci.* 2017;98:70-79.

177. Foj L, Ferrer F, Serra M, et al. Exosomal and non-exosomal urinary miRNAs in prostate cancer detection and prognosis. *Prostate.* 2017;77:573-583.

178. Crossland RE, Norden J, Bibby LA, Davis J, Dickinson AM. Evaluation of optimal extracellular vesicle small RNA isolation and qRT-PCR normalisation for serum and urine. *J Immunol Methods.* 2016;429:39-49.

179. Muralidharan J, Ramezani A, Hubal M, et al. Extracellular microRNA signature in chronic kidney disease. *Am J Physiol Renal Physiol.* 2017;312:F982-F991.

180. Delic D, Eisele C, Schmid R, et al. Urinary Exosomal miRNA Signature in Type II Diabetic Nephropathy Patients. *PLoS One.* 2016;11:e0150154.

181. Wolenski FS, Shah P, Sano T, et al. Identification of microRNA biomarker candidates in urine and plasma from rats with kidney or liver damage. *J Appl Toxicol.* 2017;37:278-286.

182. Hanke M, Hoefig K, Merz H, et al. A robust methodology to study urine microRNA as tumor marker: microRNA-126 and microRNA-182 are related to urinary bladder cancer. *Urol Oncol.* 2010;28:655-661.

183. Barutta F, Tricarico M, Corbelli A, et al. Urinary exosomal microRNAs in incipient diabetic nephropathy. *PLoS One.* 2013;8:e73798.

184. The early detection research network standard operating procedure. National Cancer Institute. 2006. Available at: https://edrn.nci.nih.gov/resources/standard-operating-procedures/standard-operating-procedures. Accessed January 29, 2018.

185. ISBER best practices for repositories presents the most effective practices for the management of specimen collections and repositories. International Society for Biological and Environmental Repositories. 2012. Available at: http://www.isber.org/?page=BPR. Accessed January 29, 2018.

186. Organization WH. WHO guidelines on drawing blood: best practices in phlebotomy. 2010.

187. Cheng HH, Yi HS, Kim Y, et al. Plasma processing conditions substantially influence circulating microRNA biomarker levels. *PLoS One.* 2013;8:e64795.

188. Moldovan L, Batte KE, Trgovcich J, et al. Methodological challenges in utilizing miRNAs as circulating biomarkers. *J Cell Mol Med.* 2014;18:371-390.

189. Page K, Guttery DS, Zahra N, et al. Influence of plasma processing on recovery and analysis of circulating nucleic acids. *PLoS One.* 2013;8:e77963.

190. Pritchard CC, Kroh E, Wood B, et al. Blood cell origin of circulating microRNAs: a cautionary note for cancer biomarker studies. *Cancer Prev Res (Phila).* 2012;5:492-497.

191. Merkerova M, Belickova M, Bruchova H. Differential expression of microRNAs in hematopoietic cell lineages. *Eur J Haematol.* 2008;81:304-310.

192. Kirschner MB, Kao SC, Edelman JJ, et al. Haemolysis during sample preparation alters microRNA content of plasma. *PLoS One.* 2011;6:e24145.

193. Kirschner MB, Edelman JJ, Kao SC, et al. The impact of hemolysis on cell-free microRNA biomarkers. *Front Genet.* 2013;4:94.

194. Pizzamiglio S, Zanutto S, Ciniselli CM, et al. A methodological procedure for evaluating the impact of hemolysis on circulating microRNAs. *Oncol Lett.* 2017;13:315-320.

195. Sowemimo-Coker SO. Red blood cell hemolysis during processing. *Transfus Med Rev.* 2002;16:46-60.

196. Hatherill J, Till G, Bruner L, Ward P. Thermal injury, intravascular hemolysis, and toxic oxygen products. *J Clin Invest.* 1986;78:629.

197. Appierto V, Callari M, Cavadini E, et al. A lipemia-independent NanoDrop-based score to identify hemolysis in plasma and serum samples. *Bioanalysis.* 2014;6:1215-1226.

198. Blondal T, Jensby Nielsen S, Baker A, et al. Assessing sample and miRNA profile quality in serum and plasma or other biofluids. *Methods.* 2013;59:S1-6.

199. Blank A, Dekker CA. Ribonucleases of human serum, urine, cerebrospinal fluid, and leukocytes. Activity staining following electrophoresis in sodium dodecyl sulfate-polyacrylamide gels. *Biochemistry.* 1981;20:2261-2267.

200. Channavajjhala SK, Rossato M, Morandini F, et al. Optimizing the purification and analysis of miRNAs from urinary exosomes. *Clin Chem Lab Med.* 2014;52:345-354.

201. Mall C, Rocke DM, Durbin-Johnson B, Weiss RH. Stability of miRNA in human urine supports its biomarker potential. *Biomark Med.* 2013;7:623-631.

202. Rounge TB, Lauritzen M, Langseth H, et al. MicroRNA biomarker discovery and high-throughput DNA sequencing are possible using long-term archived serum samples. *Cancer Epidemiol Biomarkers Prev.* 2015;24:1381-1387.

203. Aiso T, Takigami S, Yamaki A, Ohnishi H. Degradation of serum microRNAs during transient storage of serum samples at 4° C. *Ann Clin Biochem.* 2017:0004563217704233.

204. Ge Q, Zhou Y, Lu J, et al. MiRNA in plasma exosome is stable under different storage conditions. *Molecules.* 2014;19:1568-1575.

205. Grasedieck S, Scholer N, Bommer M, et al. Impact of serum storage conditions on microRNA stability. *Leukemia.* 2012;26:2414-2416.

206. Enelund L, Nielsen LN, Cirera S. Evaluation of microRNA stability in plasma and serum from healthy dogs. *Microrna.* 2017;6:42-52.

207. Kirschner MB, van Zandwijk N, Reid G. Cell-free microRNAs: potential biomarkers in need of standardized reporting. *Front Genet.* 2013;4:56.

208. Nelson PT, Wang WX, Wilfred BR, Tang G. Technical variables in high-throughput miRNA expression profiling: much work remains to be done. *Biochim Biophys Acta.* 2008;1779:758-765.

209. Webber J, Clayton A. How pure are your vesicles? *J Extracell Vesicles.* 2013;2.

210. Gardiner C, Di Vizio D, Sahoo S, et al. Techniques used for the isolation and characterization of extracellular vesicles: results of a worldwide survey. *J Extracell Vesicles.* 2016;5:32945.

211. Gonzales PA, Zhou H, Pisitkun T, et al. Isolation and purification of exosomes in urine. *Methods Mol Biol.* 2010;641:89-99.

212. Cheruvanky A, Zhou H, Pisitkun T, et al. Rapid isolation of urinary exosomal biomarkers using a nanomembrane ultrafiltration concentrator. *Am J Physiol Renal Physiol.* 2007;292:F1657-1661.

213. Witwer KW. Circulating microRNA biomarker studies: pitfalls and potential solutions. *Clin Chem.* 2015;61:56-63.

214. Gámez-Valero A, Lozano-Ramos SI, Bancu I, Lauzurica-Valdemoros R, Borràs FE. Urinary extracellular vesicles as source of biomarkers in kidney diseases. *Front Immunol.* 2015;6.

215. Li P, Kaslan M, Lee SH, Yao J, Gao Z. Progress in exosome isolation techniques. *Theranostics.* 2017;7:789-804.

216. Royo F, Zuniga-Garcia P, Sanchez-Mosquera P, et al. Different EV enrichment methods suitable for clinical settings yield different subpopulations of urinary extracellular vesicles from human samples. *J Extracell Vesicles.* 2016;5:29497.

217. Royo F, Diwan I, Tackett MR, et al. Comparative miRNA analysis of urine extracellular vesicles isolated through five different methods. *Cancers (Basel).* 2016;8.

218. Bergallo M, Gambarino S, Martino S, et al. Comparison of two available RNA extraction protocols for microRNA amplification in serum samples. *J Clin Lab Anal.* 2016;30:277-283.

219. Tanriverdi K, Kucukural A, Mikhalev E, et al. Comparison of RNA isolation and associated methods for extracellular RNA detection by high-throughput quantitative polymerase chain reaction. *Anal Biochem.* 2016;501:66-74.

220. El-Khoury V, Pierson S, Kaoma T, Bernardin F, Berchem G. Assessing cellular and circulating miRNA recovery: the impact of the RNA isolation method and the quantity of input material. *Sci Rep.* 2016;6:19529.

221. Tan GW, Khoo AS, Tan LP. Evaluation of extraction kits and RT-qPCR systems adapted to high-throughput platform for circulating miRNAs. *Sci Rep.* 2015;5:9430.

222. Brunet-Vega A, Pericay C, Quilez ME, et al. Variability in microRNA recovery from plasma: Comparison of five commercial kits. *Anal Biochem.* 2015;488:28-35.

223. Duy J, Koehler JW, Honko AN, Minogue TD. Optimized microRNA purification from TRIzol-treated plasma. *BMC Genomics.* 2015;16:95.

224. Monleau M, Bonnel S, Gostan T, et al. Comparison of different extraction techniques to profile microRNAs from human sera and peripheral blood mononuclear cells. *BMC Genomics.* 2014;15:395.

225. McAlexander MA, Phillips MJ, Witwer KW. Comparison of Methods for miRNA Extraction from Plasma and Quantitative Recovery of RNA from Cerebrospinal Fluid. *Front Genet.* 2013;4:83.

226. Moret I, Sanchez-Izquierdo D, Iborra M, et al. Assessing an improved protocol for plasma microRNA extraction. *PLoS One.* 2013;8:e82753.

227. Li Y, Kowdley KV. Method for microRNA isolation from clinical serum samples. *Anal Biochem.* 2012;431:69-75.

228. Meerson A, Ploug T. Assessment of six commercial plasma small RNA isolation kits using qRT-PCR and electrophoretic separation: higher recovery of microRNA following ultracentrifugation. *Biol Methods Protoc.* 2016;1:bpw003.

229. Becker C, Hammerle-Fickinger A, Riedmaier I, Pfaffl MW. MRNA and microRNA quality control for RT-qPCR analysis. *Methods.* 2010;50:237-243.

230. Glasel J. Validity of nucleic acid purities monitored by 260nm/280nm absorbance ratios. *Biotechniques.* 1995;18:62-63.

231. Tzimagiorgis G, Michailidou EZ, Kritis A, Markopoulos AK, Kouidou S. Recovering circulating extracellular or cell-free RNA from bodily fluids. *Cancer Epidemiol.* 2011;35:580-589.

232. Li X, Ben-Dov IZ, Mauro M, Williams Z. Lowering the quantification limit of the QubitTM RNA HS assay using RNA spike-in. *BMC Mol Biol.* 2015;16:9.

233. Schroeder A, Mueller O, Stocker S, et al. The RIN: an RNA integrity number for assigning integrity values to RNA measurements. *BMC Mol Biol.* 2006;7:3.

234. Meltzer PS. Cancer genomics: small RNAs with big impacts. *Nature.* 2005;435:745-746.

235. Analysis of miRNA content in total RNA preparations using the Agilent 2100 bioanalyzer. Tissot, C, ed. 2008. Available at: http://www.chem-agilent.com/pdf/5989-7870EN.pdf. Accessed December 2, 2017.

236. Monitoring extraction efficiency of small RNAs with the Agilent 2100 Bioanalyzer and the small RNA kit. Babu, S, ed. 2010. Available at: https://www.agilent.com/cs/library/applications/5990-6935EN.pdf. Accessed December 2, 2017.

237. Kim Y-K, Yeo J, Ha M, Kim B, Kim VN. Cell adhesion-dependent control of microRNA decay. *Mol Cell.* 2011;43:1005.

238. Gautam A, Kumar R, Dimitrov G, et al. Identification of extracellular miRNA in archived serum samples by next-generation sequencing from RNA extracted using multiple methods. *Mol Biol Rep.* 2016;43:1165-1178.

239. Guo Y, Vickers K, Xiong Y, et al. Comprehensive evaluation of extracellular small RNA isolation methods from serum in high throughput sequencing. *BMC Genomics.* 2017;18:50.

240. Andreasen D, Fog JU, Biggs W, et al. Improved microRNA quantification in total RNA from clinical samples. *Methods.* 2010;50:S6-9.

241. Chomczynski P, Sacchi N. The single-step method of RNA isolation by acid guanidinium thiocyanate–phenol–chloroform extraction: twenty-something years on. *Nat Protoc.* 2006;1:581-585.

242. Mestdagh P, Hartmann N, Baeriswyl L, et al. Evaluation of quantitative miRNA expression platforms in the microRNA quality control (miRQC) study. *Nat Methods.* 2014;11:809-815.

243. Dard-Dascot C, Naquin D, d'Aubenton-Carafa Y, et al. Systematic comparison of small RNA library preparation protocols for next-generation sequencing. *BMC Genomics.* 2018;19:118.

244. Yeri A, Courtright A, Danielson K, et al. Evaluation of commercially available small RNASeq library preparation kits using low input RNA. *BMC Genomics.* 2018;19:331.

245. Head SR, Komori HK, LaMere SA, et al. Library construction for next-generation sequencing: overviews and challenges. *Biotechniques.* 2014;56:61-64, 66, 68, passim.

246. Raabe CA, Tang TH, Brosius J, Rozhdestvensky TS. Biases in small RNA deep sequencing data. *Nucleic Acids Res.* 2014;42:1414-1426.

247. Dabney J, Meyer M. Length and GC-biases during sequencing library amplification: a comparison of various polymerase-buffer systems with ancient and modern DNA sequencing libraries. *Biotechniques.* 2012;52:87-94.

248. Baran-Gale J, Kurtz CL, Erdos MR, et al. Addressing bias in small RNA library preparation for sequencing: a new protocol recovers microRNAs that evade capture by current methods. *Front Genet.* 2015;6:352.

249. Huang X, Yuan T, Tschannen M, et al. Characterization of human plasma-derived exosomal RNAs by deep sequencing. *BMC Genomics.* 2013;14:319.

250. Zhu J, Zheng Z, Wang J, et al. Different miRNA expression profiles between human breast cancer tumors and serum. *Front Genet.* 2014;5:149.

251. Zenoni S, Ferrarini A, Giacomelli E, et al. Characterization of transcriptional complexity during berry development in Vitis vinifera using RNA-Seq. *Plant Physiol.* 2010;152:1787-1795.

252. Mills JD, Nalpathamkalam T, Jacobs HI, et al. RNA-Seq analysis of the parietal cortex in Alzheimer's disease reveals alternatively spliced isoforms related to lipid metabolism. *Neurosci Lett.* 2013;536:90-95.

253. Greenwald JW, Greenwald CJ, Philmus BJ, Begley TP, Gross DC. RNA-seq analysis reveals that an ECF σ factor, AcsS, regulates achromobactin biosynthesis in Pseudomonas syringae pv. syringae B728a. *PLoS One.* 2012;7:e34804.

254. Rajkumar AP, Qvist P, Lazarus R, et al. Experimental validation of methods for differential gene expression analysis and sample pooling in RNA-seq. *BMC Genomics.* 2015;16:548.

255. Williams AG, Thomas S, Wyman SK, Holloway AK. RNA-seq data: challenges in and recommendations for experimental design and analysis. *Curr Protoc Hum Genet.* 2014;83:11 13 11-20.

256. Anders S, Huber W. Differential expression analysis for sequence count data. *Genome Biol.* 2010;11:R106.

257. Fang Z, Cui X. Design and validation issues in RNA-seq experiments. *Brief Bioinform.* 2011;12:280-287.

258. Tam S, de Borja R, Tsao MS, McPherson JD. Robust global microRNA expression profiling using next-generation sequencing technologies. *Lab Invest.* 2014;94:350-358.

259. Liu Y, Zhou J, White KP. RNA-seq differential expression studies: more sequence or more replication? *Bioinformatics.* 2014;30:301-304.

260. ENCODE guidelines and best practices for RNA-seq. ENCODE Consortium. 2016. Available at: https://www.encodeproject.org/documents/cede0cbe-d324-4ce7-ace4-f0c3eddf5972/@@download/attachment/ENCODE%20Best%20Practices%20for%20RNA_v2.pdf. Accessed December 2, 2017.

261. Robles JA, Qureshi SE, Stephen SJ, et al. Efficient experimental design and analysis strategies for the detection of differential expression using RNA-Sequencing. *BMC Genomics.* 2012;13:484.

262. Ching T, Huang S, Garmire LX. Power analysis and sample size estimation for RNA-Seq differential expression. *RNA*. 2014;20:1684-1696.

263. Hart SN, Therneau TM, Zhang Y, Poland GA, Kocher JP. Calculating sample size estimates for RNA sequencing data. *J Comput Biol.* 2013;20:970-978.

264. Buschmann D, Haberberger A, Kirchner B, et al. Toward reliable biomarker signatures in the age of liquid biopsies - how to standardize the small RNA-Seq workflow. *Nucleic Acids Res.* 2016;44:5995-6018.

265. Schurch NJ, Schofield P, Gierlinski M, et al. How many biological replicates are needed in an RNA-seq experiment and which differential expression tool should you use? *RNA*. 2016.

266. Consortium EP. The ENCODE (ENCyclopedia of DNA Elements) project. *Science.* 2004;306:636-640.

267. Small RNA-seq data standards and processing pipeline. ENCODE Consortium. 2017. Available at: https://www.encodeproject.org/rna-seq/small-rnas/. Accessed May 17, 2018.

268. Ainsztein AM, Brooks PJ, Dugan VG, et al. The NIH extracellular RNA communication consortium. *J Extracell Vesicles.* 2015;4:27493.

269. Small RNA-seq data analysis for exRNA profiling using the exceRpt small RNA-seq pipeline. Extracellular RNA Communication Consortium. 2016. Available at: http://genboree.org/theCommons/projects/exrna-tools-may2014/wiki/Small%20RNA-seq%20Pipeline. Accessed May 17, 2018.

270. Dobin A, Davis CA, Schlesinger F, et al. STAR: ultrafast universal RNA-seq aligner. *Bioinformatics.* 2013;29:15-21.

271. Robinson MD, McCarthy DJ, Smyth GK. edgeR: a Bioconductor package for differential expression analysis of digital gene expression data. *Bioinformatics.* 2010;26:139-140.

272. Love MI, Huber W, Anders S. Moderated estimation of fold change and dispersion for RNA-seq data with DESeq2. *Genome Biol.* 2014;15:550.

273. Goecks J, Nekrutenko A, Taylor J, Galaxy T. Galaxy: a comprehensive approach for supporting accessible, reproducible, and transparent computational research in the life sciences. *Genome Biol.* 2010;11:R86.

274. Beckers M, Mohorianu I, Stocks M, et al. Comprehensive processing of high-throughput small RNA sequencing data including quality checking, normalization, and differential expression analysis using the UEA sRNA Workbench. *RNA.* 2017;23:823-835.

275. Mohorianu I, Stocks MB, Applegate CS, Folkes L, Moulton V. The UEA Small RNA workbench: a suite of computational tools for small RNA analysis. In: Dalmay T, eds. *MicroRNA Detection and Target Identification: Methods and Protocols.* New York, NY: Springer; 2017: 193-224.

276. Wan C, Gao J, Zhang H, et al. CPSS 2.0: a computational platform update for the analysis of small RNA sequencing data. *Bioinformatics.* 2017;33:3289-3291.

277. Rahman RU, Gautam A, Bethune J, et al. Oasis 2: improved online analysis of small RNA-seq data. *BMC Bioinformatics.* 2018;19:54.

278. Fehlmann T, Backes C, Kahraman M, et al. Web-based NGS data analysis using miRMaster: a large-scale meta-analysis of human miRNAs. *Nucleic Acids Res.* 2017;45:8731-8744.

279. Chen L, Heikkinen L, Wang C, et al. miRToolsGallery: a tag-based and rankable microRNA bioinformatics resources database portal. *Database.* 2018;2018.

280. Vlachos IS, Hatzigeorgiou AG. Online resources for miRNA analysis. *Clin Biochem.* 2013;46:879-900.

281. Conesa A, Madrigal P, Tarazona S, et al. A survey of best practices for RNA-seq data analysis. *Genome Biol.* 2016;17:13.

282. Perez-Riverol Y, Gatto L, Wang R, et al. Ten simple rules for taking advantage of Git and GitHub. *PLoS Comput Biol.* 2016;12:e1004947.

283. Hughes TR. 'Validation' in genome-scale research. *J Biol.* 2009;8:3.

284. Wang X. A PCR-based platform for microRNA expression profiling studies. *RNA.* 2009;15:716-723.

285. Espina V, Wulfkuhle JD, Calvert VS, et al. Laser-capture microdissection. *Nat Protoc.* 2006;1:586-603.

286. Busk PK. A tool for design of primers for microRNA-specific quantitative RT-qPCR. *BMC Bioinformatics.* 2014;15:29.

287. Benes V, Castoldi M. Expression profiling of microRNA using real-time quantitative PCR, how to use it and what is available. *Methods.* 2010;50:244-249.

288. D'haene B, Mestdagh P, Hellemans J, Vandesompele J. MiRNA expression profiling: from reference genes to global mean normalization. In: Fan J-B, eds. *Next-Generation MicroRNA Expression Profiling Technology.* 1st ed. Totowa, NJ: Humana Press; 2012: 261-272.

289. Raymond CK, Roberts BS, Garrett-Engele P, Lim LP, Johnson JM. Simple, quantitative primer-extension PCR assay for direct monitoring of microRNAs and short-interfering RNAs. *RNA.* 2005;11:1737-1744.

290. Chen C, Ridzon DA, Broomer AJ, et al. Real-time quantification of microRNAs by stem-loop RT-PCR. *Nucleic Acids Res.* 2005;33:e179.

291. TaqMan Advanced miRNA Assays—superior performance for miRNA detection and quantification. Thermo Fisher Scientific. 2016. Available at: https://www.thermofisher.com/content/dam/LifeTech/Documents/PDFs/TaqMan-Advanced-miRNA-Performance-White-Paper.pdf. Accessed October 12, 2017.

292. Rabinowits G, Gercel-Taylor C, Day JM, Taylor DD, Kloecker GH. Exosomal microRNA: a diagnostic marker for lung cancer. *Clin Lung Cancer.* 2009;10:42-46.

293. Huang Z, Huang D, Ni S, et al. Plasma microRNAs are promising novel biomarkers for early detection of colorectal cancer. *Int J Cancer.* 2010;127:118-126.

294. Lawrie CH, Gal S, Dunlop HM, et al. Detection of elevated levels of tumour-associated microRNAs in serum of patients with diffuse large B-cell lymphoma. *Br J Haematol.* 2008;141:672-675.

295. Zhu W, Qin W, Atasoy U, Sauter ER. Circulating microRNAs in breast cancer and healthy subjects. *BMC Res Notes.* 2009;2:89.

296. Spiller MP, Boon KL, Reijns MA, Beggs JD. The Lsm2-8 complex determines nuclear localization of the spliceosomal U6 snRNA. *Nucleic Acids Res.* 2007;35:923-929.

297. Peltier HJ, Latham GJ. Normalization of microRNA expression levels in quantitative RT-PCR assays: identification of suitable reference RNA targets in normal and cancerous human solid tissues. *RNA.* 2008;14:844-852.

298. Vandesompele J, De Preter K, Pattyn F, et al. Accurate normalization of real-time quantitative RT-PCR data by geometric averaging of multiple internal control genes. *Genome Biol.* 2002;3:RESEARCH0034.

299. Hellemans J, Mortier G, De Paepe A, Speleman F, Vandesompele J. qBase relative quantification framework and software for management and automated analysis of real-time quantitative PCR data. *Genome Biol.* 2007;8:R19.

300. Andersen CL, Jensen JL, Orntoft TF. Normalization of real-time quantitative reverse transcription-PCR data: a model-based variance estimation approach to identify genes suited for normalization, applied to bladder and colon cancer data sets. *Cancer Res.* 2004;64:5245-5250.

301. Pfaffl MW, Tichopad A, Prgomet C, Neuvians TP. Determination of stable housekeeping genes, differentially regulated target genes and sample integrity: BestKeeper - Excel-based tool using pair-wise correlations. *Biotechnology Letters.* 2004;26:509-515.

302. Xia M, Sherlock J, Hegerich P, et al. DataAssist–data analysis software for TaqMan real-time PCR data. *Proceedings of the International MultiConference of Engineers and Computer Scientists*. Hong Kong, March 17-19, 2010.

303. Occhipinti G, Giulietti M, Principato G, Piva F. The choice of endogenous controls in exosomal microRNA assessments from biofluids. *Tumour Biol.* 2016;37:11657-11665.

304. Livak KJ, Schmittgen TD. Analysis of relative gene expression data using real-time quantitative PCR and the 2(-Delta Delta C(T)) Method. *Methods.* 2001;25:402-408.

305. Brunet-Vega A, Pericay C, Quilez ME, et al. Data on individual PCR efficiency values as quality control for circulating miRNAs. *Data Brief.* 2015;5:321-326.

306. Pfaffl MW. A new mathematical model for relative quantification in real-time RT-PCR. *Nucleic Acids Res.* 2001;29:e45.

307. Mestdagh P, Van Vlierberghe P, De Weer A, et al. A novel and universal method for microRNA RT-qPCR data normalization. *Genome Biol.* 2009;10:R64.

308. Pritchard CC, Cheng HH, Tewari M. MicroRNA profiling: approaches and considerations. *Nat Rev Genet.* 2012;13:358-369.

309. Bustin SA, Benes V, Garson JA, et al. The MIQE guidelines: minimum information for publication of quantitative real-time PCR experiments. *Clin Chem.* 2009;55:611-622.

310. Lefever S, Hellemans J, Pattyn F, et al. RDML: structured language and reporting guidelines for real-time quantitative PCR data. *Nucleic Acids Res.* 2009;37:2065-2069.

311. Neal CS, Michael MZ, Pimlott LK, et al. Circulating microRNA expression is reduced in chronic kidney disease. *Nephrol Dial Transplant.* 2011;26:3794-3802.

312. Xiang M, Zeng Y, Yang R, et al. U6 is not a suitable endogenous control for the quantification of circulating microRNAs. *Biochem Biophys Res Commun.* 2014;454:210-214.

313. Benz F, Roderburg C, Cardenas DV, et al. U6 is unsuitable for normalization of serum miRNA levels in patients with sepsis or liver fibrosis. *Exp Mol Med.* 2013;45:e42.

314. Qi R, Weiland M, Gao XH, Zhou L, Mi QS. Identification of endogenous normalizers for serum microRNAs by microarray profiling: U6 small nuclear RNA is not a reliable normalizer. *Hepatology.* 2012;55:1640-1642.

315. Lange T, Stracke S, Rettig R, et al. Identification of miR-16 as an endogenous reference gene for the normalization of urinary exosomal miRNA expression data from CKD patients. *PloS one.* 2017;12:e0183435.

316. Khurana R, Ranches G, Schafferer S, et al. Identification of urinary exosomal noncoding RNAs as novel biomarkers in chronic kidney disease. *RNA.* 2017;23:142-152.

317. O'Shaughnessy MM, Montez-Rath ME, Lafayette RA, Winkelmayer WC. Patient characteristics and outcomes by GN subtype in ESRD. *Clin J Am Soc Nephrol.* 2015;10:1170-1178.

318. Zhang C, Liang S, Cheng S, et al. Urinary miR-196a predicts disease progression in patients with chronic kidney disease. *J Transl Med.* 2018;16:91.

319. Wang N, Zhou Y, Jiang L, et al. Urinary microRNA-10a and microRNA-30d serve as novel, sensitive and specific biomarkers for kidney injury. *PLoS One.* 2012;7:e51140.

320. Ramezani A, Devaney JM, Cohen S, et al. Circulating and urinary microRNA profile in focal segmental glomerulosclerosis: a pilot study. *Eur J Clin Invest.* 2015;45:394-404.

321. Zhang C, Zhang W, Chen HM, et al. Plasma microRNA-186 and proteinuria in focal segmental glomerulosclerosis. *Am J Kidney Dis.* 2015;65:223-232.

322. Zhang W, Zhang C, Chen H, et al. Evaluation of microRNAs miR-196a, miR-30a-5P, and miR-490 as biomarkers of disease activity among patients with FSGS. *Clin J Am Soc Nephrol.* 2014:CJN. 11561113.

323. Xiao B, Wang LN, Li W, et al. Plasma microRNA panel is a novel biomarker for focal segmental glomerulosclerosis and associated with podocyte apoptosis. *Cell Death Dis.* 2018;9:533.

324. Wang G, Tam LS, Li EK, et al. Serum and urinary free microRNA level in patients with systemic lupus erythematosus. *Lupus.* 2011;20:493-500.

325. Wang H, Peng W, Ouyang X, Li W, Dai Y. Circulating microRNAs as candidate biomarkers in patients with systemic lupus erythematosus. *Transl Res.* 2012;160:198-206.

326. Perez-Hernandez J, Forner MJ, Pinto C, et al. Increased urinary exosomal microRNAs in patients with systemic lupus erythematosus. *PLoS One.* 2015;10:e0138618.

327. Wu J, Zhang H, Wang W, et al. Plasma microRNA signature of patients with IgA nephropathy. *Gene.* 2018;649:80-86.

328. Chiang CK, Inagi R. Glomerular diseases: genetic causes and future therapeutics. *Nat Rev Nephrol.* 2010;6:539-554.

329. Alport AC. Hereditary familial congenital haemorrhagic nephritis. *Br Med J.* 1927;1:504-506.

330. Hashimura Y, Nozu K, Kaito H, et al. Milder clinical aspects of X-linked Alport syndrome in men positive for the collagen IV alpha5 chain. *Kidney Int.* 2014;85:1208-1213.

331. Pierides A, Voskarides K, Kkolou M, Hadjigavriel M, Deltas C. X-linked, COL4A5 hypomorphic Alport mutations such as G624D and P628L may only exhibit thin basement membrane nephropathy with microhematuria and late onset kidney failure. *Hippokratia.* 2013;17:207-213.

332. Woroniecka KI, Park AS, Mohtat D, et al. Transcriptome analysis of human diabetic kidney disease. *Diabetes.* 2011;60:2354-2369.

333. Abrahamson DR, Isom K, Roach E, et al. Laminin compensation in collagen alpha3(IV) knockout (Alport) glomeruli contributes to permeability defects. *J Am Soc Nephrol.* 2007;18:2465-2472.

334. Yamaguchi J, Tanaka T, Nangaku M. Recent advances in understanding of chronic kidney disease. *F1000Research.* 2015;4.

335. Nabity MB, Lees GE, Cianciolo R, et al. Urinary biomarkers of renal disease in dogs with X-linked hereditary nephropathy. *J Vet Intern Med.* 2012;26:282-293.

336. Groman RP, Bahr A, Berridge BR, Lees GE. Effects of serial ultrasound-guided renal biopsies on kidneys of healthy adolescent dogs. *Vet Radiol Ultrasound.* 2004;45:62-69.

337. Adiconis X, Borges-Rivera D, Satija R, et al. Comparative analysis of RNA sequencing methods for degraded or low-input samples. *Nat Methods.* 2013;10:623-629.

338. Kim D, Langmead B, Salzberg SL. HISAT: a fast spliced aligner with low memory requirements. *Nat Methods.* 2015;12:357-360.

339. Anders S, Pyl PT, Huber W. HTSeq--a Python framework to work with high-throughput sequencing data. *Bioinformatics.* 2015;31:166-169.

340. Benjamini Y, Hochberg Y. Controlling the false discovery rate - a practical and powerful approach to multiple testing. *J Roy Stat Soc B Met.* 1995;57:289-300.

341. Mi H, Poudel S, Muruganujan A, Casagrande JT, Thomas PD. PANTHER version 10: expanded protein families and functions, and analysis tools. *Nucleic Acids Res.* 2016;44:D336-342.

342. Zhang Y, Wang H. Integrin signalling and function in immune cells. *Immunology.* 2012;135:268-275.

343. Jubala CM, Wojcieszyn JW, Valli VE, et al. CD20 expression in normal canine B cells and in canine non-Hodgkin lymphoma. *Vet Pathol.* 2005;42:468-476.

344. Vernau W, Moore PF. An immunophenotypic study of canine leukemias and preliminary assessment of clonality by polymerase chain reaction. *Vet Immunol Immunopathol.* 1999;69:145-164.

345. Ju W, Eichinger F, Bitzer M, et al. Renal gene and protein expression signatures for prediction of kidney disease progression. *Am J Pathol.* 2009;174:2073-2085.

346. Gomez IG, MacKenna DA, Johnson BG, et al. Anti-microRNA-21 oligonucleotides prevent Alport nephropathy progression by stimulating metabolic pathways. *J Clin Invest.* 2015;125:141-156.

347. Tomkowicz B, Rybinski K, Foley B, et al. Interaction of endosialin/TEM1 with extracellular matrix proteins mediates cell adhesion and migration. *Proc Natl Acad Sci USA*. 2007;104:17965-17970.

348. Smith SW, Eardley KS, Croft AP, et al. CD248+ stromal cells are associated with progressive chronic kidney disease. *Kidney Int.* 2011;80:199-207.

349. Wilhelm A, Aldridge V, Haldar D, et al. CD248/endosialin critically regulates hepatic stellate cell proliferation during chronic liver injury via a PDGF-regulated mechanism. *Gut.* 2016;65:1175-1185.

350. Bartis D, Crowley LE, D'Souza VK, et al. Role of CD248 as a potential severity marker in idiopathic pulmonary fibrosis. *BMC Pulm Med.* 2016;16:51.

351. Eikmans M, Aben JA, Koop K, et al. Genetic factors in progressive renal disease: the good ones, the bad ones and the ugly ducklings. *Nephrol Dial Transplant.* 2006;21:257-260.

352. Lin J, Patel SR, Cheng X, et al. Kielin/chordin-like protein, a novel enhancer of BMP signaling, attenuates renal fibrotic disease. *Nat Med.* 2005;11:387-393.

353. Zeisberg M, Bottiglio C, Kumar N, et al. Bone morphogenic protein-7 inhibits progression of chronic renal fibrosis associated with two genetic mouse models. *Am J Physiol Renal Physiol.* 2003;285:F1060-1067.

354. Cheng S, Pollock AS, Mahimkar R, Olson JL, Lovett DH. Matrix metalloproteinase 2 and basement membrane integrity: a unifying mechanism for progressive renal injury. *FASEB J.* 2006;20:1898-1900.

355. Chambers JC, Zhang W, Lord GM, et al. Genetic loci influencing kidney function and chronic kidney disease. *Nat Genet.* 2010;42:373-375.

356. Sakurai Y, Motohashi H, Ogasawara K, et al. Pharmacokinetic significance of renal OAT3 (SLC22A8) for anionic drug elimination in patients with mesangial proliferative glomerulonephritis. *Pharm Res.* 2005;22:2016-2022.

357. Deguchi T, Takemoto M, Uehara N, et al. Renal clearance of endogenous hippurate correlates with expression levels of renal organic anion transporters in uremic rats. *J Pharmacol Exp Ther.* 2005;314:932-938.

358. Sinner DI, Kim GJ, Henderson GC, Igal RA. StearoylCoA desaturase-5: a novel regulator of neuronal cell proliferation and differentiation. *PLoS One.* 2012;7:e39787.

359. Edeling M, Ragi G, Huang S, Pavenstadt H, Susztak K. Developmental signalling pathways in renal fibrosis: the roles of Notch, Wnt and Hedgehog. *Nat Rev Nephrol.* 2016;12:426-439.

360. Xu Y, Shi QL, Ma H, et al. High thymidine kinase 1 (TK1) expression is a predictor of poor survival in patients with pT1 of lung adenocarcinoma. *Tumour Biol.* 2012;33:475-483.

361. Kagan HM, Li W. Lysyl oxidase: properties, specificity, and biological roles inside and outside of the cell. *J Cell Biochem.* 2003;88:660-672.

362. Liu SB, Ikenaga N, Peng ZW, et al. Lysyl oxidase activity contributes to collagen stabilization during liver fibrosis progression and limits spontaneous fibrosis reversal in mice. *FASEB J.* 2016;30:1599-1609.

363. Murawaki Y, Kusakabe Y, Hirayama C. Serum lysyl oxidase activity in chronic liver disease in comparison with serum levels of prolyl hydroxylase and laminin. *Hepatology.* 1991;14:1167-1173.

364. Sivakumar P, Gupta S, Sarkar S, Sen S. Upregulation of lysyl oxidase and MMPs during cardiac remodeling in human dilated cardiomyopathy. *Mol Cell Biochem.* 2008;307:159-167.

365. Goto Y, Uchio-Yamada K, Anan S, et al. Transforming growth factor-beta1 mediated up-regulation of lysyl oxidase in the kidneys of hereditary nephrotic mouse with chronic renal fibrosis. *Virchows Arch.* 2005;447:859-868.

366. Breyer MD, Susztak K. The next generation of therapeutics for chronic kidney disease. *Nat Rev Drug Discov.* 2016;15:568-588.

367. Quezada-Calvillo R, Simsek M, Juarez J, Nichols B. Protein synthesis controls the activity of maltase-glucoamylase and sucrase-isomaltase in non-intestinal tissues. *FASEB J.* 2015;29:596.518.

368. Zhou Q, Xiong Y, Huang XR, et al. Identification of genes associated with Smad3-dependent renal injury by RNA-seq-based transcriptome analysis. *Sci Rep.* 2015;5:17901.

369. Rubel D, Frese J, Martin M, et al. Collagen receptors integrin alpha2beta1 and discoidin domain receptor 1 regulate maturation of the glomerular basement membrane and loss of integrin alpha2beta1 delays kidney fibrosis in COL4A3 knockout mice. *Matrix Biol.* 2014;34:13-21.

370. Yhee JY, Yu CH, Kim JH, Sur JH. Effects of T lymphocytes, interleukin-1, and interleukin-6 on renal fibrosis in canine end-stage renal disease. *J Vet Diagn Invest.* 2008;20:585-592.

371. Jedlicka J, Soleiman A, Draganovici D, et al. Interstitial inflammation in Alport syndrome. *Hum Pathol.* 2010;41:582-593.

372. Sayers R, Kalluri R, Rodgers KD, et al. Role for transforming growth factor-beta1 in Alport renal disease progression. *Kidney Int.* 1999;56:1662-1673.

373. Chu CP, Hokamp JA, Cianciolo RE, et al. RNA-seq of serial kidney biopsies obtained during progression of chronic kidney disease from dogs with X-linked hereditary nephropathy. *Sci Rep.* 2017;7:16776.

374. Trionfini P, Benigni A, Remuzzi G. MicroRNAs in kidney physiology and disease. *Nat Rev Nephrol.* 2015;11:23-33.

375. Ichii O, Horino T. MicroRNAs associated with the development of kidney diseases in humans and animals. *J Toxicol Pathol.* 2018;31:23-34.

376. Ichii O, Otsuka S, Ohta H, et al. MicroRNA expression profiling of cat and dog kidneys. *Res Vet Sci.* 2014;96:299-303.

377. Koenig EM, Fisher C, Bernard H, et al. The beagle dog MicroRNA tissue atlas: identifying translatable biomarkers of organ toxicity. *BMC Genomics.* 2016;17:649.

378. Friedlander MR, Mackowiak SD, Li N, Chen W, Rajewsky N. miRDeep2 accurately identifies known and hundreds of novel microRNA genes in seven animal clades. *Nucleic Acids Res.* 2012;40:37-52.

379. Wong N, Wang X. miRDB: an online resource for microRNA target prediction and functional annotations. *Nucleic Acids Res.* 2015;43:D146-152.

380. Wang X, El Naqa IM. Prediction of both conserved and nonconserved microRNA targets in animals. *Bioinformatics.* 2007;24:325-332.

381. Mi H, Huang X, Muruganujan A, et al. PANTHER version 11: expanded annotation data from Gene Ontology and Reactome pathways, and data analysis tool enhancements. *Nucleic Acids Res.* 2017;45:D183-D189.

382. Fabregat A, Jupe S, Matthews L, et al. The Reactome Pathway Knowledgebase. *Nucleic Acids Res.* 2018;46:D649-D655.

383. Ichii O, Otsuka S, Sasaki N, et al. Altered expression of microRNA miR-146a correlates with the development of chronic renal inflammation. *Kidney Int.* 2012;81:280-292.

384. Pellegrini KL, Gerlach CV, Craciun FL, et al. Application of small RNA sequencing to identify microRNAs in acute kidney injury and fibrosis. *Toxicol Appl Pharmacol.* 2016;312:42-52.

385. Zhu Y, Yu J, Yin L, et al. MicroRNA-146b, a sensitive indicator of mesenchymal stem cell repair of acute renal injury. *Stem Cells Transl Med.* 2016;5:1406-1415.

386. Zhong X, Chung AC, Chen HY, Meng XM, Lan HY. Smad3-mediated upregulation of miR-21 promotes renal fibrosis. *J Am Soc Nephrol.* 2011;22:1668-1681.

387. Zarjou A, Yang S, Abraham E, Agarwal A, Liu G. Identification of a microRNA signature in renal fibrosis: role of miR-21. *Am J Physiol Renal Physiol.* 2011;301:F793-801.

388. Chau BN, Xin C, Hartner J, et al. MicroRNA-21 promotes fibrosis of the kidney by silencing metabolic pathways. *Sci Transl Med.* 2012;4:121ra118.

389. Xu X, Kriegel AJ, Liu Y, et al. Delayed ischemic preconditioning contributes to renal protection by upregulation of miR-21. *Kidney Int.* 2012;82:1167-1175.

390. Lai JY, Luo J, O'Connor C, et al. MicroRNA-21 in glomerular injury. *J Am Soc Nephrol.* 2015;26:805-816.

391. Hennino MF, Buob D, Van der Hauwaert C, et al. MiR-21-5p renal expression is associated with fibrosis and renal survival in patients with IgA nephropathy. *Sci Rep.* 2016;6:27209.

392. Zhong X, Chung AC, Chen HY, et al. MiR-21 is a key therapeutic target for renal injury in a mouse model of type 2 diabetes. *Diabetologia.* 2013;56:663-674.

393. Wang G, Kwan BC, Lai FM, et al. Elevated levels of miR-146a and miR-155 in kidney biopsy and urine from patients with IgA nephropathy. *Dis Markers.* 2011;30:171-179.

394. Alipour MR, Khamaneh AM, Yousefzadeh N, Mohammad-nejad D, Soufi FG. Upregulation of microRNA-146a was not accompanied by downregulation of pro-inflammatory markers in diabetic kidney. *Mol Biol Rep.* 2013;40:6477-6483.

395. Lu J, Kwan BC, Lai FM, et al. Glomerular and tubulointerstitial miR-638, miR-198 and miR-146a expression in lupus nephritis. *Nephrology (Carlton).* 2012;17:346-351.

396. Baker MA, Davis SJ, Liu P, et al. Tissue-specific microRNA expression patterns in four types of kidney disease. *J Am Soc Nephrol.* 2017;28:2985-2992.

397. Liu X, Fu B, Chen D, et al. MiR-184 and miR-150 promote renal glomerular mesangial cell aging by targeting Rab1a and Rab31. *Exp Cell Res.* 2015;336:192-203.

398. Zhou H, Hasni SA, Perez P, et al. MiR-150 promotes renal fibrosis in lupus nephritis by downregulating SOCS1. *J Am Soc Nephrol.* 2013;24:1073-1087.

399. Wang B, Komers R, Carew R, et al. Suppression of microRNA-29 expression by TGF-beta1 promotes collagen expression and renal fibrosis. *J Am Soc Nephrol.* 2012;23:252-265.

400. Qin W, Chung AC, Huang XR, et al. TGF-beta/Smad3 signaling promotes renal fibrosis by inhibiting miR-29. *J Am Soc Nephrol.* 2011;22:1462-1474.

401. Lin CL, Lee PH, Hsu YC, et al. MicroRNA-29a promotion of nephrin acetylation ameliorates hyperglycemia-induced podocyte dysfunction. *J Am Soc Nephrol.* 2014;25:1698-1709.

402. Hsu YC, Chang PJ, Ho C, et al. Protective effects of miR-29a on diabetic glomerular dysfunction by modulation of DKK1/Wnt/beta-catenin signaling. *Sci Rep.* 2016;6:30575.

403. Lin DH, Yue P, Pan C, Sun P, Wang WH. MicroRNA 802 stimulates ROMK channels by suppressing caveolin-1. *J Am Soc Nephrol.* 2011;22:1087-1098.

404. Anglicheau D, Sharma VK, Ding R, et al. MicroRNA expression profiles predictive of human renal allograft status. *Proc Natl Acad Sci USA.* 2009;106:5330-5335.

405. Soltaninejad E, Nicknam MH, Nafar M, et al. Differential expression of microRNAs in renal transplant patients with acute T-cell mediated rejection. *Transpl Immunol.* 2015;33:1-6.

406. Langmead B, Trapnell C, Pop M, Salzberg SL. Ultrafast and memory-efficient alignment of short DNA sequences to the human genome. *Genome Biol.* 2009;10:R25.

407. Hu J, Ge H, Newman M, Liu K. OSA: a fast and accurate alignment tool for RNA-Seq. *Bioinformatics.* 2012;28:1933-1934.

408. Bockmeyer CL, Sauberlich K, Wittig J, et al. Comparison of different normalization strategies for the analysis of glomerular microRNAs in IgA nephropathy. *Sci Rep.* 2016;6:31992.

409. Deiuliis JA. MicroRNAs as regulators of metabolic disease: pathophysiologic significance and emerging role as biomarkers and therapeutics. *Int J Obes (Lond).* 2016;40:88-101.

410. Thompson AG, Gray E, Heman-Ackah SM, et al. Extracellular vesicles in neurodegenerative disease - pathogenesis to biomarkers. *Nat Rev Neurol.* 2016;12:346-357.

411. Garcia-Elias A, Alloza L, Puigdecanet E, et al. Defining quantification methods and optimizing protocols for microarray hybridization of circulating microRNAs. *Sci Rep.* 2017;7:7725.

412. Ferrero G, Cordero F, Tarallo S, et al. Small non-coding RNA profiling in human biofluids and surrogate tissues from healthy individuals: description of the diverse and most represented species. *Oncotarget.* 2018;9:3097-3111.

413. Yeri A, Courtright A, Reiman R, et al. Total extracellular small RNA profiles from plasma, saliva, and urine of healthy subjects. *Sci Rep.* 2017;7:44061.

414. Fuchs RT, Sun Z, Zhuang F, Robb GB. Bias in ligation-based small RNA sequencing library construction is determined by adaptor and RNA structure. *PLoS One.* 2015;10:e0126049.

415. Serino G, Pesce F, Sallustio F, et al. In a retrospective international study, circulating miR-148b and let-7b were found to be serum markers for detecting primary IgA nephropathy. *Kidney Int.* 2016;89:683-692.

416. Liu Y, Gao G, Yang C, et al. Stability of miR-126 in urine and its potential as a biomarker for renal endothelial injury with diabetic nephropathy. *Int J Endocrinol.* 2014;2014.

417. Shyamasundar S, Ong C, Yung LYL, Dheen ST, Bay BH. MiR-128 regulates genes associated with inflammation and fibrosis of rat kidney cells in vitro. *Anat Rec.* 2017.

418. Diagnosis ICGSSoITAaP, Pressler B, Vaden S, et al. Consensus guidelines for immunosuppressive treatment of dogs with glomerular disease absent a pathologic diagnosis. *J Vet Intern Med.* 2013;27 Suppl 1:S55-59.

419. Cianciolo RE, Mohr FC, Aresu L, et al. World small animal veterinary association renal pathology initiative: classification of glomerular diseases in dogs. *Vet Pathol.* 2016;53:113-135.

420. Langenberger D, Bartschat S, Hertel J, et al. MicroRNA or not MicroRNA? In: Norberto de Souza O, Telles GP, Palakal M, eds. *Advances in Bioinformatics and Computational Biology.* Berlin, Heidelberg, Germany: Springer; 2011: 1-9.

421. Felicetti F, Feo A, Coscia C, et al. Exosome-mediated transfer of miR-222 is sufficient to increase tumor malignancy in melanoma. *J Transl Med.* 2016;14:56.

422. Li H, Ma Y, Chen B, Shi J. MiR-182 enhances acute kidney injury by promoting apoptosis involving the targeting and regulation of TCF7L2/Wnt/beta-catenins pathway. *Eur J Pharmacol.* 2018;831:20-27.

423. Wilflingseder J, Sunzenauer J, Toronyi E, et al. Molecular pathogenesis of post-transplant acute kidney injury: assessment of whole-genome mRNA and miRNA profiles. *PloS one.* 2014;9:e104164.

424. Ramachandran K, Saikumar J, Bijol V, et al. Human miRNome profiling identifies microRNAs differentially present in the urine after kidney injury. *Clin Chem.* 2013;59:1742-1752.

425. Pavkovic M, Robinson-Cohen C, Chua AS, et al. Detection of Drug-Induced Acute Kidney Injury in Humans Using Urinary KIM-1, miR-21, -200c, and -423. *Toxicol Sci.* 2016;152:205-213.

426. Chen C, Lu C, Qian Y, et al. Urinary miR-21 as a potential biomarker of hypertensive kidney injury and fibrosis. *Sci Rep.* 2017;7:17737.

427. Xu J, Li R, Workeneh B, et al. Transcription factor FoxO1, the dominant mediator of muscle wasting in chronic kidney disease, is inhibited by microRNA-486. *Kidney Int.* 2012;82:401-411.

428. Vinas JL, Burger D, Zimpelmann J, et al. Transfer of microRNA-486-5p from human endothelial colony forming cell-derived exosomes reduces ischemic kidney injury. *Kidney Int.* 2016;90:1238-1250.

429. Cantaluppi V, Gatti S, Medica D, et al. Microvesicles derived from endothelial progenitor cells protect the kidney from ischemia-reperfusion injury by microRNA-dependent reprogramming of resident renal cells. *Kidney Int.* 2012;82:412-427.

430. Park S, Moon S, Lee K, et al. Urinary and blood microRNA-126 and-770 are potential noninvasive biomarker candidates for diabetic nephropathy: a meta-analysis. *Cell Physiol Biochem.* 2018;46:1331-1340.

431. Bai XY, Ma Y, Ding R, et al. MiR-335 and miR-34a Promote renal senescence by suppressing mitochondrial antioxidative enzymes. *J Am Soc Nephrol.* 2011;22:1252-1261.

432. Fogo AB. Causes and pathogenesis of focal segmental glomerulosclerosis. *Nat Rev Nephrol.* 2015;11:76-87.

433. Wang C, Blough E, Arvapalli R, et al. Acetaminophen attenuates glomerulosclerosis in obese Zucker rats via reactive oxygen species/p38MAPK signaling pathways. *Free Radic Biol Med.* 2015;81:47-57.

434. Yang SM, Chan YL, Hua KF, et al. Osthole improves an accelerated focal segmental glomerulosclerosis model in the early stage by activating the Nrf2 antioxidant pathway and subsequently inhibiting NF-kappaB-mediated COX-2 expression and apoptosis. *Free Radic Biol Med.* 2014;73:260-269.

435. Ahmadvand H, Tavafi M, Khosrowbeygi A. Amelioration of altered antioxidant enzymes activity and glomerulosclerosis by coenzyme Q10 in alloxan-induced diabetic rats. *J Diabetes Complications.* 2012;26:476-482.

436. Adlakha YK, Saini N. MicroRNA-128 downregulates Bax and induces apoptosis in human embryonic kidney cells. *Cell Mol Life Sci.* 2011;68:1415-1428.